1995

Characterization of Nylon-11 Degradation

Leslie Christian McCullough
College of William & Mary - Arts & Sciences

Characterization of Nylon-11 Degradation

A Thesis

Presented to the Department of Chemistry

The College of William and Mary in Virginia

In Partial Fulfillment

Of the Requirements for the Degree of

Master of Arts

---

by

Leslie C. McCullough
1995

APPROVAL SHEET

This thesis is submitted in partial fullfillment

of the requirements for the degree of

Master of Arts

Leslie C McCullough

Approved, August 1995

David E. Kranbuehl

Gary W. Rice

David W. Thompson

Table of Contents

Acknowledgements

I would like to thank Dr. Kranbuehl for helping me get into the master's program late. I would also like to thank the many undergraduates who worked on this project, especially Heidi Aandahl, Nicole Haralampus, and Wendy Newby. Without them most of this data would never have been taken. Lastly, I would like to thank David Hood and Rhonda Barksdale for everything.

List of Figures

Abstract

In this study the degradation of nylon-11, Rilsan, was monitored under accelerated aging conditions. Rilsan is a trade name for poly(imino-1-oxoundecamethylene), nylon-11. The accelerated aging of the Rilsan was accomplished in three sealed $103 \pm 2°C$ CO_2 saturated oil pots. The pots contained the following solutions: 95% water/5% ASTM 3 oil; 5% water/95% ASTM 3 and IRM 903 oils; and 100% Petroleum Crude Oil Class 3 from the North Sea. Frequency dependent electromagnetic sensors were imbedded in the Rilsan and measurements were taken periodically throughout the aging process. Mechanical tension tests, viscosity, differential scanning calorimetry, hardness, light scattering, and Fourier transform infrared measurements were also taken.

For the samples aged in all three environments, the mechanical properties, the molecular weight, and the dielectric values were found to decline as the material degraded. For the 95% water pot, the physical properties were correlated with the dielectric measurements. This allowed physical properties to be predicted from dielectric values. Since dielectric measurements can be made in situ, life monitoring of these materials is possible.

I. Introduction

This study is the third phase of a larger study on the aging of Rilsan pipe. The overall goal of the study is to characterize the degradation of the Rilsan pipe. The characterization is accomplished by frequency dependent electromagnetic sensing (FDEMS) and correlating the results with mechanical and viscosity measurements. The in situ FDEMS monitoring provides a sensitive, convenient, automated means for monitoring polymers in their actual operating environment. FDEMS has numerous advantages: nondestructive; reproducibility; sensitivity; in situ capability; remote sensing; automation.[1] Development of an in situ FDEMS monitoring system of Rilsan pipe will enable pipe failure prediction, potentially saving time, money, and the environment.

Oil reserves were found under the North Sea in the 1960's. The first Norwegian oil field went into production in 1971 followed by the first British oil field in 1975.[2] These two countries remain the primary holders of oil resources in the North Sea. The sea has been divided into numerous sectors. The following countries have sectors and control the development and collection of royalties: United Kingdom, Norway, Denmark, Germany, and Netherlands. (Figure 1-1)

The North Sea is known for its unpredictable weather. Winter storms with winds up to 100 mph are common. The violent weather can make the North Sea unnavigable during the winter. Exploratory drilling can only be done during good

weather, mostly in the summer months. Permanent platforms for oil rigs, however, are in place year round and must be able to withstand winter storms and collisions with floating ice. It is imperative that the pipes do not rupture as it would cause an environmental catastrophe.

The North Sea averages depths of 100 ft. in the south and 400 ft. in the north. These relatively shallow depths allow for the use of fixed platforms. Fixed platforms consist of two or three sections with the bottom section being secured to the sea floor and the top section used for the base of drilling. The platform often has room for storage and the housing of personnel. (Figure 1-2) Up to 42 wells can be drilled from one platform.[3] Because of the high costs involved in building and operating these platforms, no oil company owns more than 25% of any one platform.

The high cost of offshore drilling and the potential environmental hazards have led to the need for reliable, flexible materials for use as pipes. Steel pipe, which is traditionally used in land based oil rigs, is not entirely suitable for use with offshore platforms. Motions from surface water and under water currents make flexible pipe a necessity. The Rilsan pipe is used as the fluid gas barrier in flexible pipes for the transport of oil and gas from the ocean floor to the surface. Nylons are suited to this application because they are stable in the presence of hydrocarbons.

Metal degradation and fatigue can be visually detected and repaired or

replaced prior to failure. However, polymers and composites can fail catastrophically with no warning. Therefore, a method of life monitoring is critical.

Rilsan accelerated aging was performed in three oil and water pots at 103 $\pm$ 2°C. The pipe in use on the platform is subjected to an average oil-water temperature of 70°C. The higher temperature was used at William and Mary to obtain a complete study of degradation over a reasonable period of time. The pots were pressurized with CO_2 and only opened when measurements were taken. Dielectric, mechanical, molecular weight, DSC, and hardness measurements were taken at approximately the same intervals.

The aging was done in a controlled environment and can not be directly correlated to the varying conditions of an oil platform. However, it does demonstrate the relationship between dielectric measurements and macroscopic properties. The movement of the individual ions on a microscopic level, detected through dielectric measurements, gives information about the macroscopic state of the material. Changes on the macroscopic level are caused by changes on the microscopic level. Due to this, FDEMS dielectric sensors can indirectly monitor the mechanical properties of Rilsan pipe over time.

Figure 1-1[4]

The North Sea and bordering countries

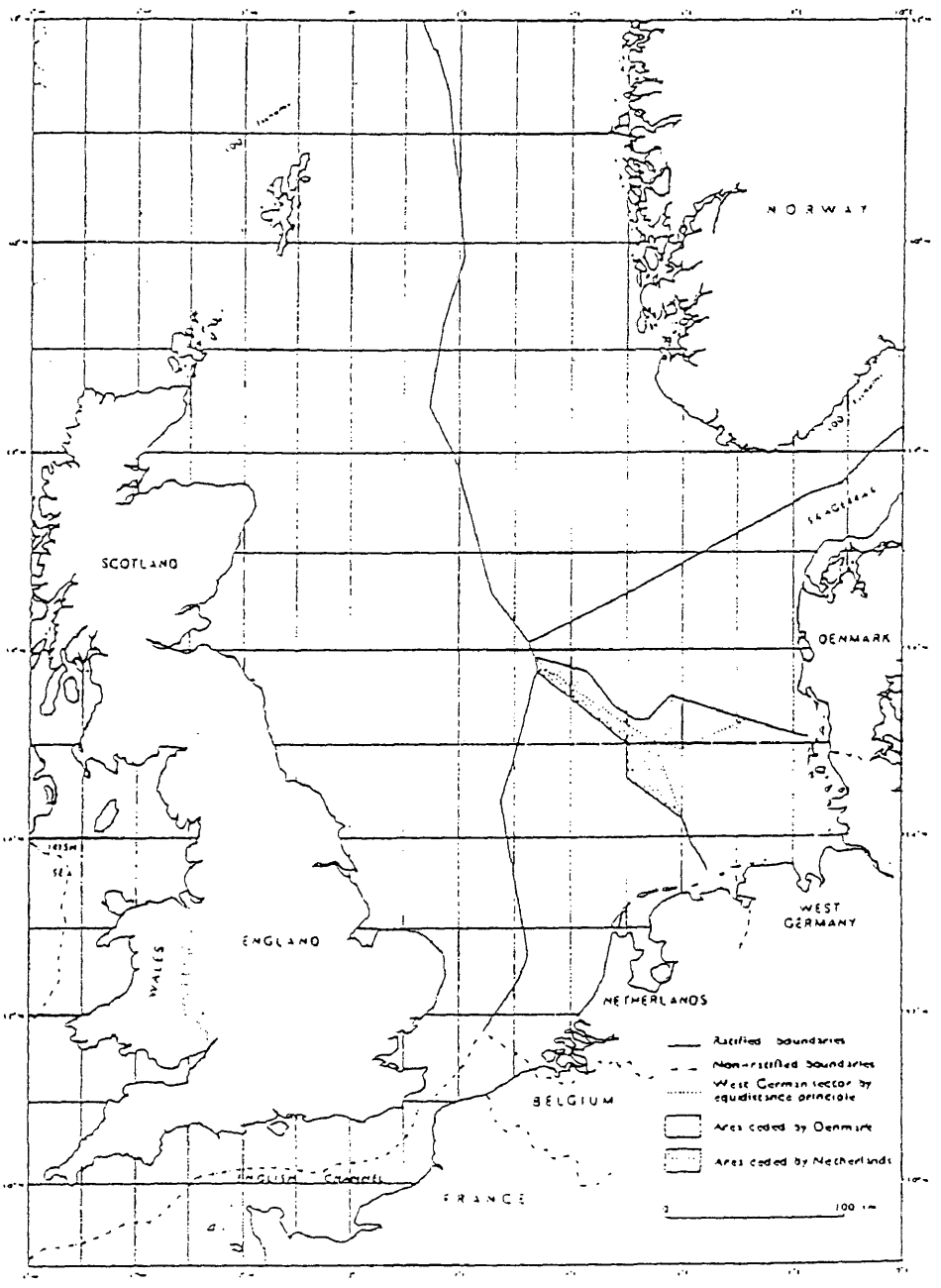

Fig 21. International division of the North Sea

Figure 1-2[5]

Rotary-drilling Rig

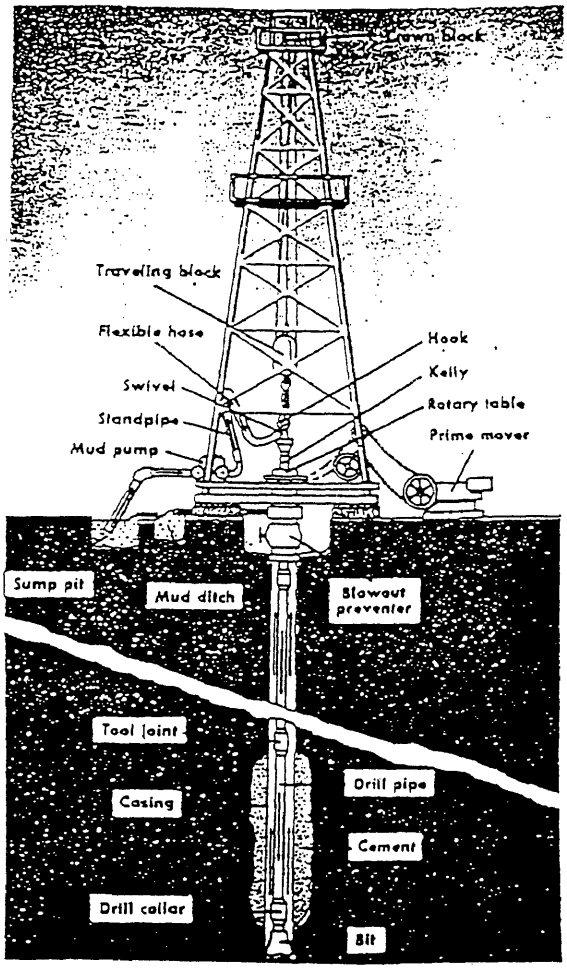

Offshore Drilling Rigs

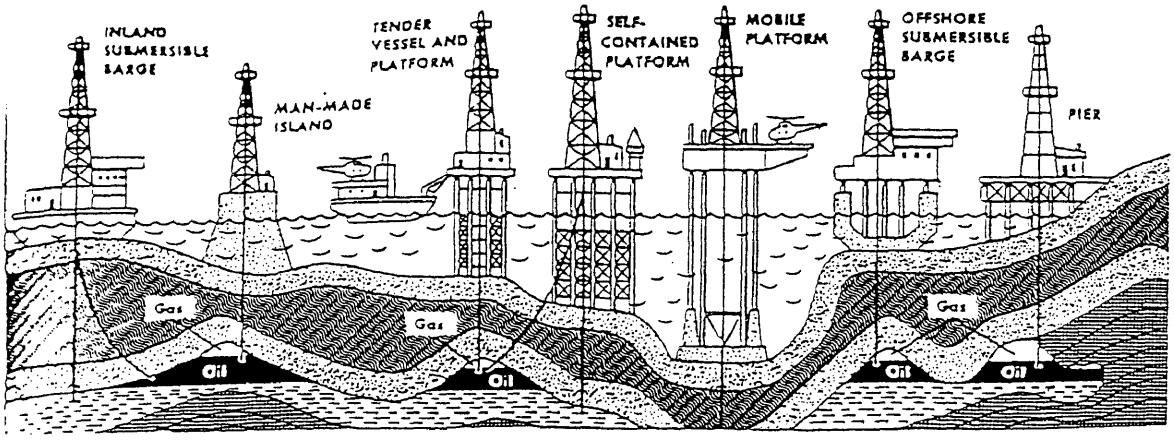

References

1. Kranbuehl, D., D. Hood, L. McCullough, H. Aandahl, N. Haralampus, and W. Newby. "Frequency Dependent Electromagnetic Sensing (FDEMS) For Life Monitoring of Polymers in Structural Composites During Use." 1995.

2. Collier's Encyclopedia. 1987. vol 17 p. 645.

3. The World Book Encyclopedia. 1993. vol 15 pp. 338-342.

4. Chapman, Keith. North Sea Oil and Gas: A Geographical Perspective. North Pomfret, VT: David & Charles, 1976. p. 72.

5. Collier's Encyclopedia. 1987. vol 17 pp. 647 & 649.

II. Chemistry of Rilsan

The nylon studied was Rilsan BESNO P40TL. Rilsan is a trade name for poly(imino-1-oxoundecamethylene), nylon-11, made by Aquitane Chemicals Inc. Nylon-11 has the following formula:

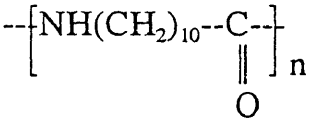

BESNO P40TL is a code used to indicate certain additives and properties of the polymer. B is a manufacture reference. ES refers to blow molding, extrusion of profiles. N means it has medium viscosity. P40 indicates that the sample is very flexible. T indicates that it is temperature resistant and L means that it is light stabilized.[1]

Nylon-11 is synthesized by a condensation polymerization of ω-aminoundecanoic acid at 200-220°C with continuous removal of the water formed. The reaction is forced to completion under pressure.

The amidation is a rapid reaction over 180°C with virtually no side reactions. The polymer is generally linear with no isomerism. Under favorable conditions nylon molecular weights of 20,000 - 30,000 are obtainable.[2] Tensile strength increases with greater molecular weight and levels off at a maximum value.[3] Therefore, polymers of high molecular weight are desired to achieve maximum strength.

The amidation reaction is second order with respect to the functional groups. It depends on the concentration of both unreacted -NH_2 and -COOH.[4] The general rate law for this would be

$$\frac{d[A]}{dt} = -k[A]\,[B]$$

where A and B represent the two functional groups.

The literature reports melting temperatures of 185-188°C for nylon-11. The nylon used in this study has a melting point of approximately 180°C before aging and reaches a maximum melting point of approximately 187°C during aging. The lower melting point is most likely due to the fact that the literature values are for pure nylon-11 while the sample under study has additives.

Nylons are semi-crystalline polymers. The crystallinity is due to the regularity of the molecules along the chain and the strong polarity and hydrogen bonding of the amide linkages. The high melting point and opacity result from the polymer's crystallinity. Nylon-6, with a melting temperature of 215°C, has a higher melting point due to its shorter chain segments which enhance crystallinity.

Semi-crystalline polymers have chains that go through several crystallites with amorphous regions in between. High tensile strength is attributed to these amorphous regions. They hold the crystallites together with primary bonds.[5] The amorphous regions allow the polymer to withstand more force before breaking

than it would if it was entirely crystalline. The amorphous regions also allow the semi-crystalline polymer to be flexible.

The highly polar amide linkages enable nylons to absorb water. Nylon-11 absorbs considerably less water than the other commercially used nylons, nylon-6 and nylon-66, 2-3% compared to 8-10% at saturation. Water absorption increases the toughness of the nylon because it makes the polymer less brittle.[6]

The main route of degradation is through acid hydrolysis. This is essentially the reverse of the condensation polymerization by which nylons are synthesized. A molecule of water is added across the amide bond resulting in chain scission. A mechanism for this process is shown in Figure 2-1. This chain scission lowers the molecular weight, which makes the polymer more brittle and lowers the tensile strength.[7] Lowering the molecular weight makes the alignment for crystallization easier and the crystallinity of the material would likely increase at this point.

The hydrolysis of nylon-6 in 40% H_2SO_4 at 50°C proceeds as uniform first order splitting.[9] The hydrolysis of the amide linkages is the same regardless of the length of the carbon chain. The hydrolysis of nylon-11 in solution with CO_2 and water in excess would be a first order reaction dependent on the concentration of amide bonds.

In order for hydrolysis to take place in the solid state, water must first diffuse into the polymer. The rate of hydrolysis depends on the amount of acid

Figure 2-1
Mechanism for acid hydrolysis of an amide bond[8]

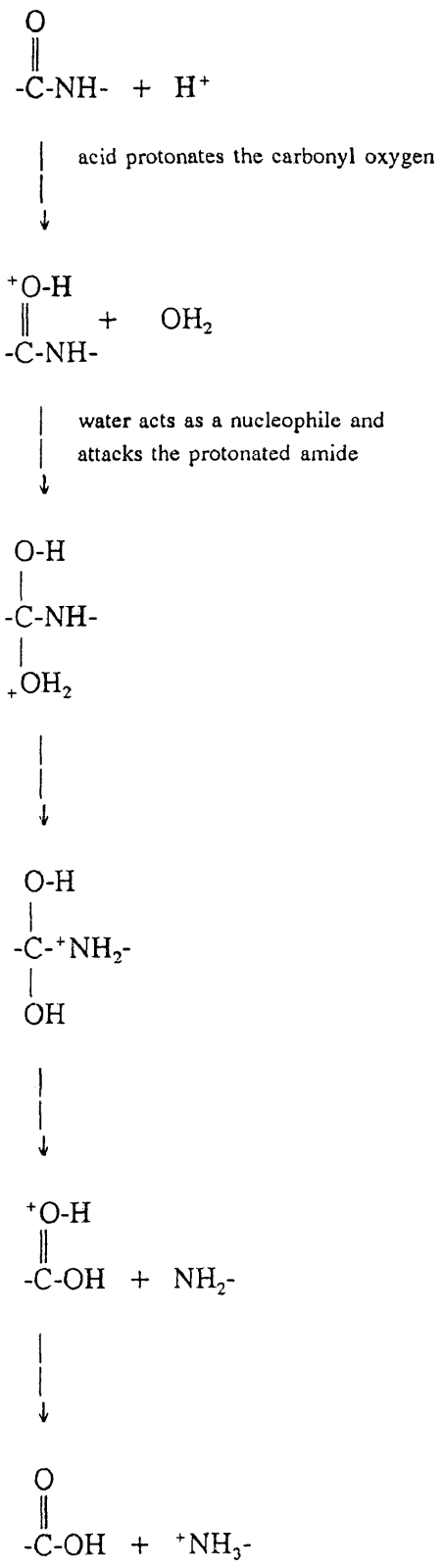

present as well as the concentration of the amide. For a cross section of nylon pipe, the rate of diffusion of water would initially determine the rate of the chain scission. Diffusion is favored at temperatures above T_g because there is constant cooperative segmental movement.[10] T_g for nylon-11 is 43°C[11] which is well below the temperature of the aging environment. Once water is present in the nylon the rate process would be determined by the amide concentration since the water is in excess.

Water acts as a plasticizer and can actually increase the strength of the nylon before hydrolysis begins. There is plasticizer or stabilizer present in the original samples of nylon pipe. The plasticizer may be either joined by or replaced by water after the nylon is in the water bath. As the original plasticizer leaves it opens up space for water to enter. The highly polar amide bonds favor water absorption. Water is absorbed more rapidly during the initial period of the aging study because crystallinity tends to lower the permeability of water into the polymer.

Crystallinity also lowers the rate of hydrolysis. Crystalline regions are more resistant to hydrolysis than amorphous regions. In the hydrolysis of poly(ethylene terephthalate) the order of hydrolytic activity is:
unoriented amorphous > unoriented crystalline > oriented crystalline.[12]
Nylon would follow the same pattern. The amorphous regions would be the areas first attacked. As these chains are shortened and subsequently aligned to form

crystallites the hydrolysis reaction would slow.

As the amorphous regions are replaced by areas of more crystallinity, the permeation of water into the polymer slows. The hydrolysis by the water that has diffused into the nylon also slows. From these factors it would be expected that the greatest changes in nylon properties would occur during the initial stages of the degradation process.

References

1. Kohan, Melvin I., editor. Nylon Plastics. New York: John Wiley & Sons, 1973. pp. 645-646.

2. Flory, Paul J. Principles of Polymer Chemistry. Ithaca, NY: Cornell University Press, 1953. p. 94.

3. Flory, p. 6.

4. Flory, p. 83.

5. Sperling, L.H. Introduction to Physical Polymer Science, 2nd edition. New York: John Wiley & Sons, Inc., 1992. p. 215.

6. Birley, A.W., R.J. Heath, and M.J. Scott. Plastics Materials: Properties and Applications, 2nd edition. New York: Chapman and Hall, 1988. p. 105.

7. Sperling, p. 511.

8. Solomons, T.W. Graham. Organic Chemistry, 4th edition. New York: John Wiley & Sons, 1988. p. 847.

9. Flory, p. 86.

10. Seymour, Ramond B. Plastics vs. Corrosives. New York: John Wiley & Sons, 1982. p. 26.

11. Brandrup, J. and E.H. Immergut, ed. Polymer Handbook, 3rd edition. New York: John Wiley & Sons, 1989. p. III/168.

12. Reich, Leo and Salvatore S. Stivala. Elements of Polymer Degradation. New York: McGraw-Hill Book Company, 1971. p. 69.

III. Methods of Data Acquisition

Frequency Dependent Electromagnetic Sensing

Frequency dependent electromagnetic sensing (FDEMS) provides a convenient method for monitoring the aging or degradation of polymeric materials. Impedance measurements taken in the hertz to kilohertz frequency range provide information on the changing chemical and physical properties of the material.

A sensor is used to measure capacitance (C) and conductance (G), both dependent on sample geometry, from the dielectric impedance. Capacitance and conductance are used to calculate the intensive geometry independent complex permittivity, ϵ^*.

$$\epsilon^* = \epsilon' - i\epsilon''$$

[1]

where ϵ' is the dielectric permittivity and ϵ'' is the dielectric loss factor associated with the time dependent orientation polarization and conduction. These are calculated from

$$\epsilon' = \frac{C_{material}}{C_o}$$

[2]

and

$$\epsilon'' = \frac{G_{material}}{C_o \omega}$$

[3]

where C_o is the air-filled capacitance of the sensor and ω is $2\pi f$ with f, frequency, in hertz. The air-filled capacitance is constant over all frequencies.

The real and imaginary components of ϵ^* have both a dipolar and an ionic component.

$$\epsilon' = \epsilon'_d + \epsilon'_i$$

[4]

$$\epsilon'' = \epsilon''_d + \epsilon''_i$$

[5]

The dipolar component results from the rotational diffusion of bound charges and molecular dipole moments. The frequency dependence of the dipolar component can be shown by the Cole-Davidson function:

$$\epsilon^*_d = \frac{\epsilon_r - \epsilon_u}{(1 - i2\pi f\tau)^\beta} + \epsilon_u$$

[6]

where ϵ_r and ϵ_u are the limiting low and high frequency values of ϵ_d, τ is the characteristic relaxation time, and β is the Cole-Davidson distribution parameter

$(0<\beta<1)$ which measures the distribution in relaxation times. This dipolar component dominates the dielectric signal at high frequencies and in highly viscous media.[1]

The ionic component arises from the translational diffusion of charge resulting in localized layers of charge near the electrodes. Therefore, the ionic component often dominates at low frequencies, low viscosities, and high temperatures. Johnson and Cole derived equations for the ionic contribution to ϵ^{*2}

$$\epsilon'_i=\epsilon'_d+C_oZ_o\sin\left(\frac{n\pi}{2}\right)\omega^{-(n+1)}\left(\frac{\sigma}{\epsilon_o}\right)^2$$

[7]

$$\epsilon''_i=\epsilon''_d+\left(\frac{\sigma}{\epsilon_o\omega}\right)-C_oZ_o\cos\left(\frac{n\pi}{2}\right)\omega^{-(n+1)}\left(\frac{\sigma}{\epsilon_o}\right)^2$$

[8]

where ϵ_o is the permittivity in a vacuum (8.85×10^{-14} Farads/cm) and C_o is the air replaceable capacitance in Farads. $Z = Z_o(i\omega)^{-n}$ is the electrode impedance induced by the ions, σ ($ohm^{-1}cm^{-1}$) is the specific conductivity and n is between 0 and 1.[3] The first term in equation [7] describes the conductance of ions translating through the medium. The second term results from the electrode polarization and makes impedance measurements difficult to interpret and use as the measured frequency becomes significantly lower.

By ignoring these electrode polarization effects, the ionic conductivity is

related to the loss factor by the equation:

$$\sigma = \epsilon_o \omega \epsilon''_i \qquad [9]$$

The dipolar component of the loss factor can be determined by subtracting the ionic component from the complex permittivity.

$$\epsilon''_d = \epsilon^* - \frac{\sigma}{\epsilon_o \omega} \qquad [10]$$

The magnitude of the ionic mobility, σ, and the rotational mobility, τ, determined from the frequency dependence of $\epsilon^**\omega$ can be quantitatively related to the reaction advancement, degradation through hydrolysis. This is due to the dependence of σ and τ on the extent of reaction and physical state of the polymer. These molecular level dielectric measurements are useful because the mobility on the molecular level is related to the macroscopic state of the material.

FDEMS measurements were made with a geometry independent microsensor, patented by Kranbuehl. The sensor consists of a fine array of two interdigitated comb electrodes on one side (active side) and is constructed of noble metals and high temperature ceramics. The DekDyne sensor is inert and designed to withstand temperatures exceeding 400°C and pressures up to 1000 psi. (Figure 3-1)

Frequency dependent impedance measurements were taken using a Hewlett-Packard 4263A LCR Meter controlled by a microcomputer.

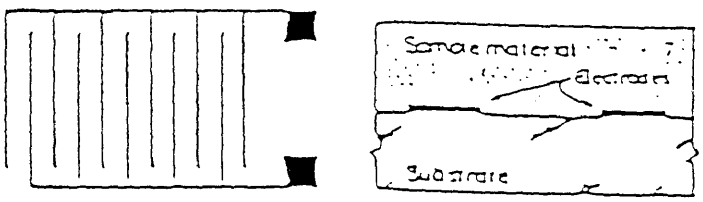

DekDyne sensor

Figure 3-1

Mechanical Testing

The mechanical tests were performed according to ASTM Designation: D 638 - 87b Standard Test Method for Tensile Properties of Plastics. Dogbone samples were cut to the dimensions shown in Figure 3-2. Units are in inches.

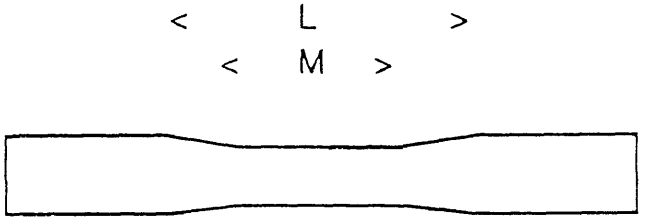

M=2:552

a(W)=0.487	b(W)=0.247	c(W)=0.243	d(W)=0.244	e(W)=0.467
a(T)=0.232	b(T)=0.231	c(T)=0.229	d(T)=0.228	e(T)=0.229

Mechanical tensile test piece (Dogbone)

Figure 3-2

One end of the sample was clamped into a stationary grip and the other into a movable grip. (Figure 3-3) The movable grip was raised at a rate of 0.5"/min. Load at break, percent extension at break, load at yield, and percent extension at yield were obtained in this manner. The data revealed the strength of the material.

Changes in the strength of the material are observed over the period of aging.

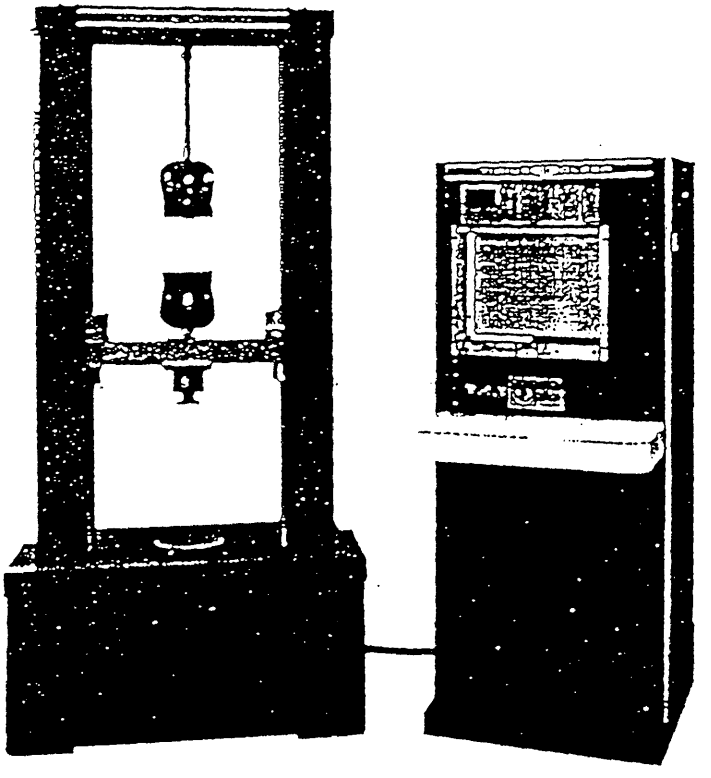

Universal testing machine for tension or compression.[4]

Figure 3-3

Viscosity

Samples of nylon at various stages of aging were dissolved in m-cresol to enable solution viscosity measurements. The viscosity measurements were performed in an Ubbelohde viscometer at a constant temperature of 25°C. (Figure 3-4) The flow time was used to calculate the viscosity average molecular weight.

$$\eta_{sp} = \left(\frac{t}{t_o}\right) - 1$$

[11]

t_o = flow time for solvent

Plotting η_{sp}/c vs. c for various concentrations yields a straight line with a y-intercept equal to the intrinsic viscosity, $[\eta]$.

Intrinsic viscosity is related to molecular weight by the Mark-Houwink equation

$$[\eta] = kM^a$$

[12]

k and a are constants. For this system k is 0.081 ml/g and a is 0.74.[5]

Flow times at low concentrations are not as reliable as those at higher concentrations. Due to the inherent error in the low concentration measurements, the slope calculated for the fresh nylon samples, using concentrations of 0.000828

g/ml and 0.003298 g/ml, was used as the slope for all of the samples. Concentrations of approximately 0.003 g/ml were used for all of the samples.

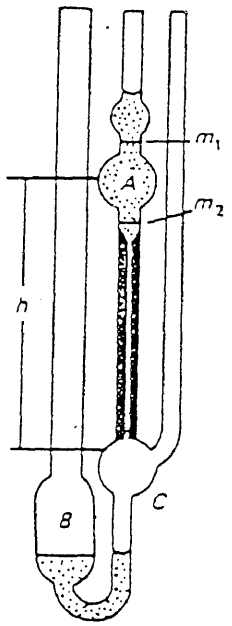

Ubbelohde Viscometer

Figure 3-4

Differential Scanning Calorimetry

Differential scanning calorimetry (DSC) measures the change in heat capacity for first and second order phase transitions. DSC measurements were taken using a Perkin-Elmer DSC-7. For Rilsan the phase transition of interest is melting of the material. Melting is a first order phase transition. The second

order phase transition, the glass transition (T_g), is not reported here for Rilsan. The DSC plot shows a peak where the maximum point represents the melting temperature, T_m, and the area under the peak is the change in enthalpy, ΔH. Measurements were taken from 100 - 200°C at a heating rate of 5°C per minute. The curve was integrated between 160 and 200°C to calculate ΔH.

ΔH can be used to calculate the degree of crystallinity with the following equation:

$$\%crystallinity = \frac{\Delta H_{melt}}{\Delta H^{o}_{melt}} x100\% \qquad [13]$$

where ΔH_{melt} is the enthalpy of the sample and ΔH^{o}_{melt} is the enthalpy for a purely crystalline sample of the material. ΔH^{o}_{melt} for nylon-11 is 54.1 cal/g (226 J/g).[14] From equation [13], enthalpy can be used to follow any changes in crystallinity.

Since nylon is a semi-crystalline polymer, samples tested in the DSC could be from amorphous or crystalline regions. The small (5 - 10 mg) sample is not necessarily representative of the larger sample. To help eliminate this problem multiple samples were used and averaged. However, DSC measurements still can only be used to indicate a general trend.

Hardness Tests

Hardness measurements were taken with a Barber Colman model GYZJ 935 impressor. Hardness is measured by the distance of indention and recovery that occurs when a sharp steel point is pressed into the surface under constant load and then released.[6] Hardness is a relative measurement that illustrates changes in the nylon as it ages.

Light Scattering

Light scattering was performed with a Dawn B laser light scattering photometer made by Wyatt Technology Corporation. The instrument uses a 5mW He-Ne laser to provide a steady, intense beam of vertically polarized light at a wavelength of 632.8 nm.

The light scattering experiment enabled the determination of the weight average molecular weight for fresh nylon. Light scattering solutions must be dust free. Consequently, the solutions were filtered through 0.45 micron filters. M-cresol, the solvent used in the viscosity study, is extremely viscous and difficult to work with. To combat this problem a 70/30 m-cresol/heptane solution was

used. This reduced the viscosity without affecting the solubility of the nylon.[7,8]

Fourier Transform Infrared Spectroscopy

Fourier transform infrared spectroscopy (FTIR) was used to monitor the degradation of the nylon samples. Spectra were acquired using a Nicolet 20DXB FTIR Spectrometer. As a sample degrades, the amount of amide groups decrease and carboxylic acid groups increase.

Weight Loss Study

Various weight loss studies were performed to determine the amount of plasticizer in the fresh nylon pipe and the amount of water absorbed while in a pot. The weight loss studies helped show the rate of diffusion of water into the nylon.

There are two types of diffusion, Fickian and non-Fickian. Fickian

diffusion follows Fick's laws.[9,10]

$$1st: J = -D\frac{\delta c}{\delta x} \qquad [14]$$

$$2nd: \frac{\delta c}{\delta t} = \frac{\delta}{\delta x}\left[D\frac{\delta c}{\delta x}\right] \qquad [15]$$

where J is flux, D is the diffusion coefficient, c is concentration, x is distance, and t is time. Most diffusion is Fickian. An example of non-Fickian diffusion is the dissolution of a high polymer by a good solvent.[11]

The diffusion of interest in this study, water into a slab of nylon, would be Fickian. The nylon acts as the solvent and the water as the solute. It is a dilute solution. The concentration profile of this system is

$$\frac{c(t) - c(initial)}{c(final) - c(initial)} = erf(B)$$

$$B = \frac{z}{\sqrt{4D_{eff}t}} \qquad [16][12]$$

erf is the error function. For values of B between 0 and 0.75, erf(B) $\approx$ B. For B = 2, erf(B) $\approx$ ½(B).[15] Therefore, erf(B) = B is a reasonable approximation. It follows from equation [16] that the speed with which the water penetrates the nylon is proportional to the square root of time. Weights were used in place of

concentrations because they are easier to measure.

Three weight loss studies were performed. The first used a vacuum oven at 80°C to prevent absorption of water from the air. The second placed samples in the 95% water pot and the 95% oil pot. The third study placed samples in an air oven at 105°C.

References

1. Kranbuehl, David. "Cure Monitoring," Encyclopedia of Composites. New York: VCH Publishers, 1990.

2. Johnson, J.F. and R.H. Cole. Journal of the American Chemical Society. 73 4536. 1951.

3. Kranbuehl, D.E., et al. "Dielectric properties of the polymerization of an aromatic polyimide," Polymer. 1986. vol 27 p. 13.

4. Shah, Vishu. Handbook of Plastics Testing Technology. New York: John Wiley & Sons, 1987. p. 27.

5. Brandrup, J. and E.H. Immergut, ed. Polymer Handbook, 3rd edition. New York: John Wiley & Sons, 1989. p. VII/25

6. Allcock, H.R. and F.W. Lampe. Contemporary Polymer Chemistry, 2nd edition. Englewood Cliffs, NJ: Prentice Hall, 1990. p. 529.

7. Allcock, pp. 348-363.

8. Sperling, L.H. Introduction to Physical Polymer Science, 2nd edition. New York: John Wiley & Sons, Inc., 1992. pp. 85-96.

9. Atkins, P.W. Physical Chemistry, 4th edition. New York: W.H. Freeman and Company, 1990. pp. 735-738 & pp. 766-767.

10. Sperling, pp. 146-151.

11. Cussler, E.L. Diffusion: Mass transfer in fluid systems. New York: Cambridge University Press, 1984. p. 132.

12. Cussler, p. 36.

13. Crank, J. and G.S. Park, ed. Diffusion in Polymers. New York: Academic Press, 1968.

14. Inoue, M. "Studies on Crystallization of High Polymers by Differential Thermal Analysis." Journal of Polymer Science. Part A. New York: John Wiley & Sons, Inc., 1963. p. 2700

15. Atkins, p.956.

IV. Experimental Setup

Nylon pipe was flattened to $^1/_4$" thick panels in a heated hydraulic press. These panels were then used to make 2" squares for the sensor plates and dogbones for the mechanical tests.

A DekDyne sensor was used to measure the impedance of the nylon. Teflon coated copper leads were attached to the sensor with an epoxy solder. Sensors were imbedded between two flattened pieces of nylon pipe by heating the system so that the nylon flowed. This technique kept the active side of the sensors in contact with the material and sealed the edges so that water could not come in direct contact with the sensor.

Two sets of sensors were used in this study. Three different pots, 95% water, 95% oil, and crude oil, were used as the aging environments. The 95% water pot consisted of 95% deionized water and 5% ASTM 3 oil. The 95% oil pot was 95% oil and 5% deionized water. The oil was a mixture of ASTM 3 oil and IRM 903 oil. The third pot was pure crude oil from the North Sea. The oil was Petroleum Crude Oil Class 3 UN 1267 309 III received from Amitec LTD. Each of these mixtures was in a tightly sealed paint pot. (Figure 4-1) Each system was kept at 103 $\pm$ 2°C and occasionally charged with CO_2 to keep the system acidic.

The acidity of these pots was determined by using the Standard Test Method

for Acid and Base Number by Color-Indicator Titration, ASTM designation: D 974-92. The pots were all slightly acidic with acid numbers near 2 for the 95% water and 95% oil pots and near zero for the crude oil pot.

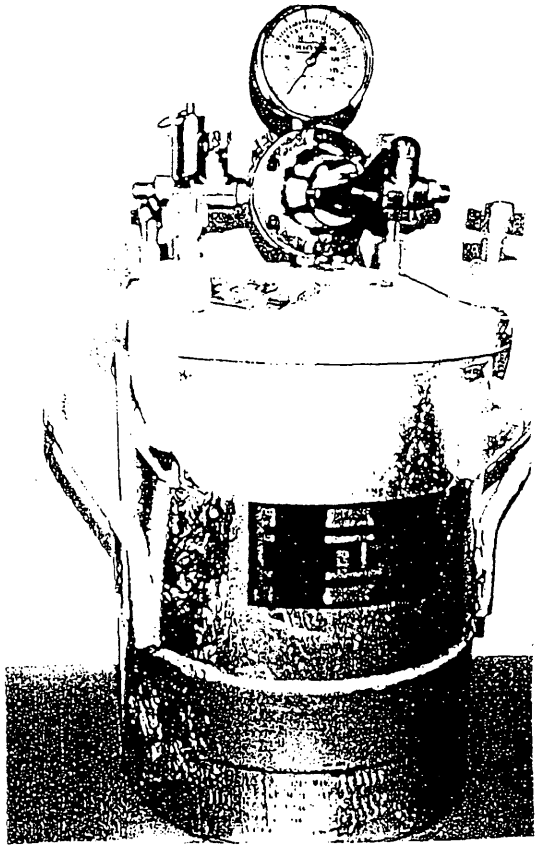

Paint pot containing aging environment

Figure 4-1

The first part of this study used 12 sensors: 1L, 1M, 1R, 2L, 2M, 2R, 3T, 3M, 3B, 4T, 4M, and 4B.

Sensor panels one and two had three sensors imbedded between two $^{1}/_{4}$"

pieces of nylon. These three sensors were on the same level and were designated left, middle, and right.(1L, 1M, 1R, 2L, 2M, and 2R) The nylon panels were bolted between two 3" square, $^1/_8$" thick steel plates to prevent the nylon from flexing and cracking the sensor. The steel plates also limited the absorption of the oil/water solution into the polymer. Silicon caulking material was used to seal the edges between the two plates so that absorption was primarily via the active side. The plate on the active side had an array of small holes. (Figure 4-2) The plate on the nonactive side was solid.

Sensor panels three and four also had three sensors in them. These were arranged in a top, middle, and bottom orientation.(3T, 3M, 3B, 4T, 4M, and 4B) Three $^1/_4$" nylon pieces were used. Therefore, the bottom sensor had the most nylon on its active side. The steel plate on the active side had four slits in it. (Figure 4-2) The nonactive side had a solid steel plate.

Sensor panels one and three were in the 95% oil pot. Sensor panels two and four were in the 95% water pot.

A second set of sensors (C1L, C1R, C2, C3L, C3R, and C4) were in the 95% oil and crude oil pots. Sensor panels C1 and C3 had a right and left sensor and the steel plate on the active side had an array of holes. Sensor panels C2 and C4 had only one sensor imbedded between two round steel plates $2^3/_8$" in diameter. The plates on both the active and nonactive sides had holes. Sensors C1 and C2 were in the 95% oil pot. Sensors C3 and C4 were in the crude oil pot.

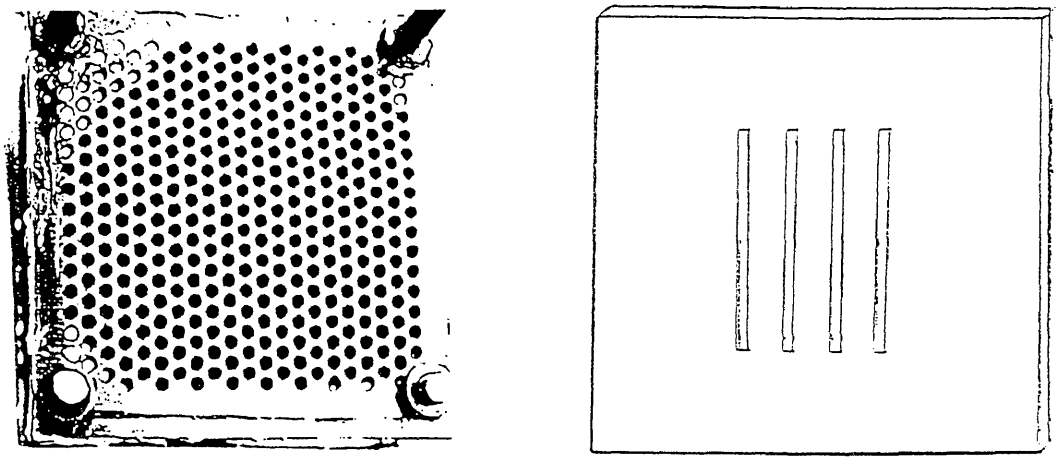

a b

Stainless Steel plates for active side of sensors
a) with array of holes; b) with four slits

Figure 4-2

The sensor leads were inserted through a pressure seal in the lid of the pot for ease in taking measurements during the study. Consequently, this allowed the pot to remain sealed while dielectric measurements were taken. Five minute measurements were taken periodically throughout the aging process at 5 frequencies (0.1, 0.12, 1, 10, and 100 kHz.) These impedance measurements were converted to log ϵ' and log (ϵ"*ω).

The mechanical pieces were placed between two $6^1/_2$" square, $^1/_8$" steel

plates. One of these plates was solid and the other had an array of small holes. Silicon caulk was used to seal the edges between the plates so that diffusion would primarily occur from only one direction. (Figure 4-3)

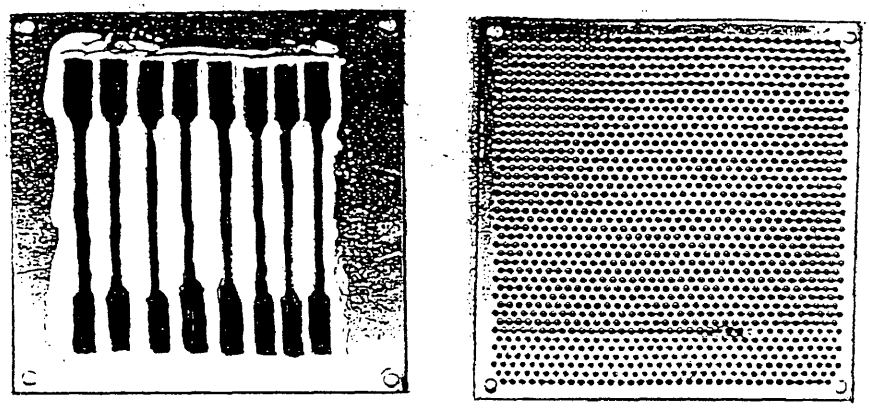

Dogbones with stainless steel plates

Figure 4-3

Mechanical pieces were periodically removed from the baths. In addition to undergoing the tensile tests, the mechanical pieces were used for DSC, viscosity, and hardness testing. Samples for DSC and viscosity testing were also occasionally taken from sensor panels.

The mechanical data for phases one and two was analyzed along with the new data from phase three. Phase one accelerated aging was performed in a 95%

water pot at 130°C and phase two in a 95% water pot at 105°C. The mechanical pieces from both of these phases were also used for viscosity tests.

Balmoral Field Study

For this aspect of the study, four FDEMS sensors were placed on an oil platform in the North Sea. These were mounted on a spool piece with four ports. The spool piece is on the platform at the top of the pipe. These spectator samples are subjected to the same flow of oil as the actual pipe. The average temperature the pipe is exposed to is 70°C. This is an attempt to monitor the system on line.

DekDyne ceramic sensors were imbedded in aged fresh nylon. The aged fresh nylon pipe had been sitting in a warehouse for approximately eight years but had not been exposed to an accelerated aging environment, ie. a heated oil and/or water solution. This pipe was used in the fabrication of these sensors because the pipe on the platform has been in use for about a decade. Using older nylon is believed to better approximate the actual pipe.

The nylon and the sensor are in a circular stainless steel case, or plug. The bottom half is solid and has a cavity for the polymer sample. There are two

different types of lids; one with a large hole in the center with three rings of small holes surrounding the large hole and one with only the three rings of small holes. (Figures 4-5) These sensors were placed in a bomb calorimeter filled with deionized water and pressurized to 25 atm with oxygen to impregnate the nylon with water. Four sensors of this type were installed on a drill platform in the North Sea. Measurements have been taken twice a day (except day 0) over a period of 31 weeks. This aspect of the study is still underway.

Dogbones were also made from the aged fresh nylon. These were aged in the crude oil pot.

Figure 4-5 Circular sensor plug

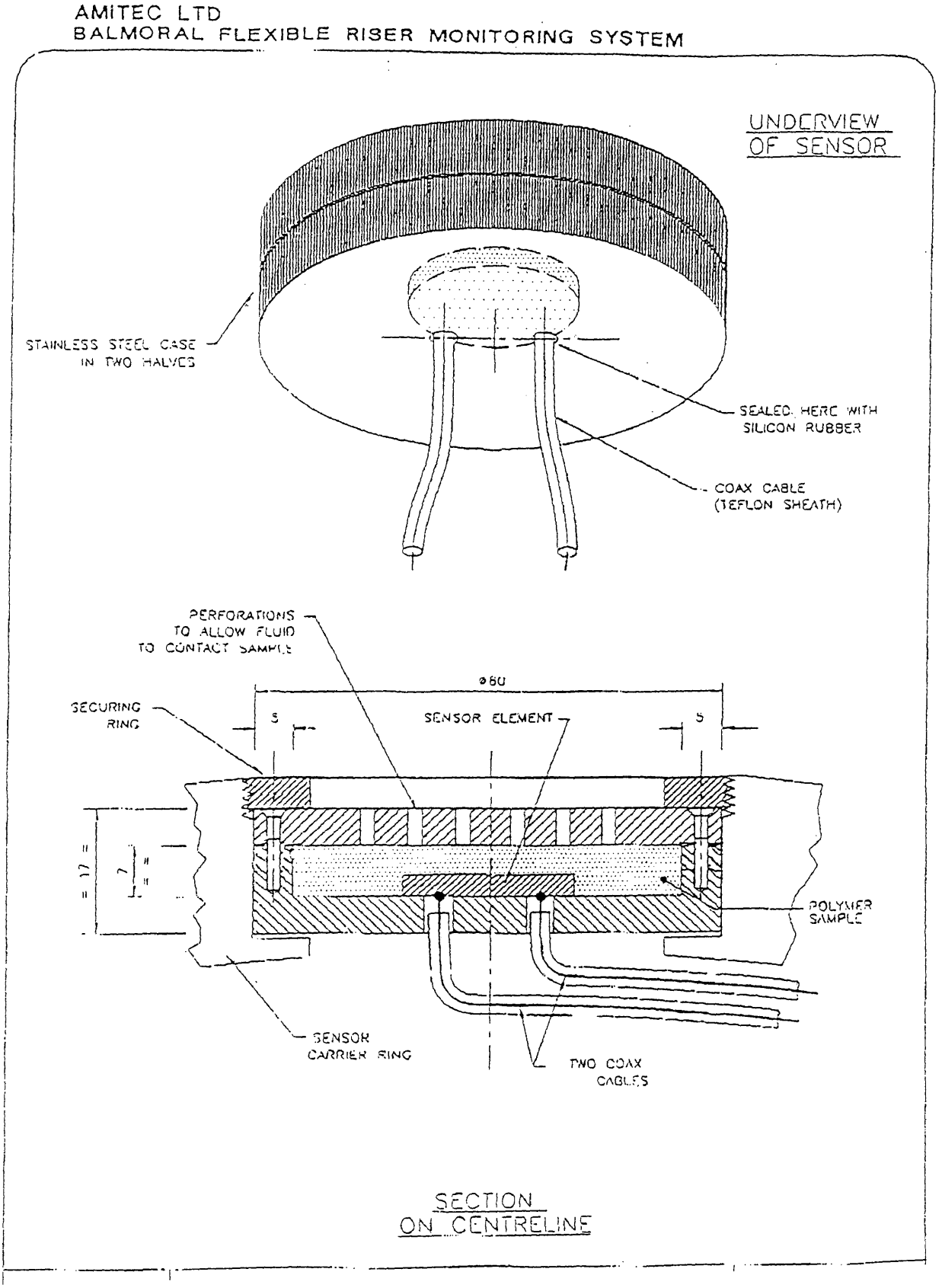

Field Aged Nylon 11

Small samples of nylon-11 pipe that had been aged in oil fields throughout the world were received from the Exxon Corporation. Viscosity samples were taken from the inside and outside of these pieces. The inside would be the side of the pipe exposed to the oil. For all of these samples the inside was darker in color. The samples had the following properties:

Property	A1	A2	D2	E1	E2	control
Service Duration (yrs)	8.8	8.8	5.25	0.83	5.6	0
Max. Temp (°C)	95	88.3	25	91.1	79	n/a
ID Hardness	94.8	88.2	90.6	91.4	89.4	86
OD Hardness	92.4	84.6	85.2	83	88.2	78.6
Extractable (wt%)	7.74	3.91	9.35	11.91	12.45	14.52
Yield Strength (psi)	4500	4645	3461	3933	3744	3562
Elong @ Yield (%)	55	59	83	76	81	100
Break Strength (psi)	4185	4089	3753	3696	4013	3975
Elong @ Break (%)	71	97	252	181	257	330
Modulus (psi)	19130	17953	10765	11624	12138	11033

V. Results and Discussion

Dielectric data was taken on the first set of sensors over a period of 225 days. Panels 3 and 4 were removed after 128 days and 1 and 2 were aged for the entire time. (Figures 5-1 through 5-16) Output for the second set of sensors are shown in figures 5-17 through 5-28. Data from the 95% water pot showed an initial increase in log ϵ' and log (ϵ"*ω) followed by a slow decline. The initial jump is due to the absorption of water into the nylon. The dielectric constant is very sensitive to moisture uptake. Due to water's polarity and fluidity, it has a much higher dielectric constant than the polymer. The presence of water in the nylon raised the measured dielectric properties. The decline in log (ϵ"*ω) following the peak represents a decrease in ionic mobility, due to the increased crystallinity that occurs with hydrolytic degradation.

Sensors C1L, C1R, and C2 (second run) in the 95% oil pot showed a similar decline to the sensors in the 95% water pot. Log ϵ' decreased by approximately a decade over 200 days and log(ϵ"*ω) decreased by approximately half a decade.

Sensors 1L, 1M, 3M, and 3B (first run) in the 95% oil pot showed a peak near day 125 as opposed to a peak near day 25 for sensors aged in the 95% water pot. This shows that there was a gradual infusion of the oil/water mixture to the sensor. This suggests that the nylon developed microcracks or did not remain

properly sealed around the edges due to aging.

The set of sensors in the crude oil showed at all five frequencies a gradual drop in value over 200 days. The dielectric values for the sensors in the crude oil dropped approximately half as much as those in the CO_2 charged, 95% water and 95% oil pots. These plots indicated that the nylon was degrading at a slower rate in the crude oil pot than in the 95% water and 95% oil pots. The rate was approximately half the CO_2 95% water or 95% oil degradation rate.

The mechanical data also demonstrated the degradation of the material. Values for load at break, percent extension at break, load at yield, and percent extension at yield are displayed in tables 5-1 through 5-7. For the 95% water pot samples, both load at break and percent extension at break remained fairly constant and then suddenly dropped off. (Figures 5-29 & 5-30) The curve of the mechanical properties is a good example of the tendency for polymers to fail catastrophically.

The mechanical pieces aged in the 95% oil and crude oil pots followed the same pattern. The 95% oil pot samples showed failure at about the same time that failure was seen in the 95% water, 103°C samples. However, a longer period of aging was required before failure of the pieces from the crude oil. (Figures 5-31 through 5-34) This supports enhanced degradation by hydrolysis.

The mechanical data from phase 1, which was aged at 130°C, dropped rapidly to about 65% of its original load after 20 days. For the 103°C data of

phases 2 and 3, the load remained nearly the same through day 50. Percent extension displayed the same pattern. For phase 1 (130°C), percent extension dropped below 100 by day 20 while for phases 2 and 3 (103°C) percent extension remained above 100 until after day 55. This indicates that the rate of degradation increases with increased temperature. The rate of degradation at 130°C is approximately three times the rate at 103°C.

The molecular weight data obtained through viscosity measurements illustrated a decrease in molecular weight over time. During degradation, the polymer molecule is cleaved giving smaller polymer molecules. See tables 5-8 through 5-16 and figures 5-37 through 5-43.

Molecular weight decreased more rapidly for phase 1 (130°C) than for phases 2 and 3 (103°C). Molecular weight fell to 20,000 g/mol after only 8 days at 130°C while it took approximately 55 days to reach this value at 105°C. Mechanical failure, considered as the point where the polymer has fallen to 30% of its original strength, occured below a molecular weight of 15,000 g/mol. Amitec LTD defines failure of the nylon as the point when it has fallen below 45% of the original percent extension at break. This also occurs below a molecular weight of 15,000 g/mol.

The enthalpy data from the DSC showed an overall increase; however, the variation in the data is a significant percent of the overall changes. The overall rise in enthalpy indicates an increase in crystallinity of the nylon. The average

crystallinity of the fresh nylon is 11%. The majority of the values for aged nylon are near twice this value. There was also a small increase in melting temperature. (Tables 5-17 through 5-22 and Figures 5-44 through 5-46)

The hardness data is in tables 5-23 through 5-26 and figure 5-47. There is an overall increase in hardness with the age of the sample.

Light scattering was done with samples of fresh nylon. The molecular weights determined are shown in table 5-27. They are comparable to the value determined with viscosity measurements. The average value determined by light scattering was 52,300 g/mol. The molecular weight determined from viscosity measurements was 49,600 g/mol.

A fresh sample and a sample aged 92 days in the 95% water pot were tested on the FTIR. There was a dramatic decrease in the peak around 1500 from the fresh to the aged sample. This indicates that there are less amide groups in the aged sample than in the fresh sample. (Figures 5-48 and 5-49)

Using the data from the weight loss study, percent weight remaining was plotted versus day for all of the samples.(Figures 5-50 through 5-63) For the fresh samples in the 80°C and 105°C ovens, the data was normalized with the following relationship:

$$\frac{wt(t) - wt(final)}{wt(initial) - wt(final)}$$

This was plotted versus the square root of time. These yielded fairly linear plots.

(Figures 5-64 and 5-65) The three samples from the 95% water and 95% oil pots were also plotted in this fashion. (Figures 5-66 through 5-68) The plots were linear, implying Fickian diffusion, until about day 64 (day^1/2 = 8). After that point the curves started to level off. This indicates that diffusion is Fickian until the sample is saturated. After saturation, diffusion is non-Fickian.

Correlations

For dielectric measurements to be most useful for life monitoring, log ϵ' and log (ϵ"*ω) must be correlated to molecular weight and mechanical properties. Correlations were done using the data from the 95% water pot. This will enable a sample's mechanical properties to be monitored in situ.

First, the raw dielectric data, log ϵ' and log (ϵ"*ω), for sensors 2L, 2M, and 4M was converted to the non-logarithmic values. These values were then normalized by dividing each value by the value from the peak day. The peak days were 22, 27, and 27, respectively. The normalized values were plotted together on the same plot. An average curve was drawn through these points. (Figures 5-69 & 5-70)

The plot of molecular weight versus day for dielectric sensor panels and mechanical pieces was used to determine the respective dielectric and mechanical days corresponding to chosen molecular weights. (Figure 5-71) Using the dielectric days, normalized ϵ' and $\epsilon''*\omega$ were found from figures 5-69 and 5-70. Using the mechanical days, load at break and percent extension at break were determined using the smooth curves for that data.(Figures 5-72 & 5-73) This analysis resulted in the following correlation plots:

- normalized ϵ' vs. molecular weight (Figure 5-74)
- normalized ϵ' vs. load at break (Figure 5-75)
- normalized ϵ' vs. % extension at break (Figure 5-76)
- normalized $\epsilon''*\omega$ vs. molecular weight (Figure 5-77)
- normalized $\epsilon''*\omega$ vs. load at break (Figure 5-78)
- normalized $\epsilon''*\omega$ vs. % extension at break (Figure 5-79)

These correlation plots enable one to monitor a sample using FDEMS and predict other macroscopic properties. This is done with sensor 2L as an illustration. The non-log values must first be normalized to the peak day. (Figures 5-80 & 5-81) Then days and dielectric values are picked from these two plots. The dielectric values are used to determine molecular weight, load at break, and percent extension at break from the correlation plots. These values are plotted against the dielectric days. (Figures 5-82 through 5-87)

Balmoral Field Data

Data for sensors 1, 3, and 4 was analyzed. Extremely noisy values that differed by more than 0.5 from the preceding value were regarded as spurious and discarded. This only needed to be done for sensors 3 and 4 and resulted in discarding approximately 15% of the original data. Every seven measurements (starting with measurement 1) were averaged. This gave one value for every 0.5 weeks. The values were then normalized by dividing by the value for week five. Week five was used because it was a relatively high point for all three sensors. The normalized values for log ϵ' and log (ϵ"*ω) were then plotted versus week for all three sensors at 1 kHz. 1 kHz was used because it is the middle of the frequency range measured. Plots were also created using the average of these sensors. (Figures 5-85 through 5-92) No degradation was evident in these samples after 31 weeks. The values for normalized log ϵ' and log (ϵ"*ω) have remained level throughout the 31 week aging process in the field. This is to be expected due to the low temperature (70°C) of the oil in the North Sea.

Table 5-1

Mechanical Test Data: Unaged Nylon

load at break (psi)	% extension at break (% of 2")	load at yield (psi)	% extension at yield (% of 2")
@ 7566	404		
@ 7692	435		
5281	317	211	52
5724	322	224	57
* ----	----	238	78
6165	322	227	58
6450	365	227	63
7139	377	239	64
7063	342	247	61
5044	177	206	35
7746	416	257	75
6865	277	269	46
5114	198	210	34
6508	339	234	53
7475	413	251	76
6823	385	236	66

* sample never broke

@ yield data was not recorded for these samples

Table 5-2

Mechanical Test Data: 95% Water Pot, 103°C

day	load at break (psi)	% extension at break (% of 2")	load at yield (psi)	% extension at yield (% of 2")
14	6782	403	255	62
14	5865	299	232	47
30	6779	370	268	54
30	6069	326	262	46
40	5784	292	240	46
40	5011	195	220	35
51	6052	381	250	55
51	6631	348	262	55
55	4389	24	144	8
55	5047	127	237	26
67	1421	3	31	1
67	1786	4	50	2
92	849	2	29	1
92	213	11	11	5

Table 5-3

Mechanical Test Data: 95% Oil Pot, 103°C

day	load at break (psi)	% extension at break (% of 2")	load at yield (psi)	% extension at yield (% of 2")
14	6487	316	253	50
14	6426	326	255	50
30	6049	287	253	43
30	5538	169	236	30
45	6169	321	259	47
45	5898	286	257	44
60	5387	94	253	22
60	5438	106	260	22
75	6134	99	282	24
90	5637	76	270	20
90	6203	63	260	15
92	2001	6	61	3
92	2132	6	67	3
92	6429	52	233	13

Table 5-4

Mechanical Test Data: Crude Oil Pot, 103°C

day	load at break (psi)	% extension at break (% of 2")	load at yield (psi)	% extension at yield (% of 2")
32	6875	337	279	52
32	6690	285	272	45
39	7067	314	298	49
39	7266	312	304	49
55	6364	143	297	28
55	6271	258	308	34
75	6508	180	310	31
90	6899	352	341	41
126	5133	87	242	20
163	2745	7	90	3

Table 5-5

Mechanical Test Data: Aged Fresh in Crude Oil Pot, 103°C

day	load at break (psi)	% extension at break (% of 2")	load at yield (psi)	% extension at yield (% of 2")
0	4315	124	179	27
0	6535	322	236	53
0	4072	108	163	23
31	5510	149	243	30
31	4950	70	184	20
70	6432	251	314	38
143	5325	112	272	24

Table 5-6

Mechanical Test Data: Phase 2, 103°C

day	load at break (psi)	% extension at break (% of 2")	load at yield (psi)	% extension at yield (% of 2")
4	5935	388	218	63
4	5922	358	220	61
4	6189	375	226	63
8	6463	391	236	64
8	6916	440	230	74
8	6566	403	233	69
15	6319	344	239	55
15	6710	377	259	59
15	6556	374	240	57
25	6007	314	236	48
25	5997	316	243	49
55	4967	245	223	38
55	5244	299	238	42
55	4778	180	210	32
60	2735	14		6
60	4660	73		19
@118	928	3	27	1

@ two 118 day samples broke while tightening clamps

Table 5-7

Mechanical Test Data: Phase 1, 130°C

day	load at break (psi)	% extension at break (% of 2")	load at yield (psi)	% extension at yield (% of 2")
@4	5942	373		
4	6087	363	232	58
4	6076	422	216	69
8	4876	163	253	27
8	5676	321	260	44
*8		352	225	43
12	4711	178	264	28
12	4865	76	251	19
12	4788	306	307	40
12	5551	235	296	31
20	4243	168	216	29
20	4456	158	206	30
20	4296	153	224	28
*30		83	154	20
30	4221	89	198	22
30	4596	126	218	26
41	4810	118	223	24
41	4307	91	220	21
41	3978	85	217	20
61	2735	14	86	6
61	4660	73	216	19
61	4484	65	233	19

* crosshead did not stop after break

Table 5-8

Viscosity Data: Solvent and fresh samples

sample	conc (g/ml)	time (min:sec)
m-cresol		27:45 27:41
fresh nylon	0.003298	50:47 51:02
fresh nylon	0.000828	33:06 33:34

M_v (fresh nylon) = 49600 g/mol

Table 5-9

Viscosity Data: Mechanical pieces from 95% Water Pot, 103°C

day	conc (g/ml)	time(min:sec)	M_v (g/mol)
14	0.003208	47:45 48:00	42400
30	0.003212	43:32 42:48	28900
40	0.003200	42:54 43:22	28900
51	0.003198	40:00 39:35	20300
55	0.003266	38:21 38:34	16500
67	0.003190	36:27 38:11	14400
92	0.003286	34:45 35:39	9340

Table 5-10

Viscosity Data: Mechanical Pieces from 95% Oil Pot, 103°C

day	conc (g/ml)	time(min:sec)	M_v (g/mol)
14	0.003198	48:06 47:46	42800
30	0.003206	43:24 43:43	30000
45	0.003196	43:04 43:07	28900
60	0.003198	37:32 37:23	14700
75	0.003270	36:57 37:56	14100
90	0.003192	37:33 36:58	14300
92	0.003306	36:48 37:39	13400

Table 5-11

Viscosity Data: Mechanical pieces from Crude Oil Pot, 103°C

day	conc (g/ml)	time(min:sec)	M_v (g/mol)
32	0.003192	43:12 43:41	29900
39	0.003198	43:32 42:56	29300
55	0.003204	45:20 44:57	34500
75	0.003174	41:40 41:53	25600
90	0.003204	41:31 41:28	24500
126	0.003202	38:45 38:54	17900
163	0.003200	39:21 40:15	20300

Table 5-12

Viscosity Data: Aged Fresh Mechanical pieces in Crude Oil Pot, 103°C

day	conc (g/ml)	time(min:sec)	M_v (g/mol)
0	0.003216	42:35 45:03	30600
31	0.003208	49:24 49:25	47000
70	0.003182	44:54 44:53	34100
143	0.003200	39:38 39:16	19400

Table 5-13

Viscosity Data: Sensors

sample	conc (g/ml)	time(min:sec)	M_v (g/mol)
95% water pot day 12 front	0.003202	47:31 47:08	40900
95% water pot day 36 front	0.003222	42:24 42:29	26800
95% water pot day 36 back	0.003254	42:51 42:56	27600
95% water pot day 128 front	0.003320	36:17 36:03	11100
95% water pot day 128 back	0.003262	37:08 38:27	15000
95% water pot day 224	0.003290	31:14 30:50	2900
95% oil pot day 12 front	0.003260	49:49 49:21	46700
95% oil pot day 36 front	0.003216	48:00 47:25	41700
95% oil pot day 36 back	0.003294	44:17 43:50	30100
95% oil pot day 42 edge	0.003254	41:56 41:42	24800
95% oil pot day 128 front	0.003234	36:01 37:31	12900
95% oil pot day 128 back	0.003260	37:24 38:23	15200
95% oil pot day 224	0.003216	34:19 34:39	8300
100°C oven day 133	0.003300	48:45 48:50	43300

95% oil pot day 151 Sensor C1	0.003196	35:27 35:52	10800
95% oil pot day 145 front	0.003200	37:10 37:13	14100
95% oil pot day 145 back	0.003202	36:23 36:41	12600

Table 5-14

Viscosity Data: Samples from phase 2, 103°C

sample	conc (g/ml)	time(min:sec)	M_v (g/mol)
55 days mechanical	0.003226	41:24 41:58	24800
118 days mechanical	0.003274	35:53 36:10	11100
sensor day 159 front	0.003344	40:32 40:41	20800
sensor 3 day 159 back	0.003210	34:54 34:56	9200

Table 5-15

Viscosity Data: Mechanical Samples from phase 1, 130°C

day	conc (g/ml)	time (min:sec)	M_v (g/mol)
4	0.003210	46:59 46:51	39500
8	0.003204	39:33 40:14	20500
20	0.003210	38:03 39:00	17100
30	0.003208	37:18 37:19	14300
41	0.003196	37:52 38:03	15900
61	0.003210	36:47 38:17	14800

Table 5-16

Viscosity Data: Field Aged Nylon

sample	conc (g/ml)	time (min:sec)	M_v (g/mol)
control unaged	0.003236	47:55 48:02	42100
A1 - inside	0.003244	42:08 41:52	25400
A1 - outside	0.003236	44:11 44:25	31600
A2 - inside	0.003092	36:25 36:51	13600
A2 - outside	0.003276	42:23 41:34	24900
D2 - inside	0.003250	46:22 46:42	37700
D2 - outside	0.003172	47:50 48:00	43200
E1 - inside	0.003240	41:46 40:47	23500
E1 - outside	0.003176	44:18 43:57	32000
E2 - inside	0.003176	40:05 40:01	21100
E2 - outside	0.003220	45:37 45:19	35100

Table 5-17

DSC Data: Unaged Nylon

ΔH (J/g)	T_m (°C)	% crystallinity
36.196	180.961	16.0
23.321	180.728	10.3
15.966	183.219	7.1

Table 5-18

DSC Data: Mechanical pieces from 95% water pot, 103°C

day	ΔH (J/g)	T_m (°C)	%crystallinity
14	52.800	183.099	23.4
14	58.195	185.369	25.8
30	48.524	189.593	21.5
30	52.748	184.660	23.3
40	55.008	182.239	24.3
40	56.953	184.375	25.2
51	57.013	184.948	25.2
51	59.512	186.554	26.3
55	54.815	188.493	24.3
55	49.379	186.699	21.8
67	53.003	187.756	23.4
67	52.148	186.466	23.1
92	54.754	187.060	24.2
92	57.225	186.991	25.3

Table 5-19

DSC Data: Mechanical pieces from 95% oil pot, 103°C

day	ΔH (J/g)	T_m (°C)	%crystallinity
14	57.193	184.711	25.3
14	50.408	183.827	22.3
30	47.596	188.926	21.1
30	54.868	189.173	24.3
45	57.463	184.688	25.4
45	58.928	185.062	26.1
60	61.184	185.369	27.1
60	61.481	185.667	27.2
75	51.758	186.194	22.9
90	50.464	187.662	22.3
92	54.233	188.729	24.0
92	55.140	187.750	24.4

Table 5-20

DSC Data: Mechanical pieces from crude oil pot, 103°C

day	ΔH (J/g)	T_m (°C)	%crystallinity
32	54.737	184.038	24.2
32	50.315	185.850	22.3
39	54.613	185.798	24.2
39	53.171	185.435	23.5
55	54.452	185.692	24.1
55	51.898	186.598	23.0
75	59.951	186.501	26.5
90	42.680	185.795	18.9
163	48.888	186.494	21.6

Table 5-21

DSC Data: Aged fresh mechanical pieces in crude oil pot, 103°C

day	ΔH(J/g)	T_m (°C)	%crystallinity
0	52.017	181.683	23.0
0	38.800	181.131	17.2
31	47.123	184.760	20.9
31	31.509	183.889	13.9
70	52.946	185.426	23.4
143	49.623	187.200	22.0

Table 5-22

DSC Data: Sensors

sample	ΔH(J/g)	T_m (°C)	%crystallinity
95% water pot day 128 - front	47.837	185.104	21.2
95% water pot day 128 - edge	41.091	184.601	18.2
95% water pot day 224 - front	41.803	184.382	18.5
95% water pot day 224 - back	45.924	184.859	20.3
95% oil pot day 128 - front	56.664	186.527	25.1
95% oil pot day 128 - edge	51.864	186.092	22.9
95% oil pot day 224 - middle	58.269	182.088	25.8

Table 5-23

Hardness Tests: Fresh Samples

sample	1st	2nd	3rd	4th	5th	average
panel	30	29	19	30	25	27
sensor	21	13	18	24	21	19
dogbone	28	25	29	28	23	27
panel	19	27	28	28	20	24

total average for fresh samples: 24

Table 5-24

Hardness Tests: Mechanical pieces 95% water pot, 103°C

day	1st reading	2nd reading	3rd reading	average
14	22	28	28	26
30	37	33	33	34
40	41	41	38	40
51	34	34	32	33
55	43	43	39	42
67	48	49	44	47
92	59	53	58	57
153	56	54	52	54

Table 5-25

Hardness Tests: Mechanical pieces 95% oil pot, 103°C

day	1st reading	2nd reading	3rd reading	average
14	38	40	36	41
30	45	42	44	44
45	43	42	41	42
60	43	43	45	44
75	51	48	48	49
90	49	50	48	49
92	57	56	58	57
153	57	55	57	56

Table 5-26

Hardness Tests: Mechanical pieces crude oil pot, 103°C

day	1st reading	2nd reading	3rd reading	average
31	42	42	43	42
32	40	38	37	38
39	44	40	41	42
55	48	44	46	46
70	50	48	46	48
75	44	42	45	44
90	47	48	47	47

Table 5-27

Light scattering: Fresh Rilsan

M_w (g/mol)
(4.76 +/- 10.0)e4
(5.32 +/-3.0)e4
(5.62 +/-3.0)e4

Figure 5-1

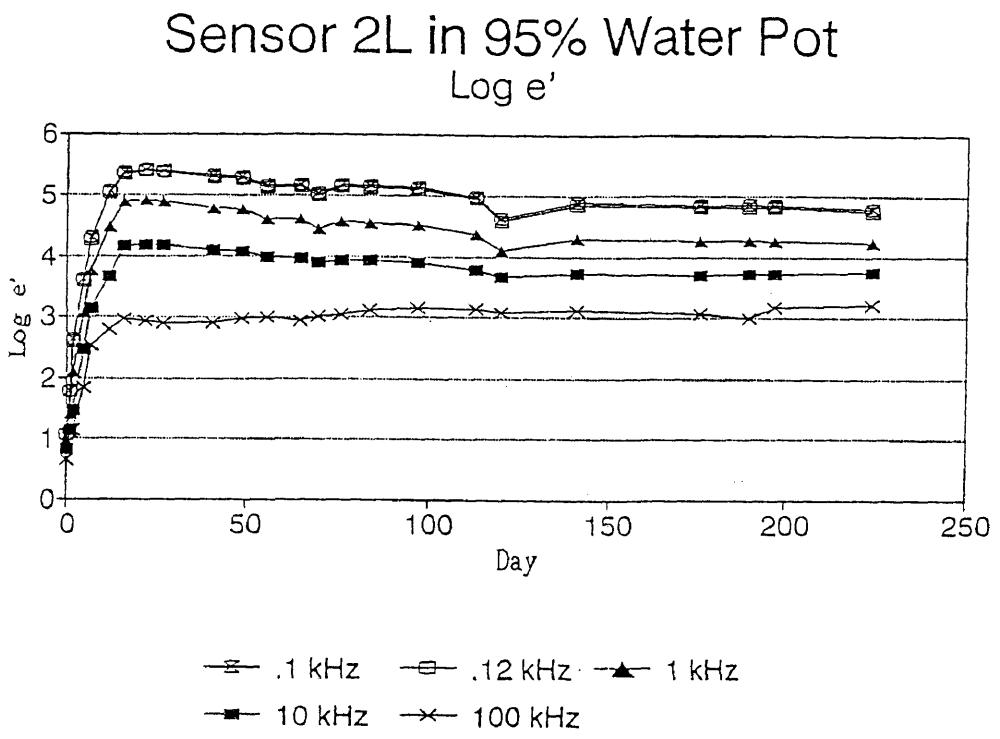

Figure 5-2

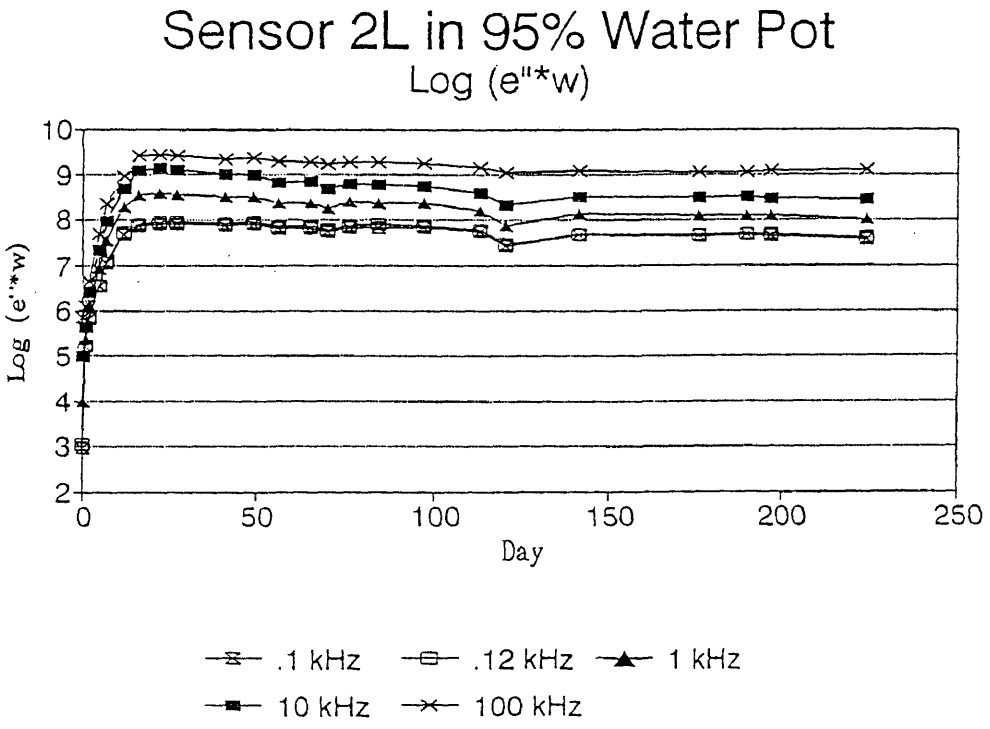

Figure 5-3

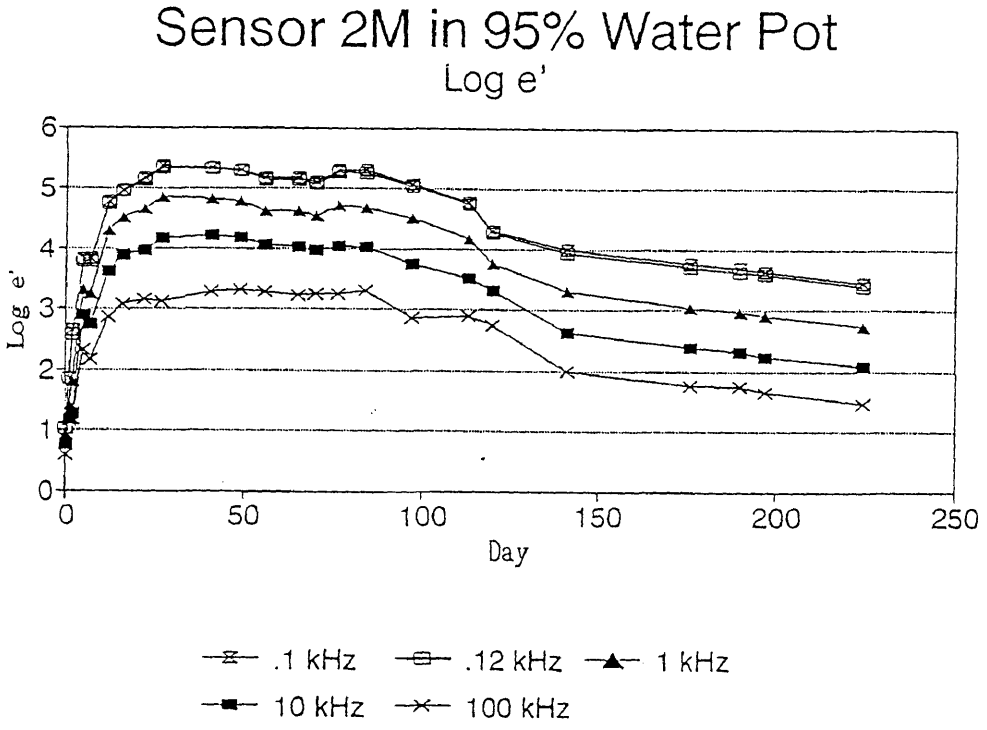

Figure 5-4

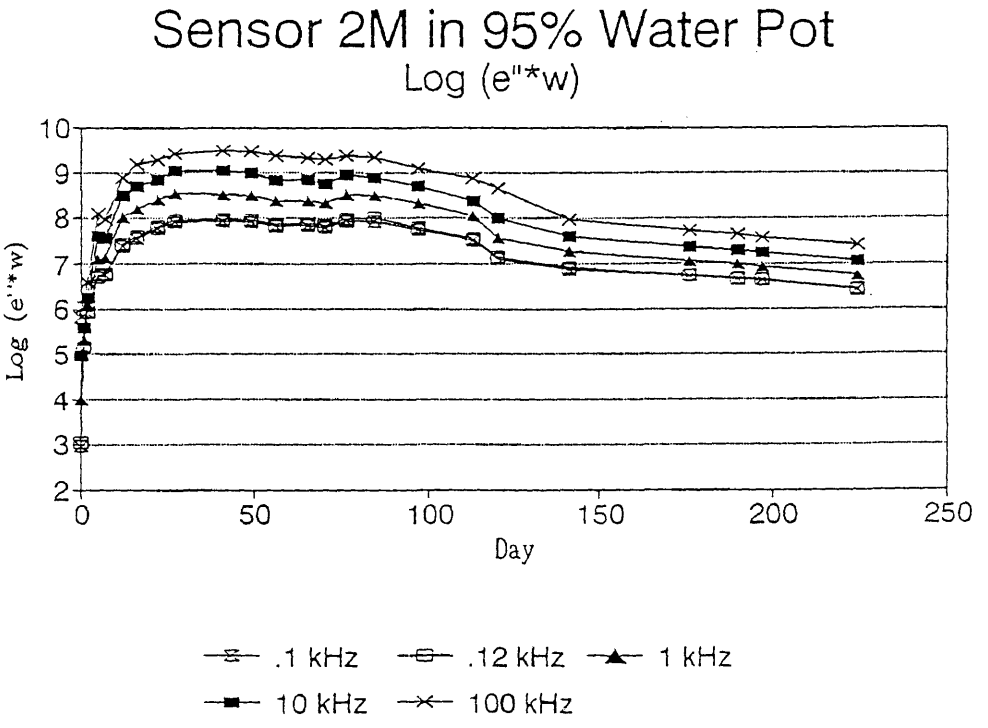

Figure 5-5

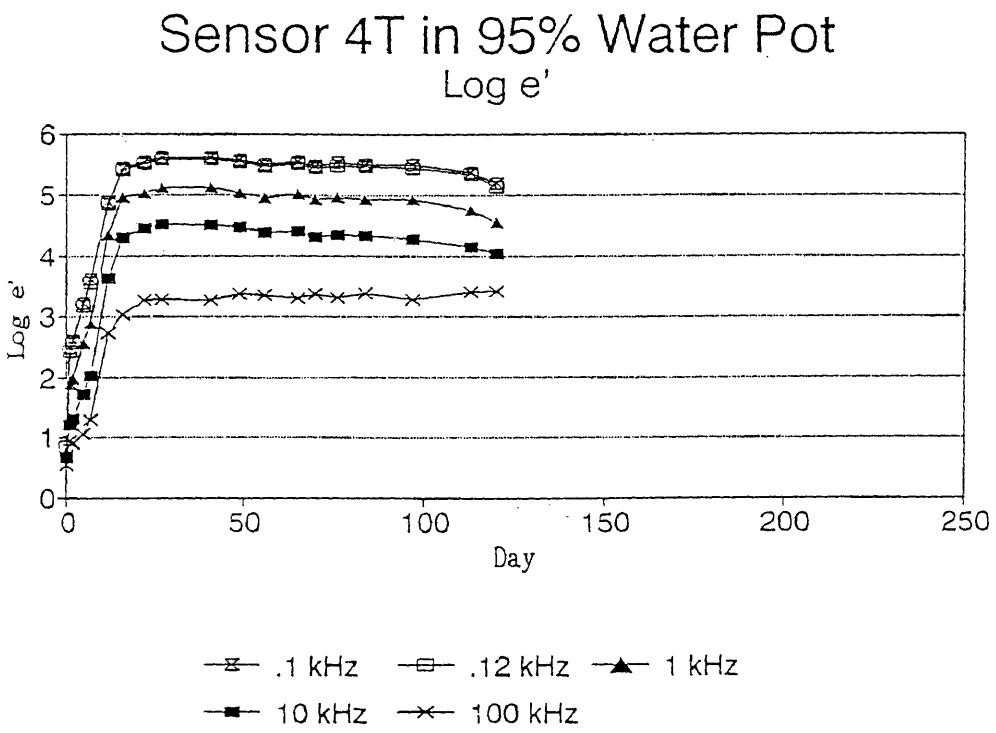

Figure 5-6

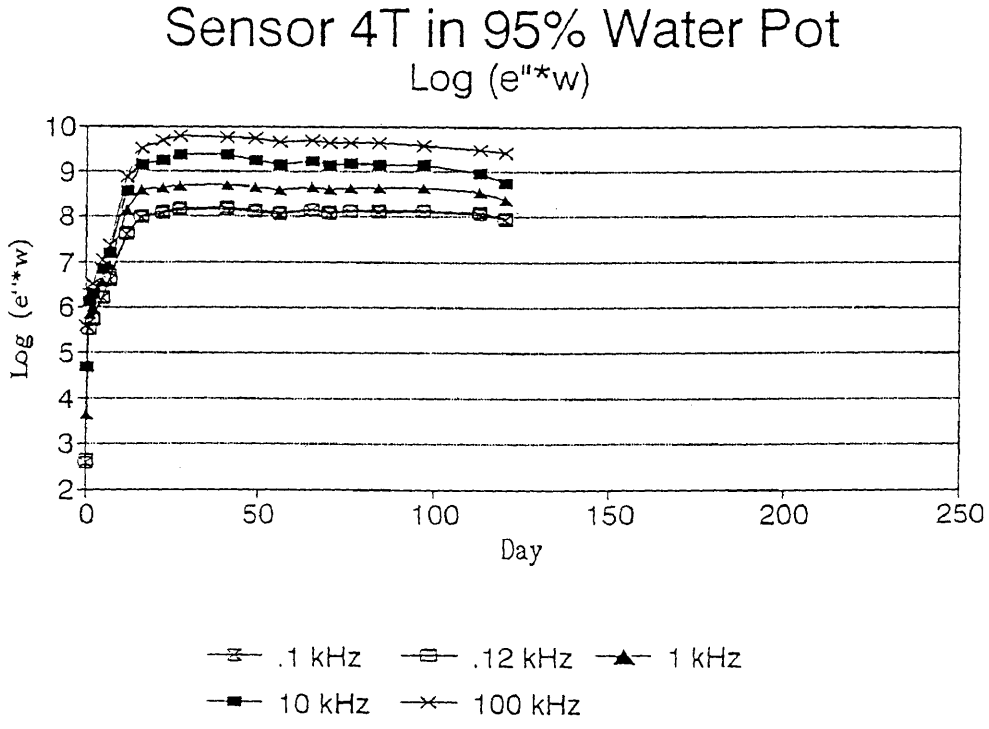

Figure 5-7

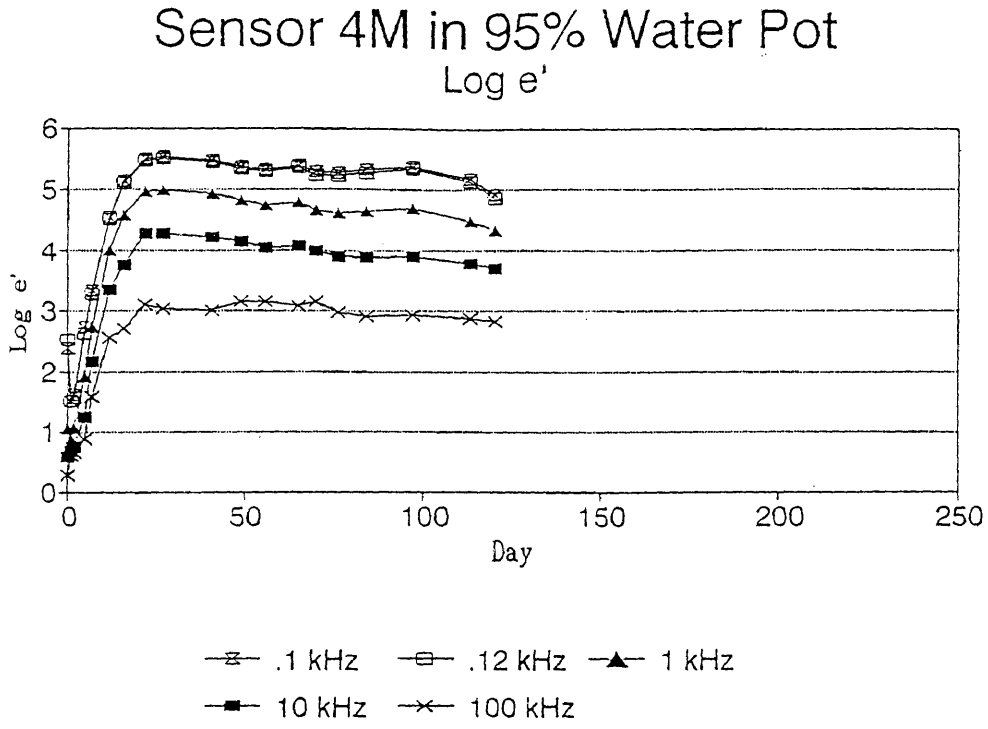

Figure 5-8

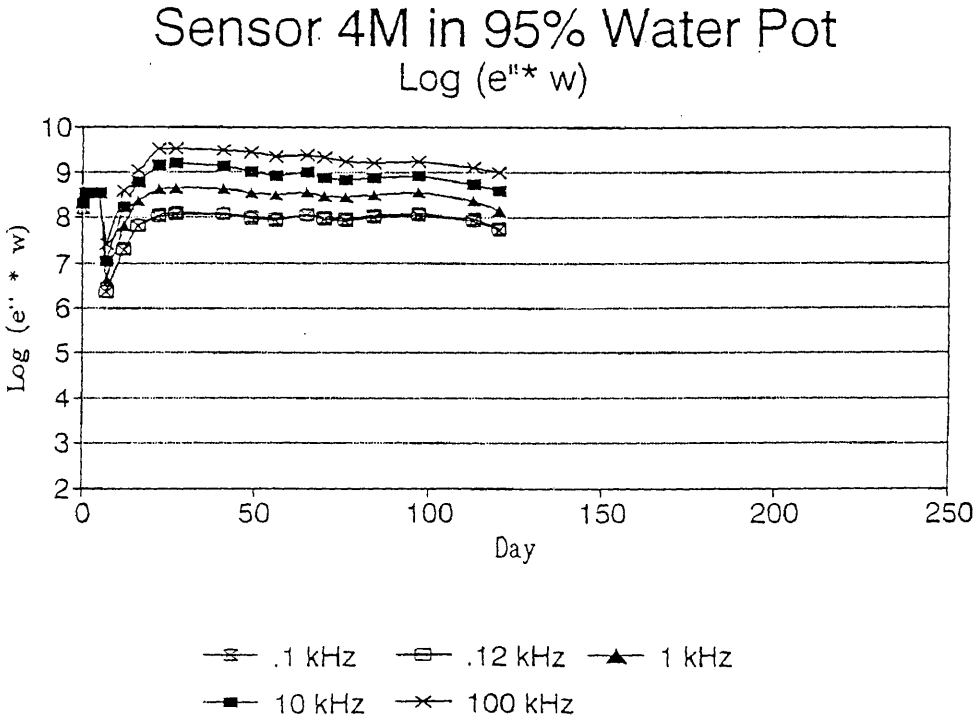

Figure 5-9

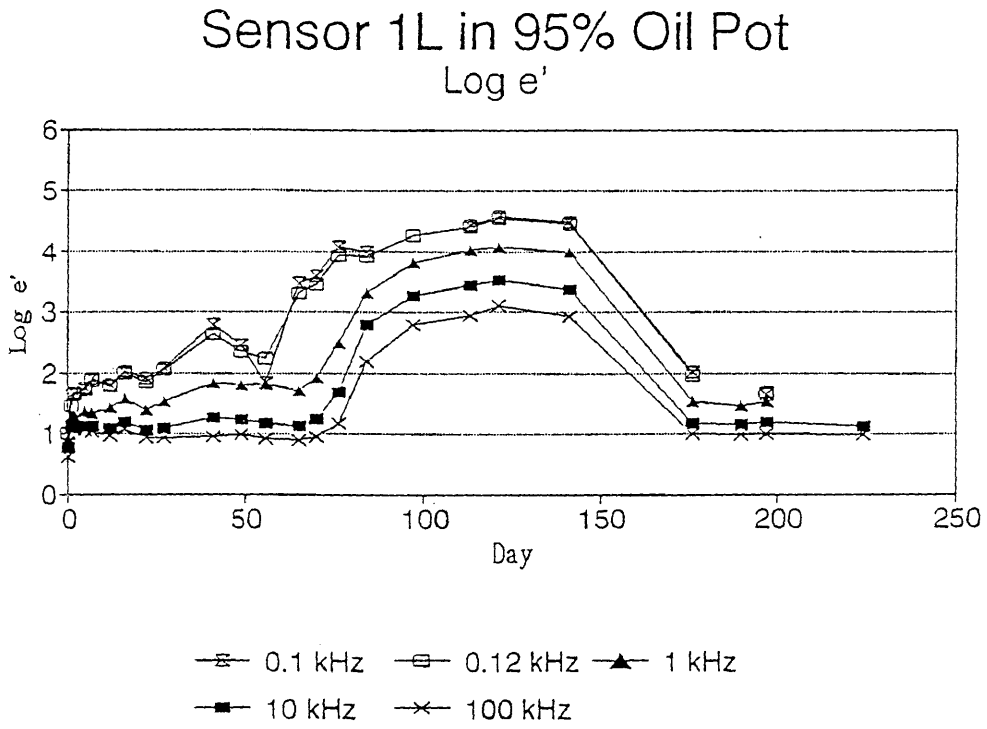

Figure 5-10

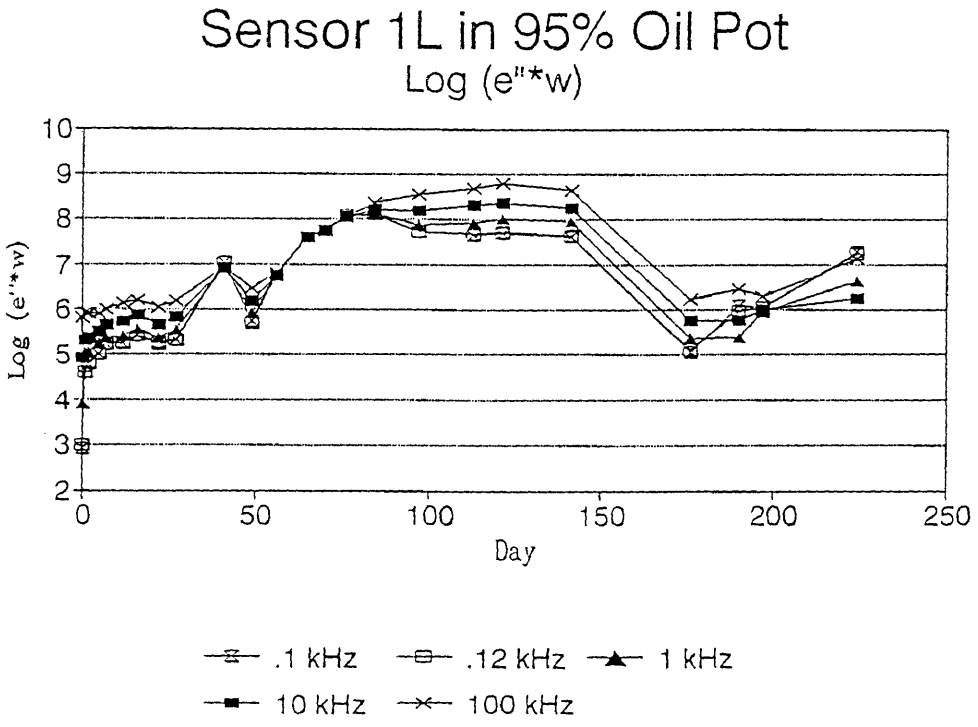

Figure 5-11

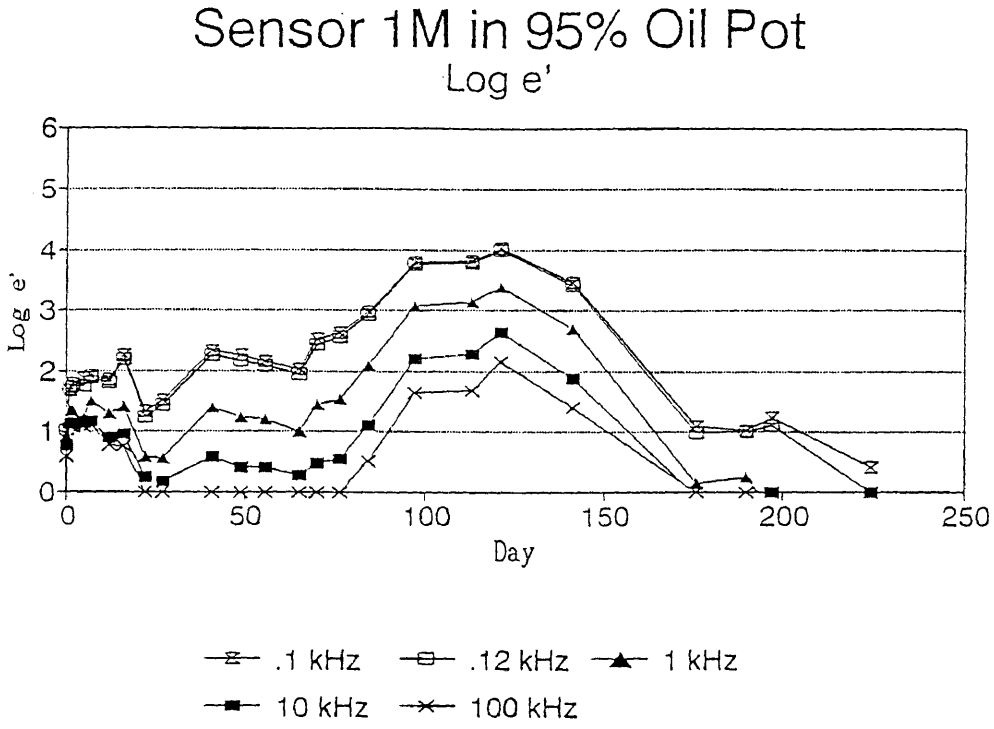

Figure 5-12

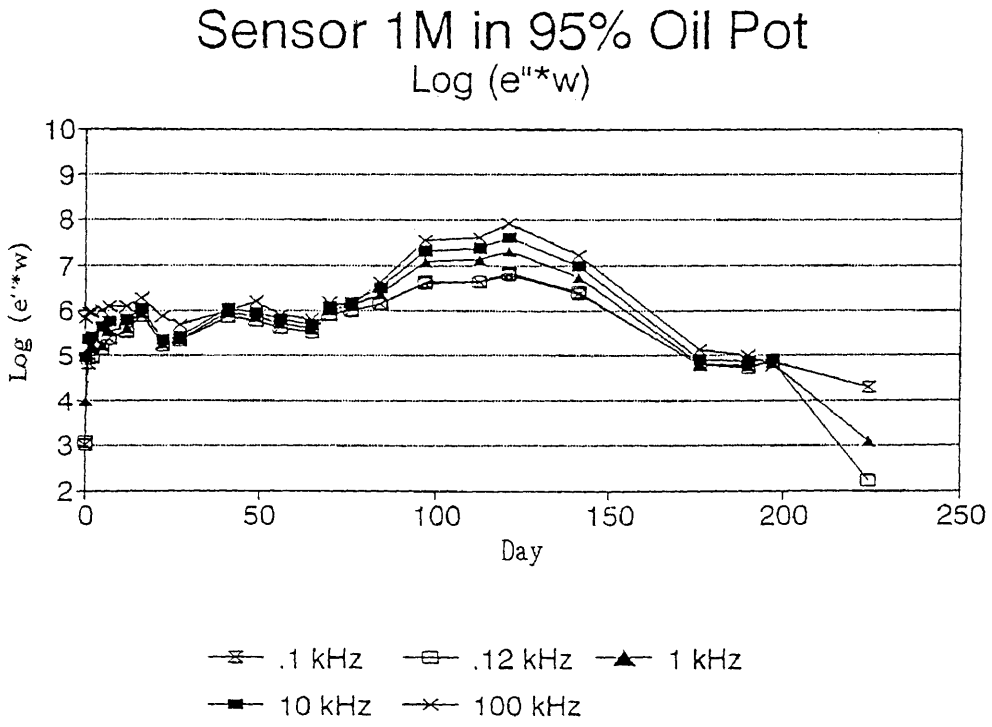

Figure 5-13

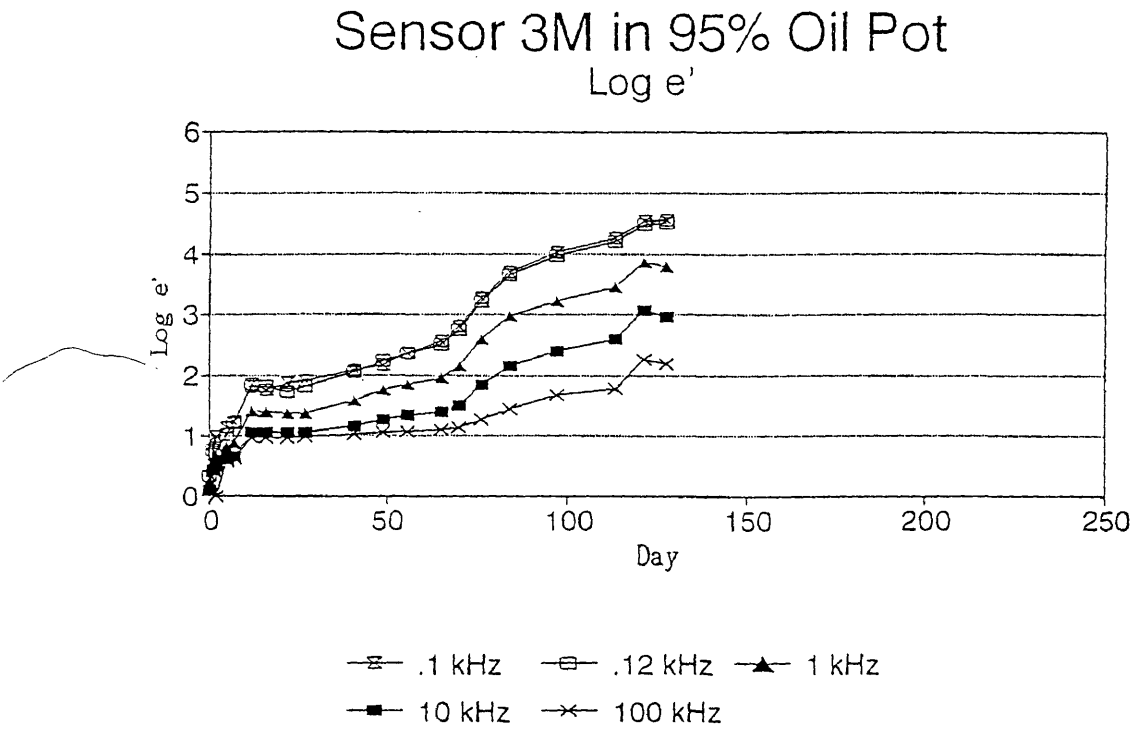

Figure 5-14

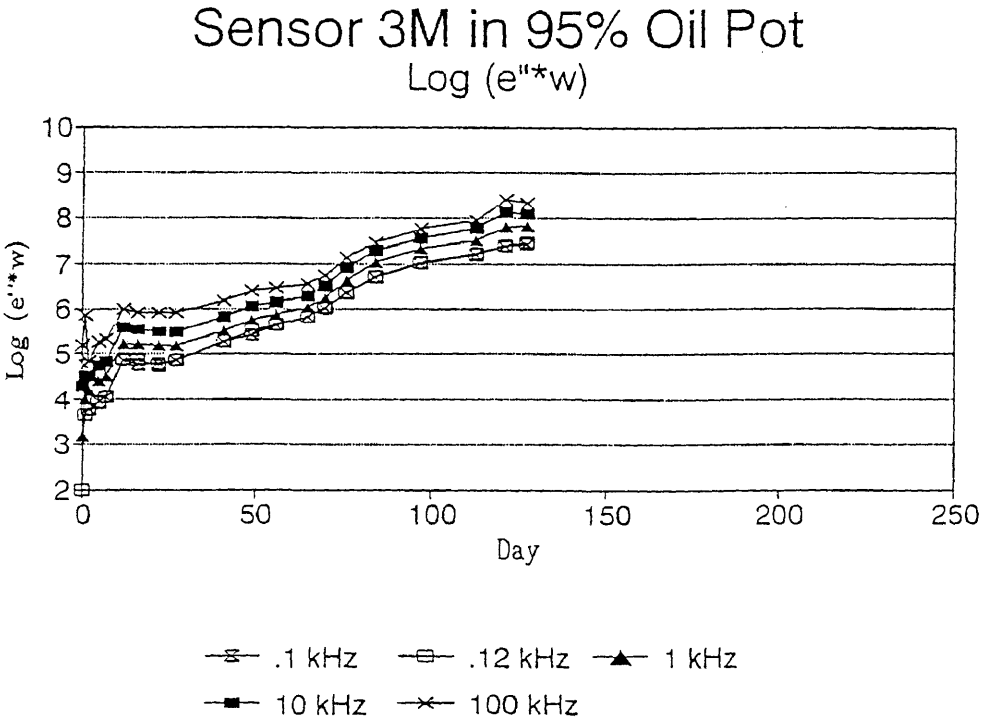

Figure 5-15

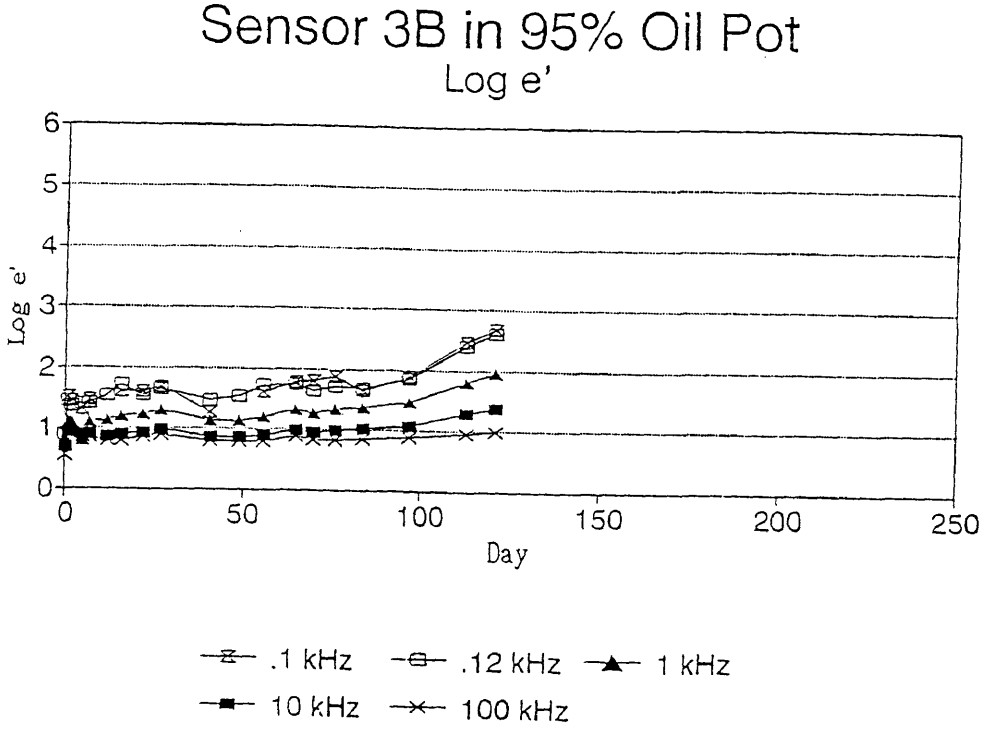

Figure 5-16

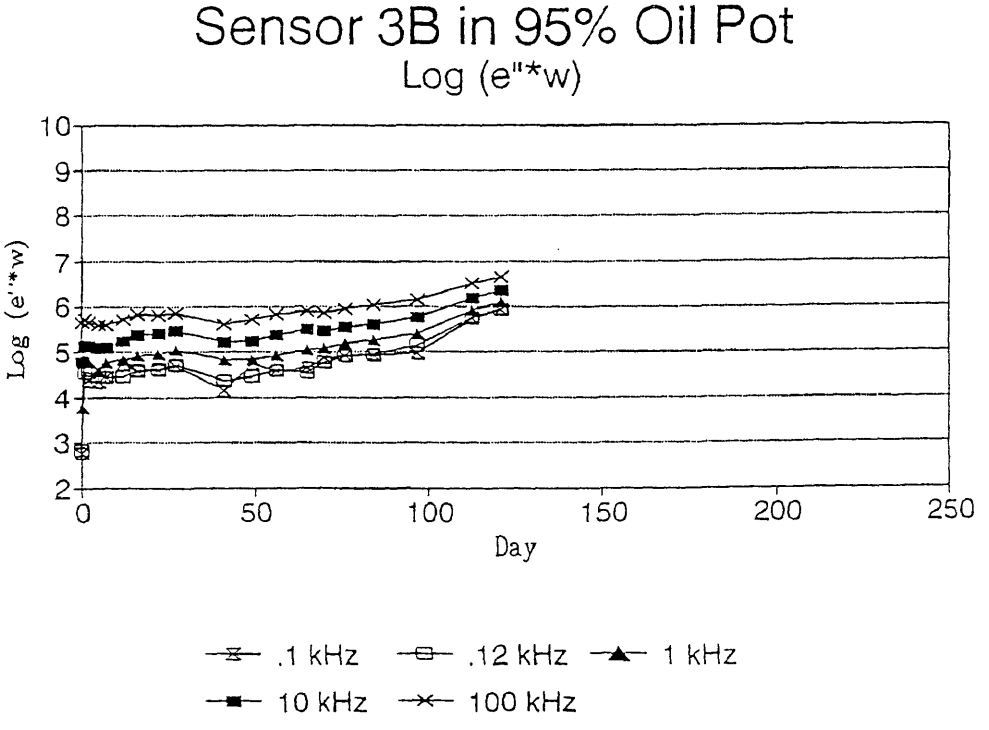

Figure 5-17

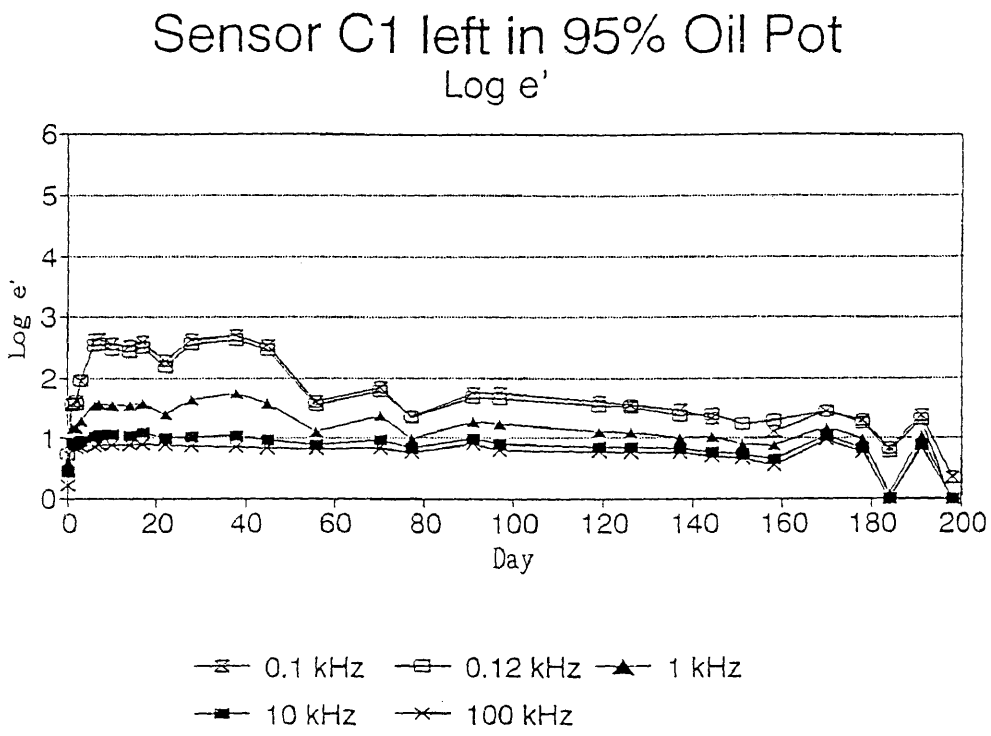

Figure 5-18

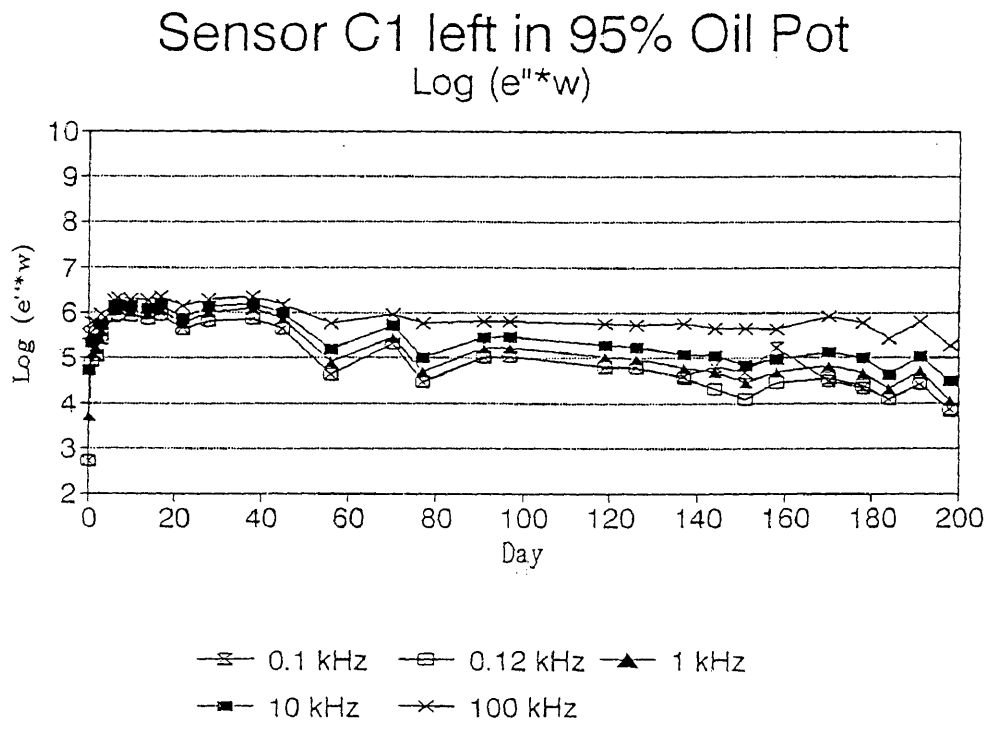

Figure 5-19

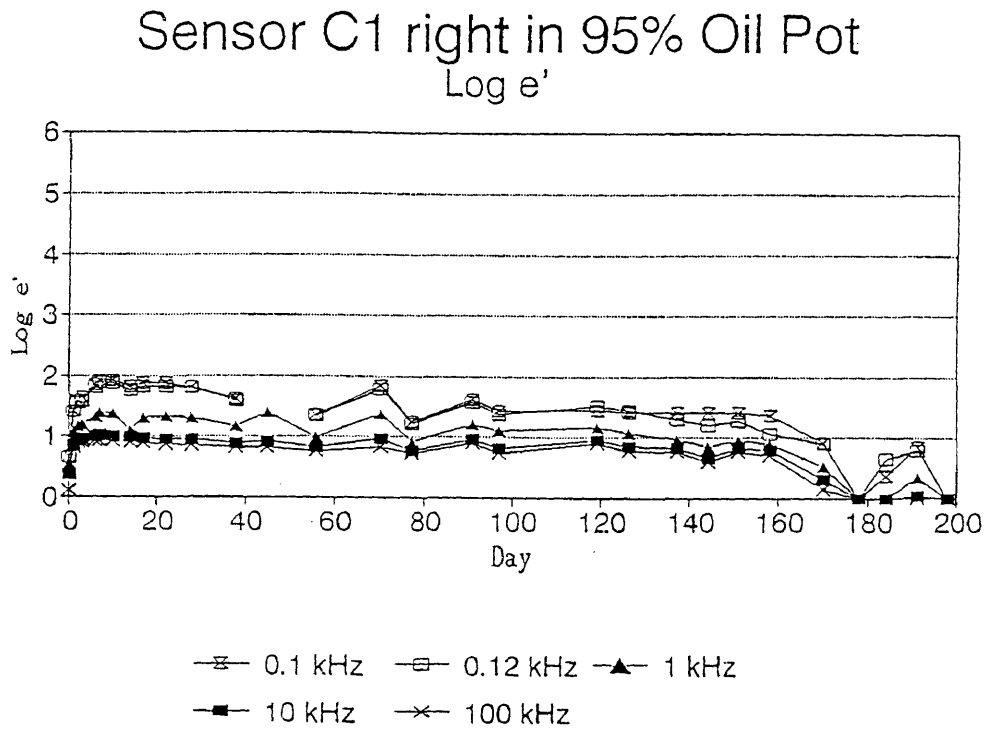

Figure 5-20

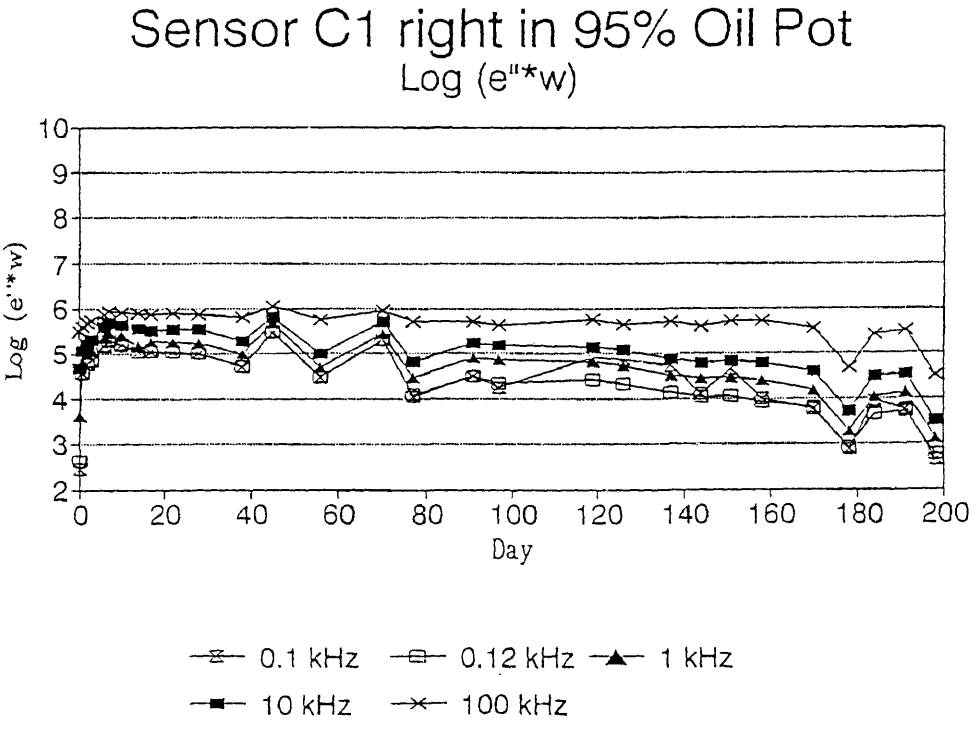

Figure 5-21

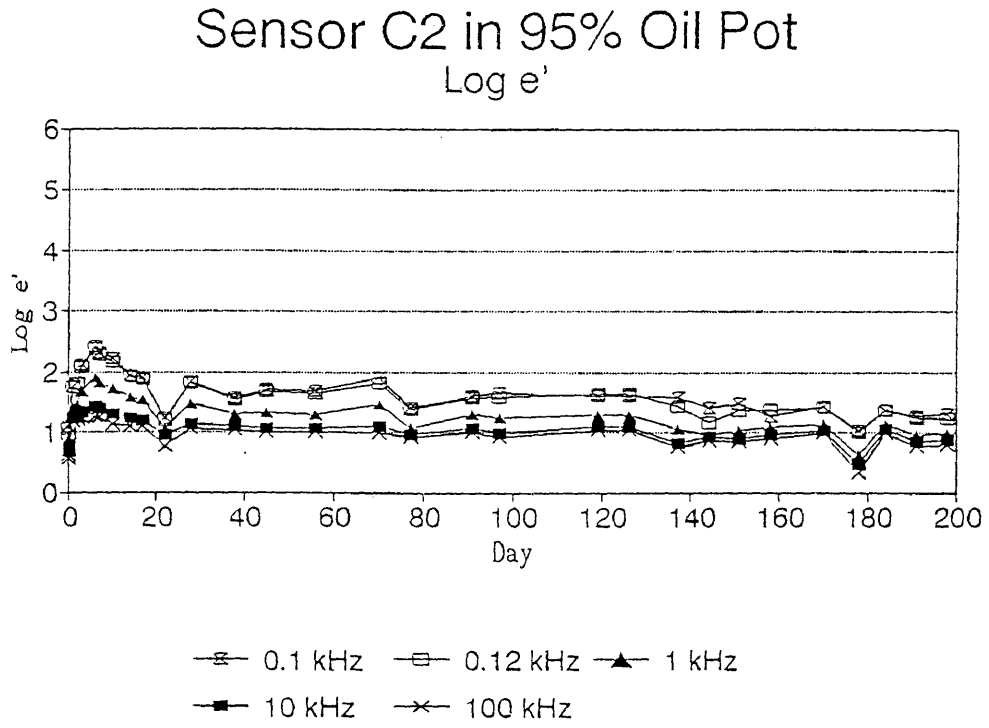

Figure 5-22

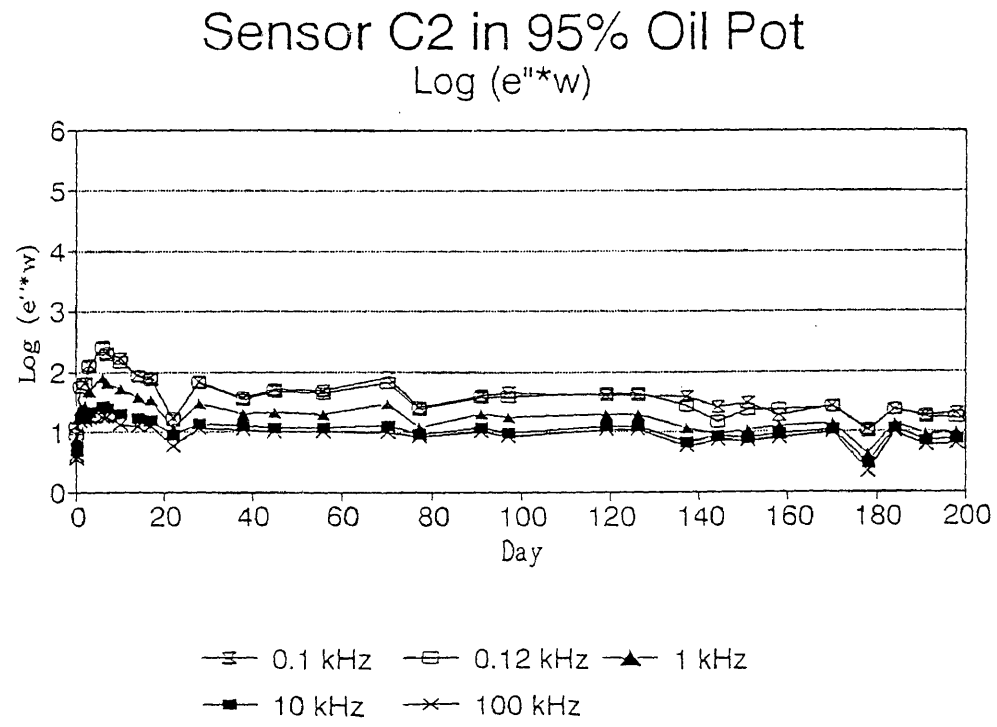

Figure 5-23

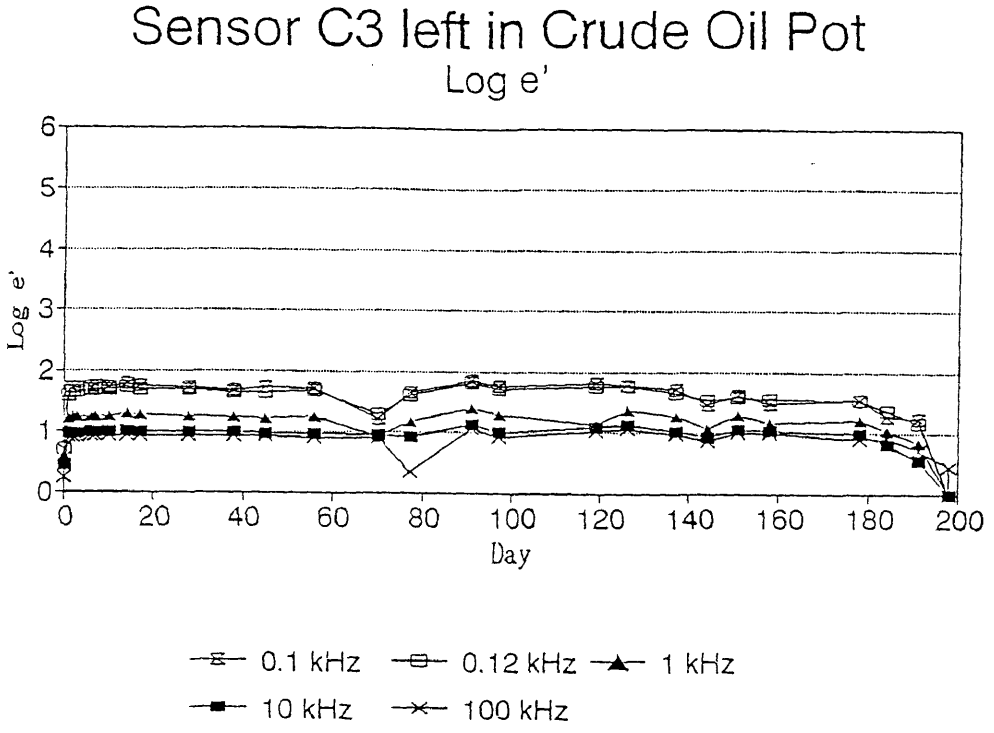

Figure 5-24

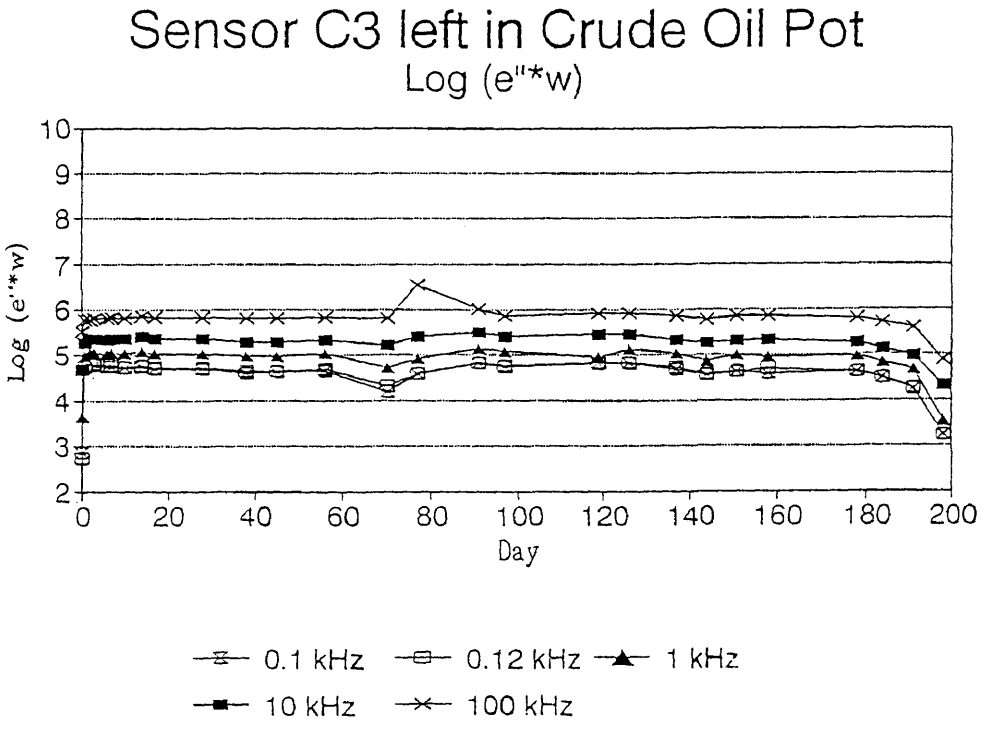

Figure 5-25

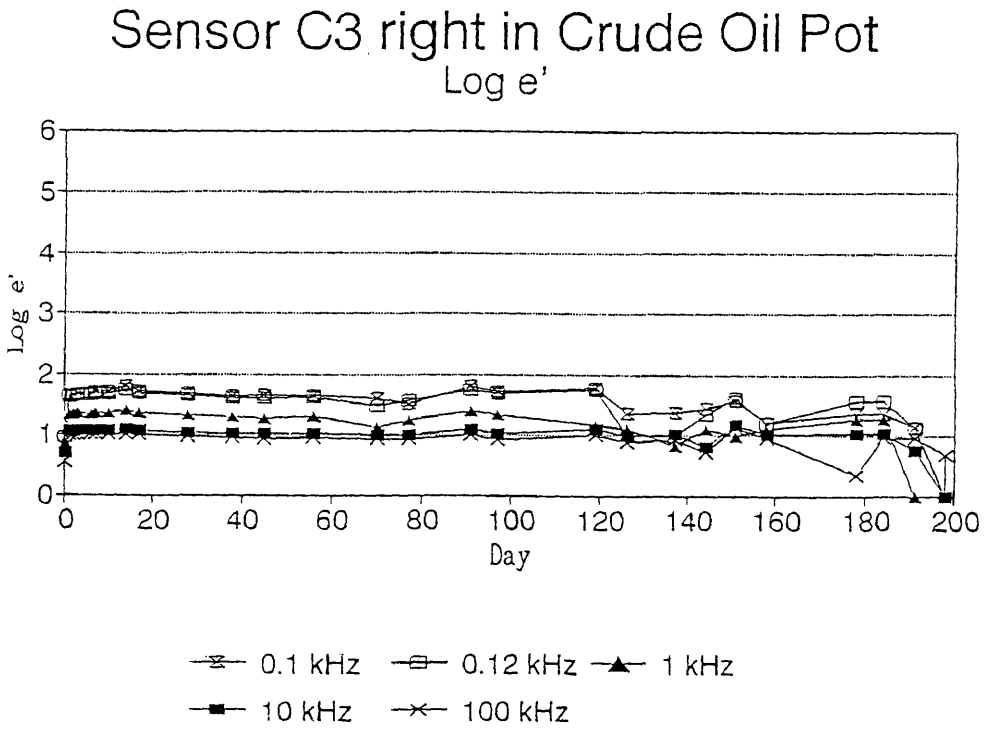

Figure 5-26

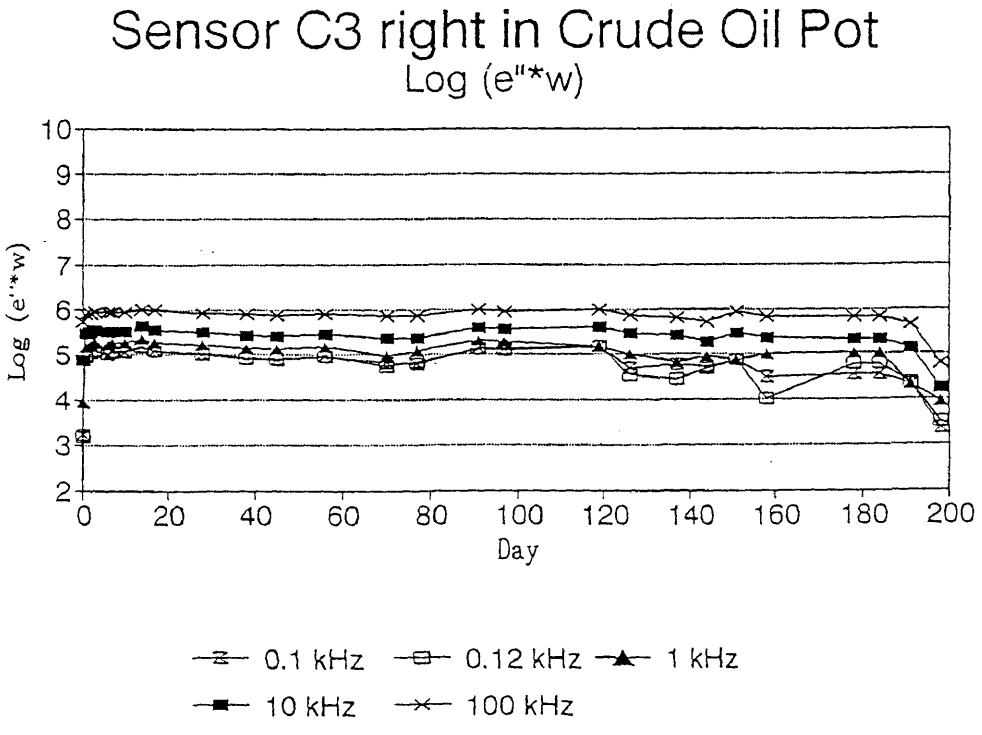

Figure 5-27

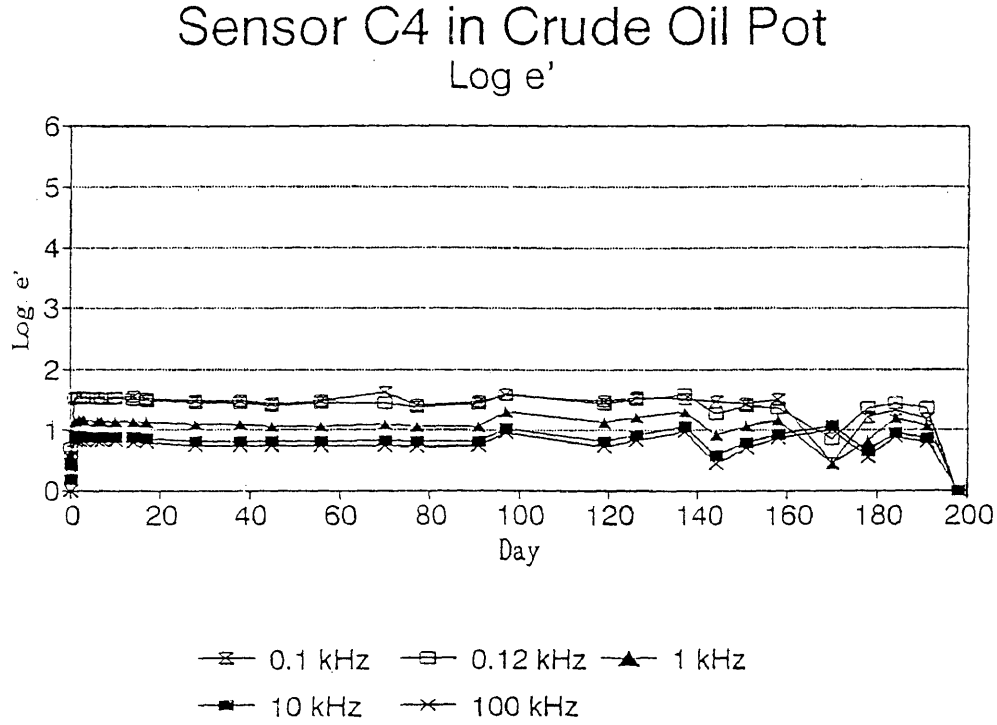

Figure 5-28

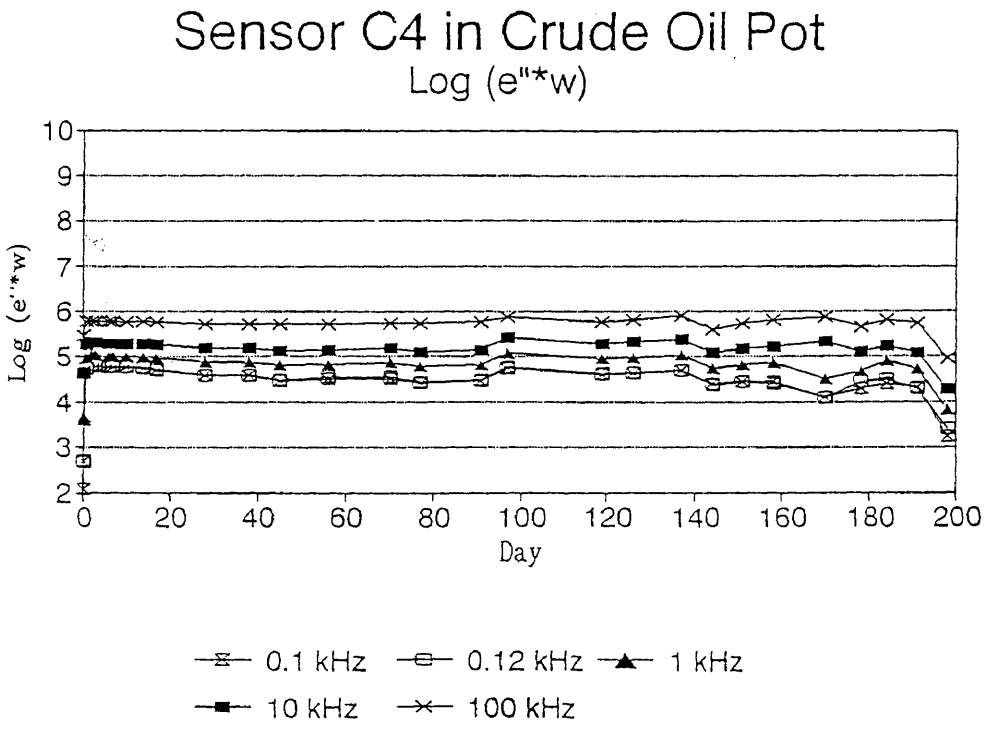

Figure 5-29

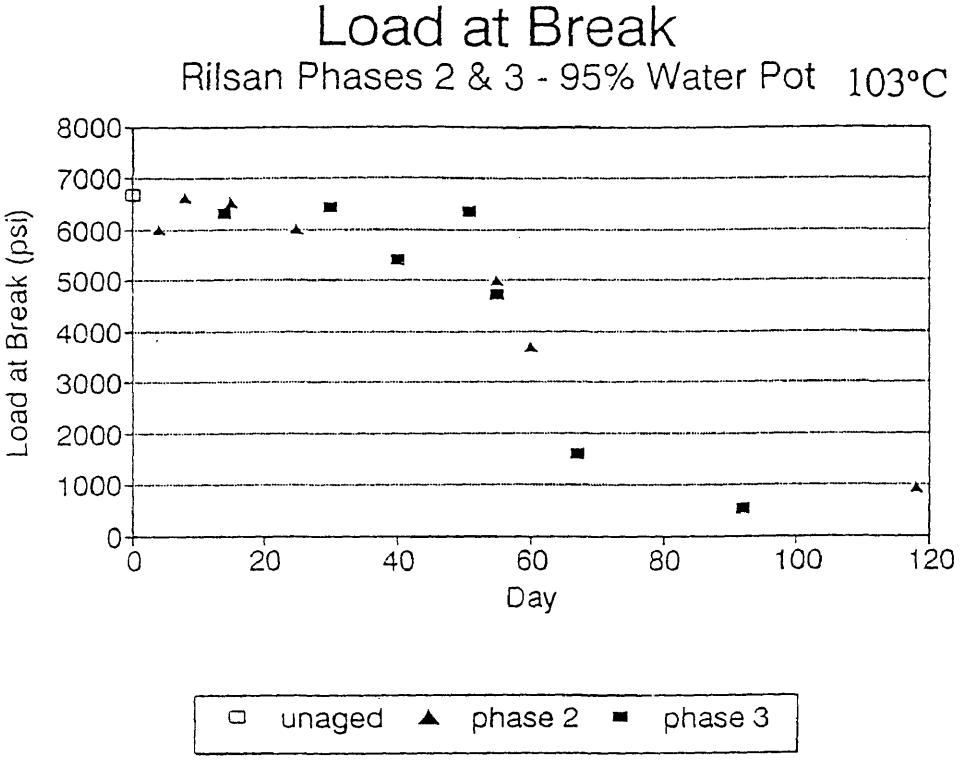

Figure 5-30

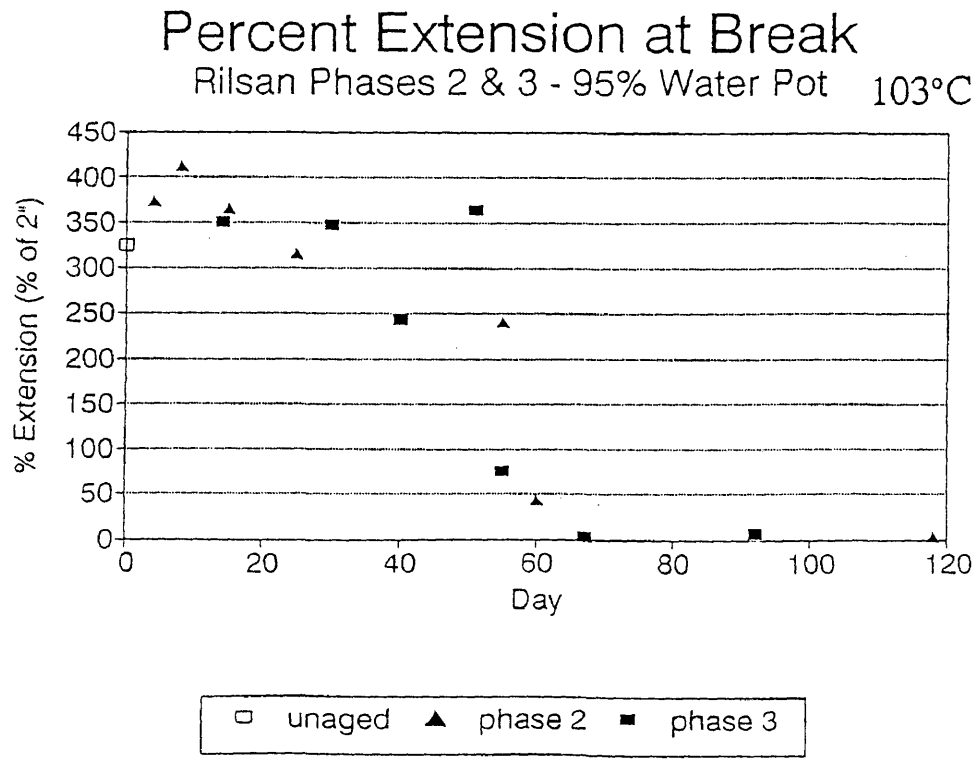

Figure 5-31

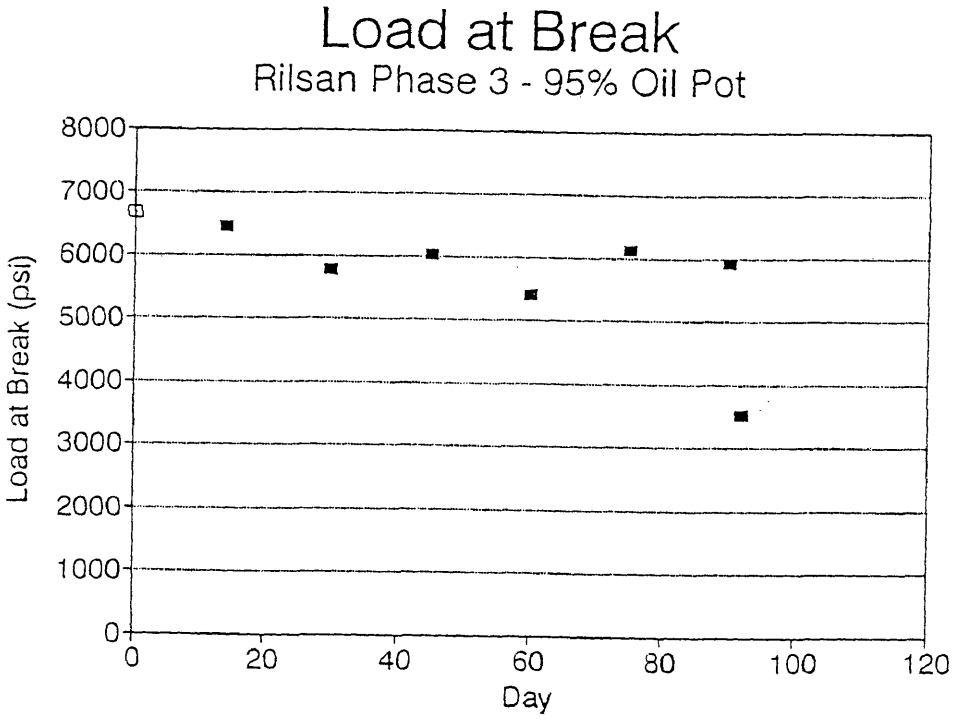

Figure 5-32

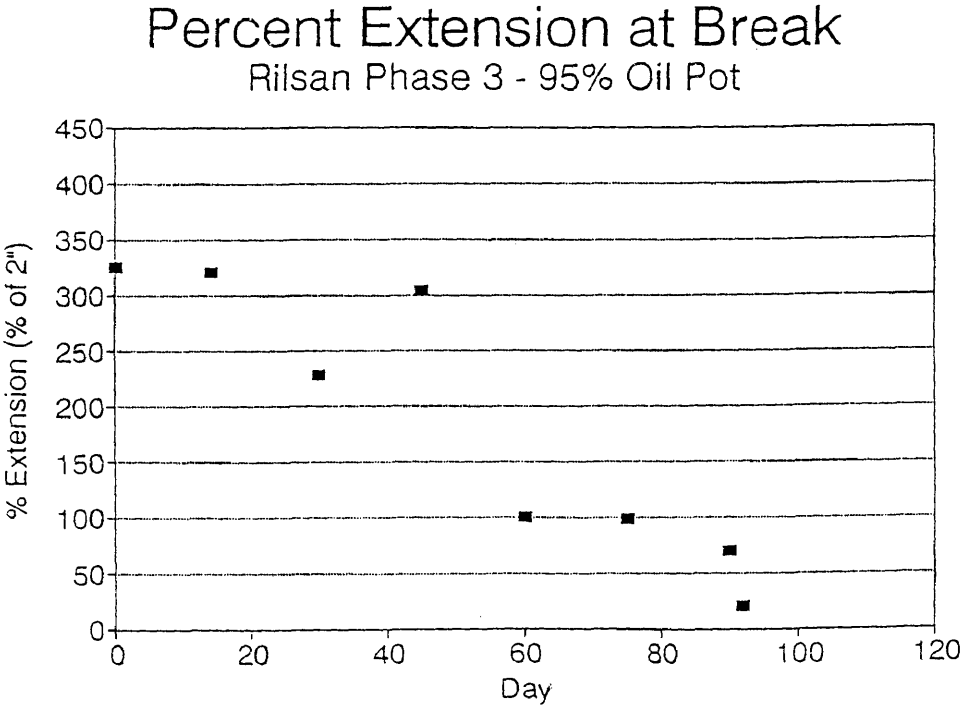

Figure 5-33

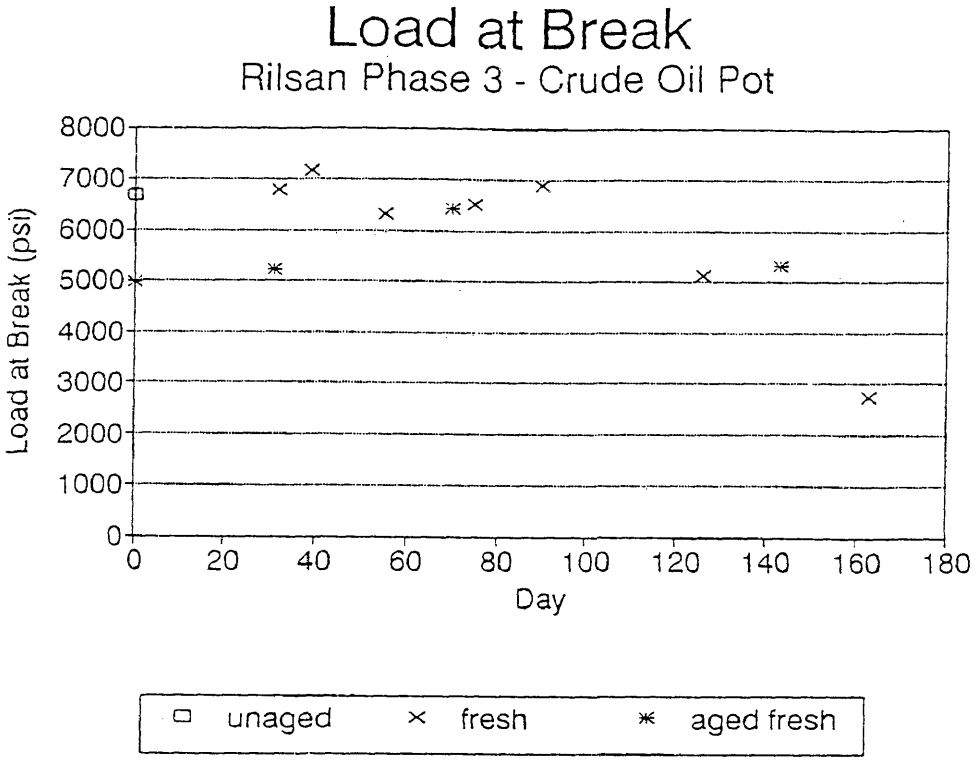

Figure 5-34

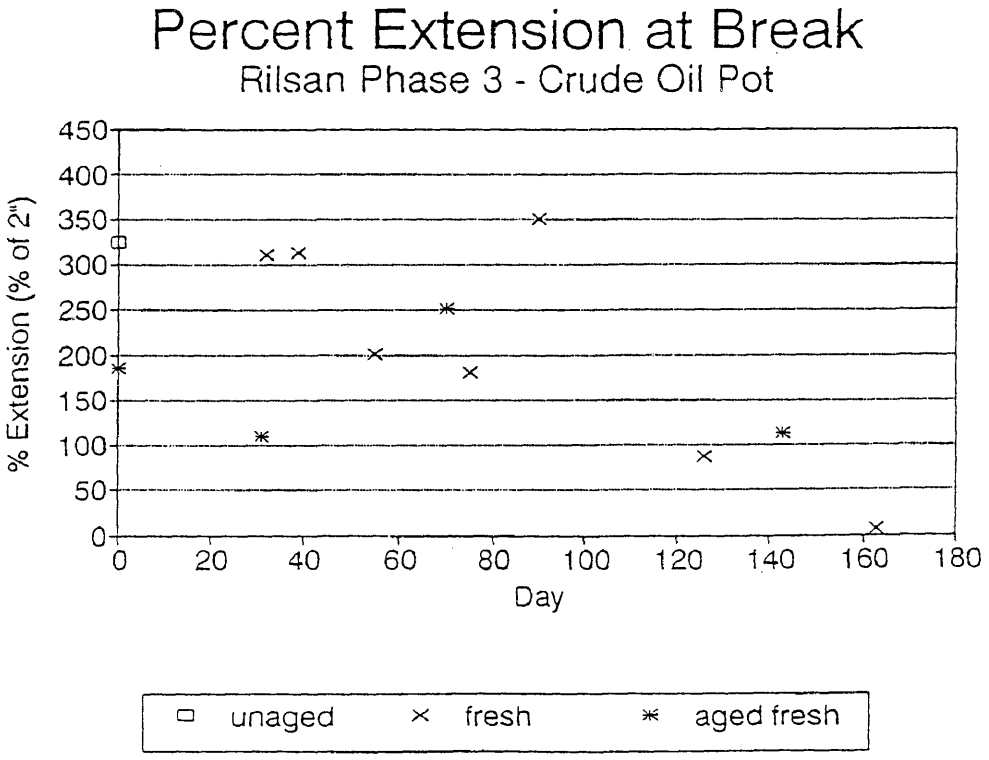

Figure 5-35

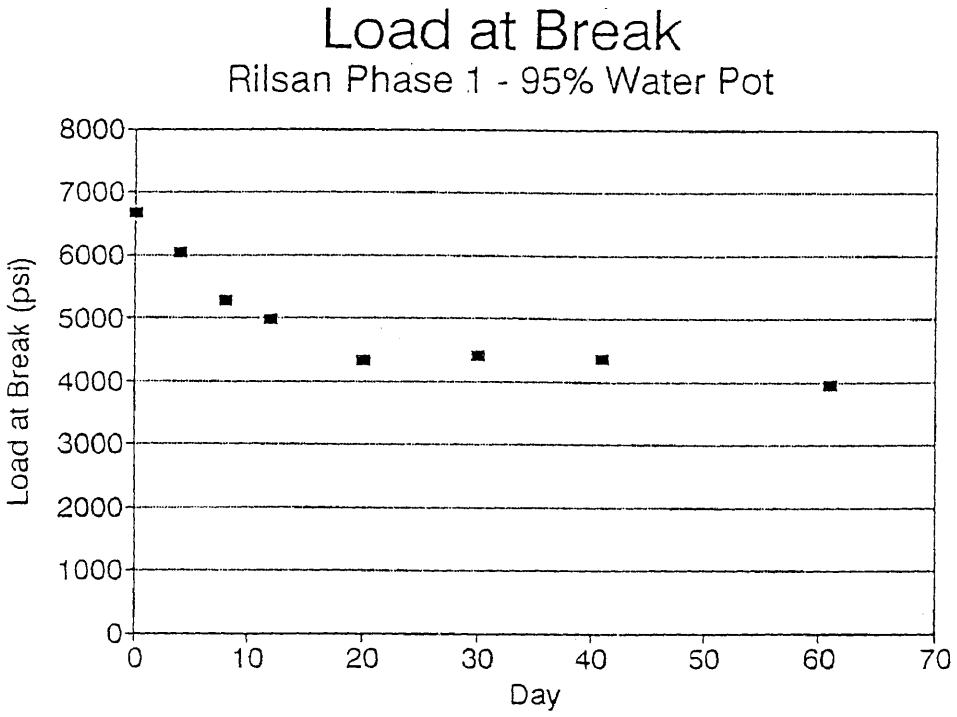

Figure 5-36

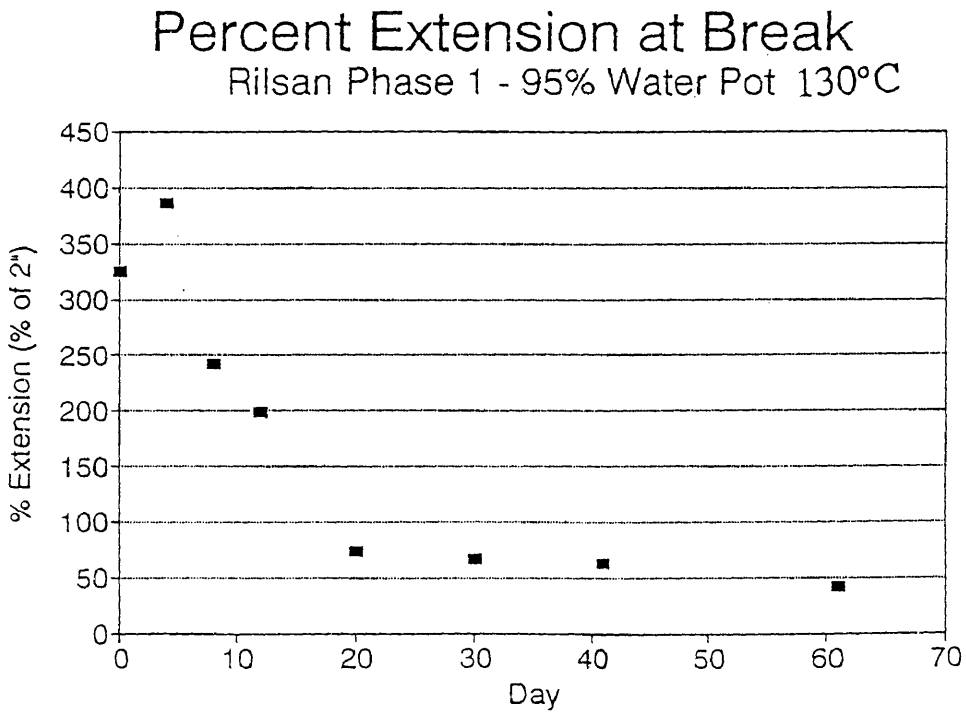

Figure 5-37

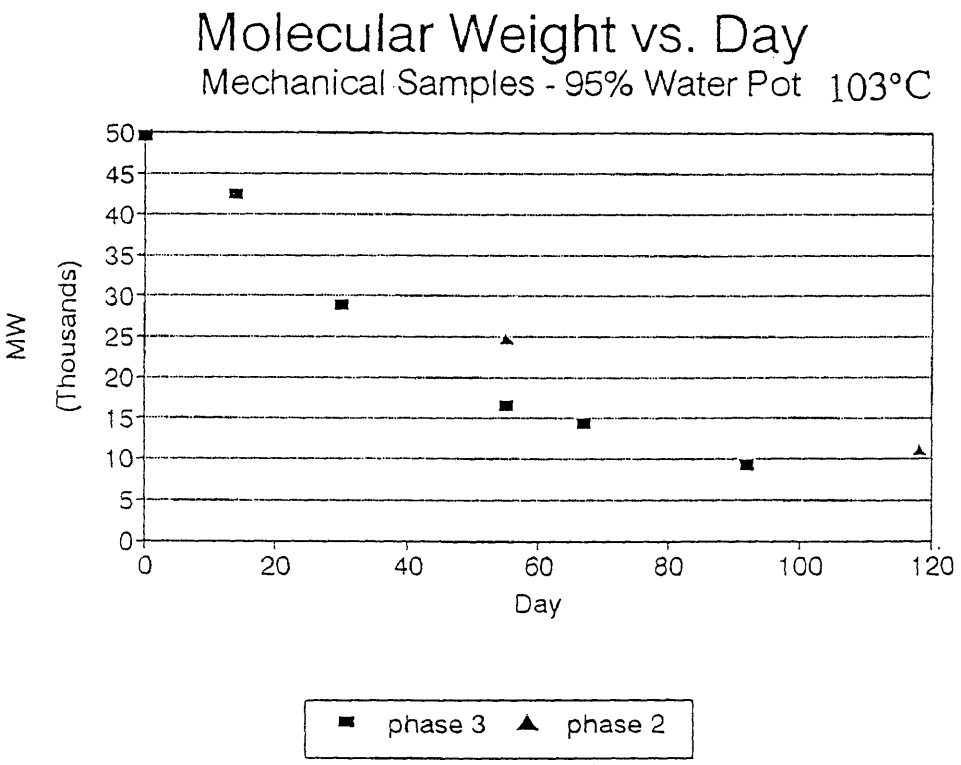

Figure 5-38

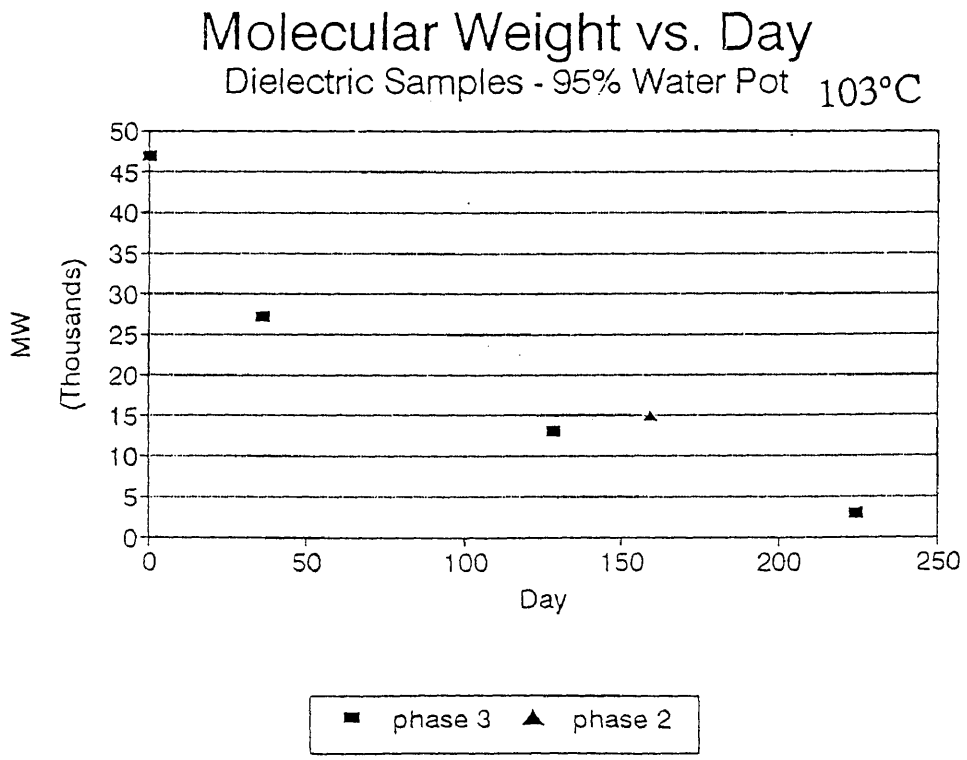

Figure 5-39

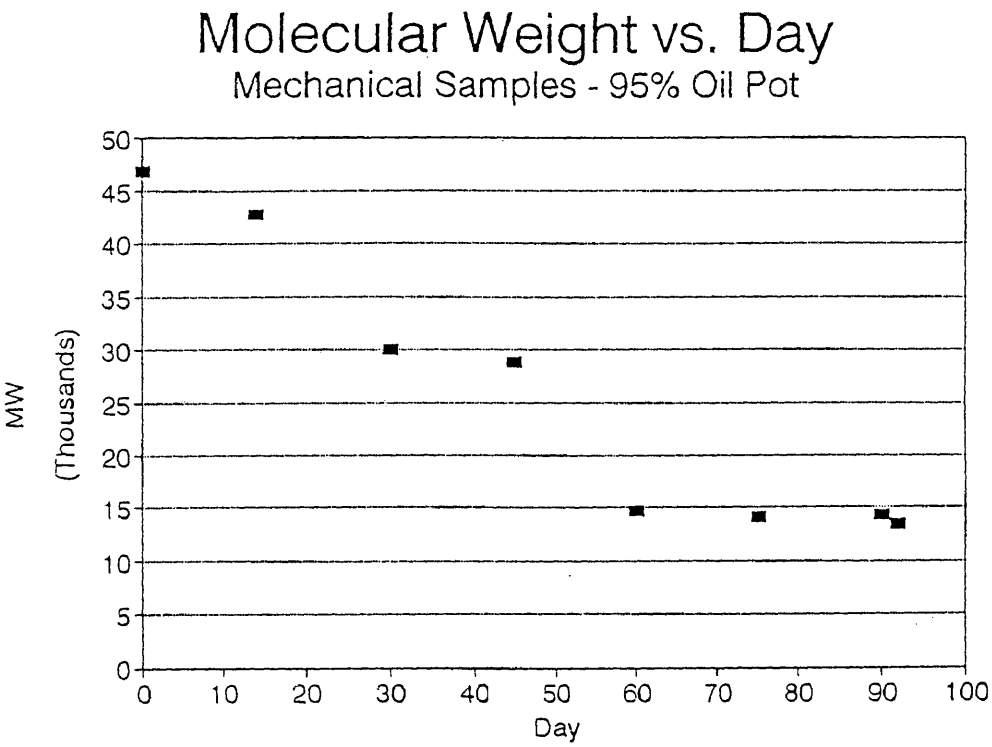

Figure 5-40

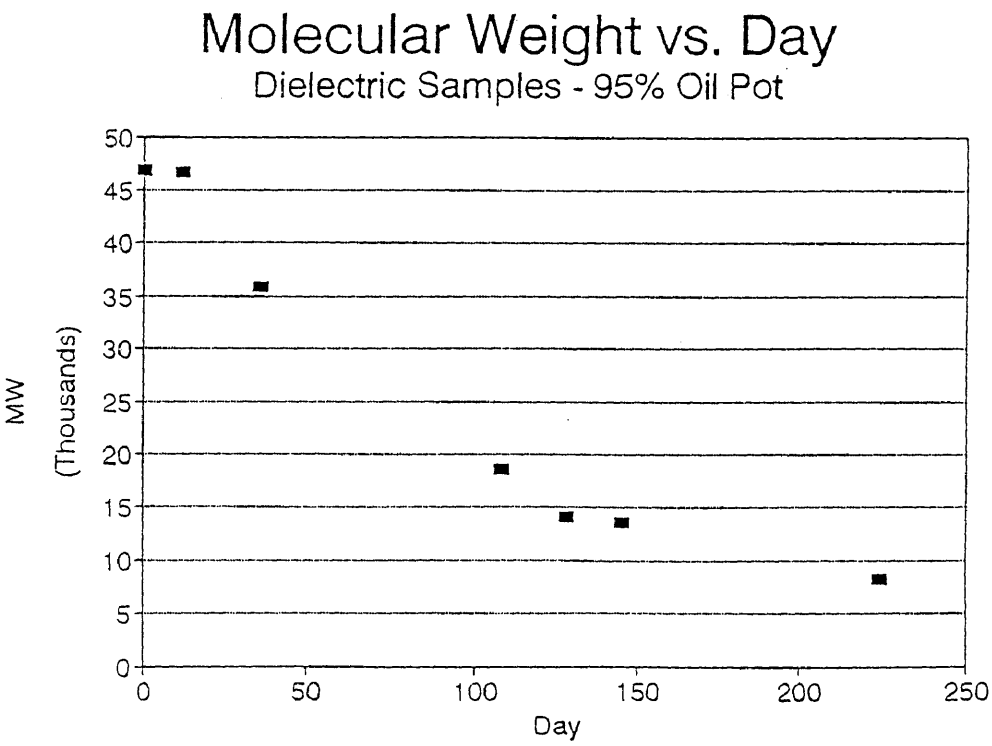

Figure 5-41

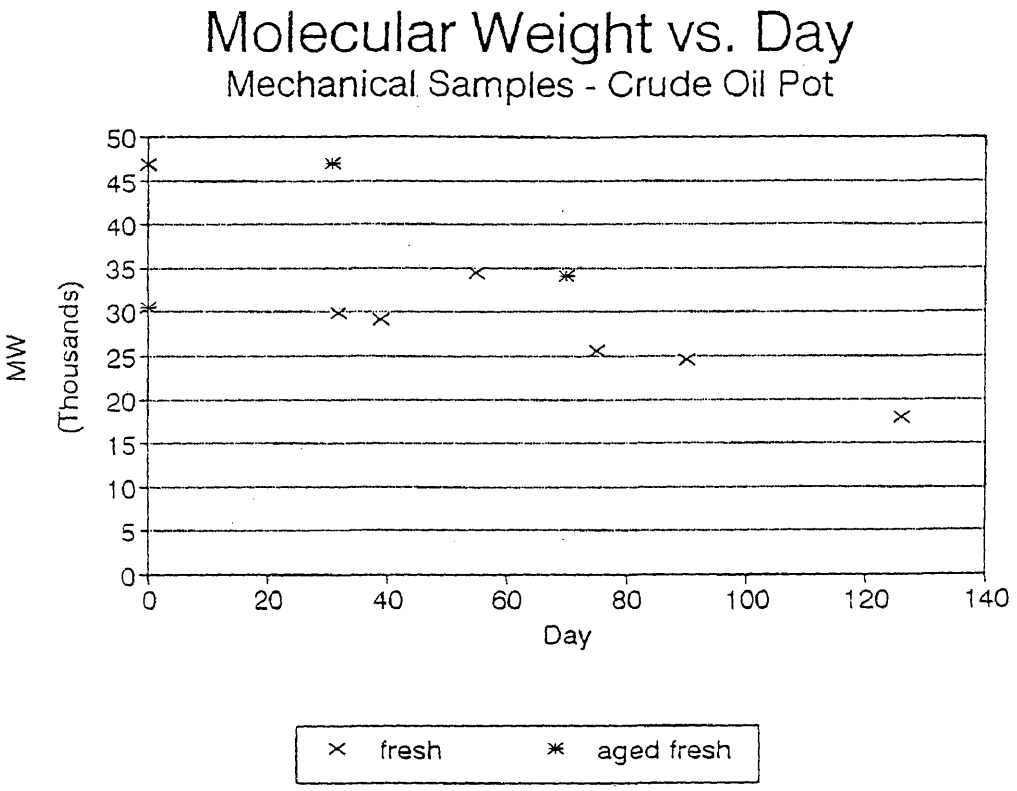

Figure 5-42

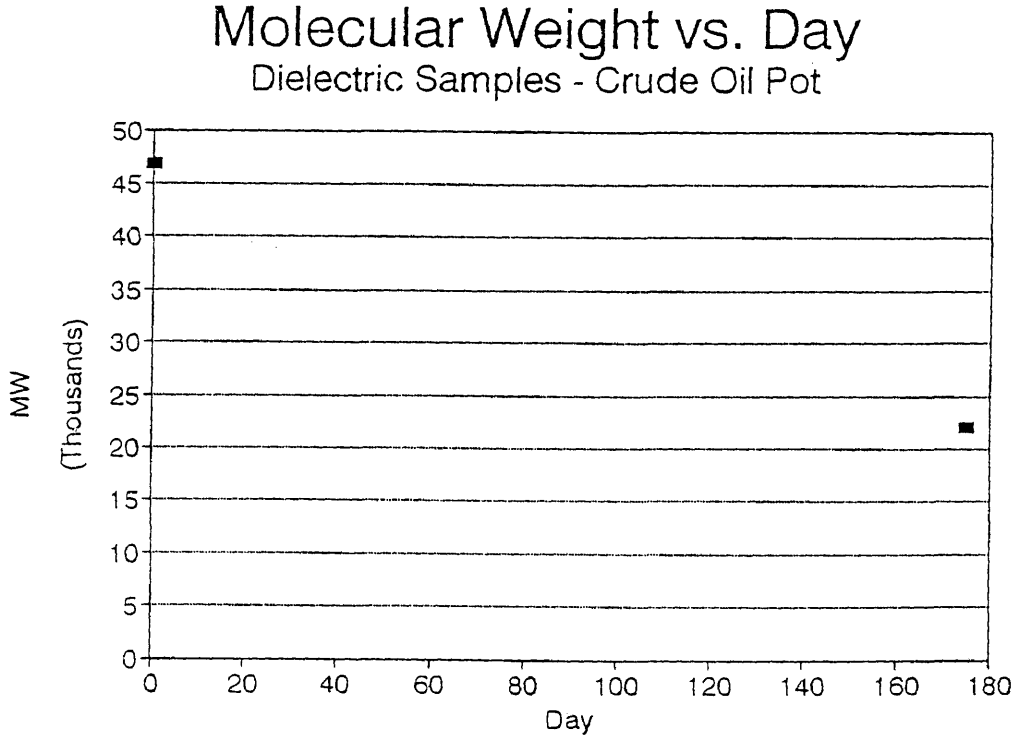

Figure 5-43

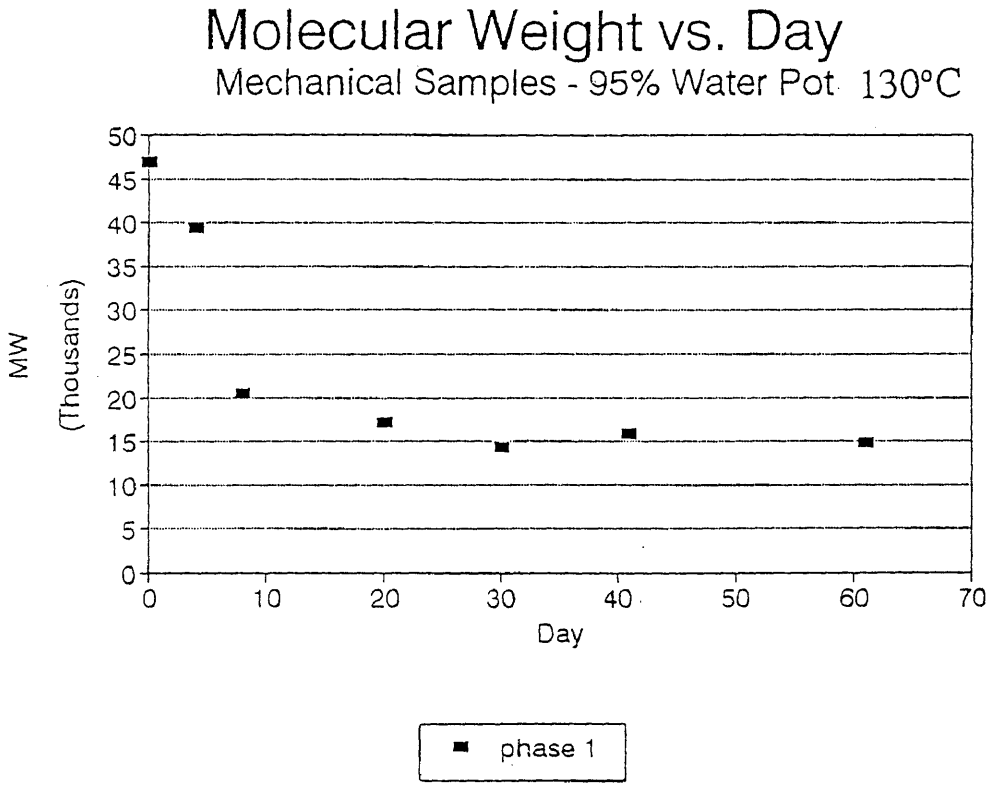
Molecular Weight vs. Day
Mechanical Samples - 95% Water Pot 130°C
MW
(Thousands)
50
45
40
35
30
25
20
15
10
5
0
0
10
20
30
40
50
60
70
Day
phase 1

Figure 5-44

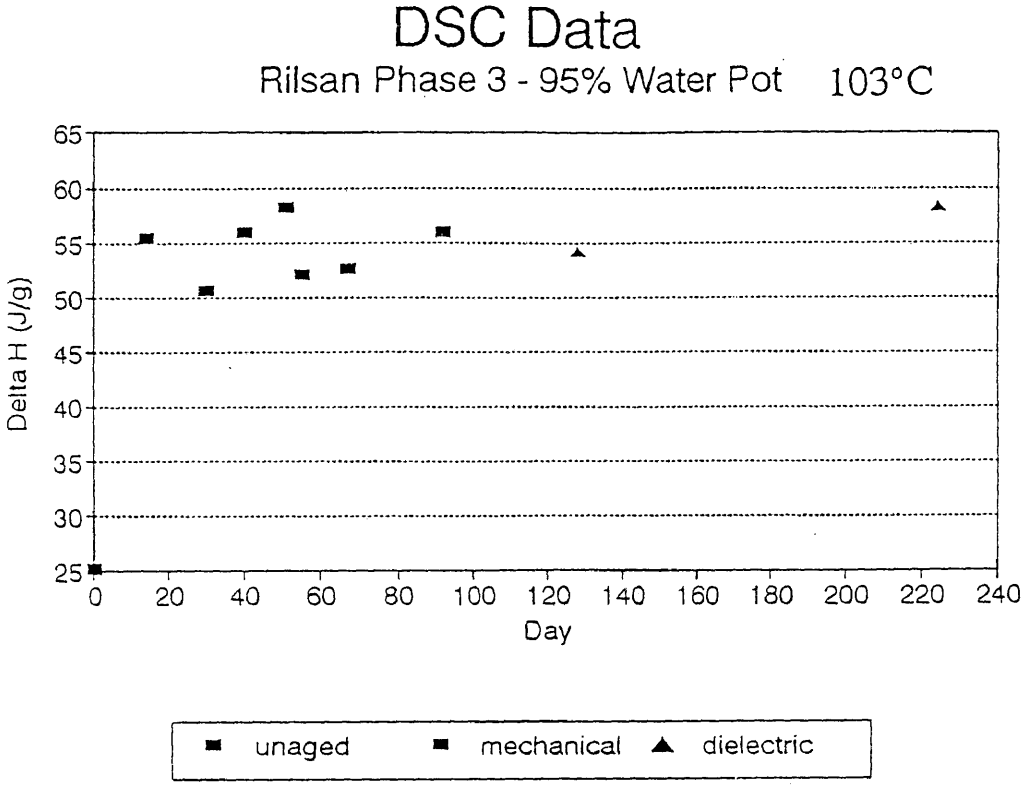

Figure 5-45

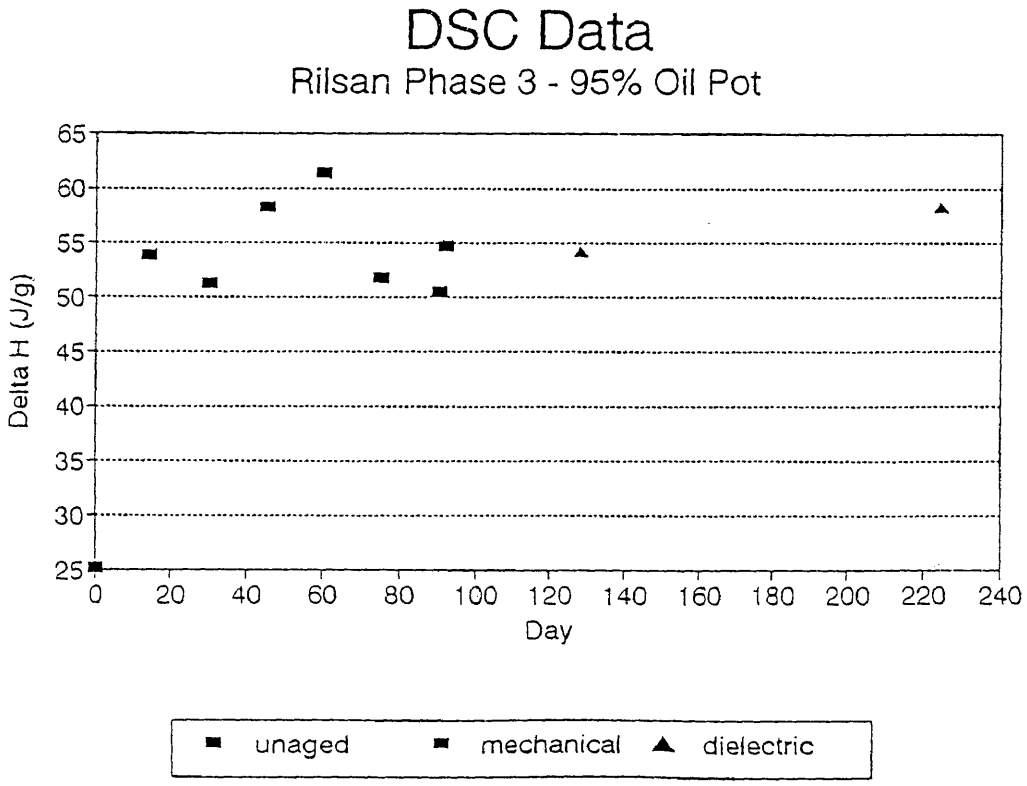

Figure 5-46

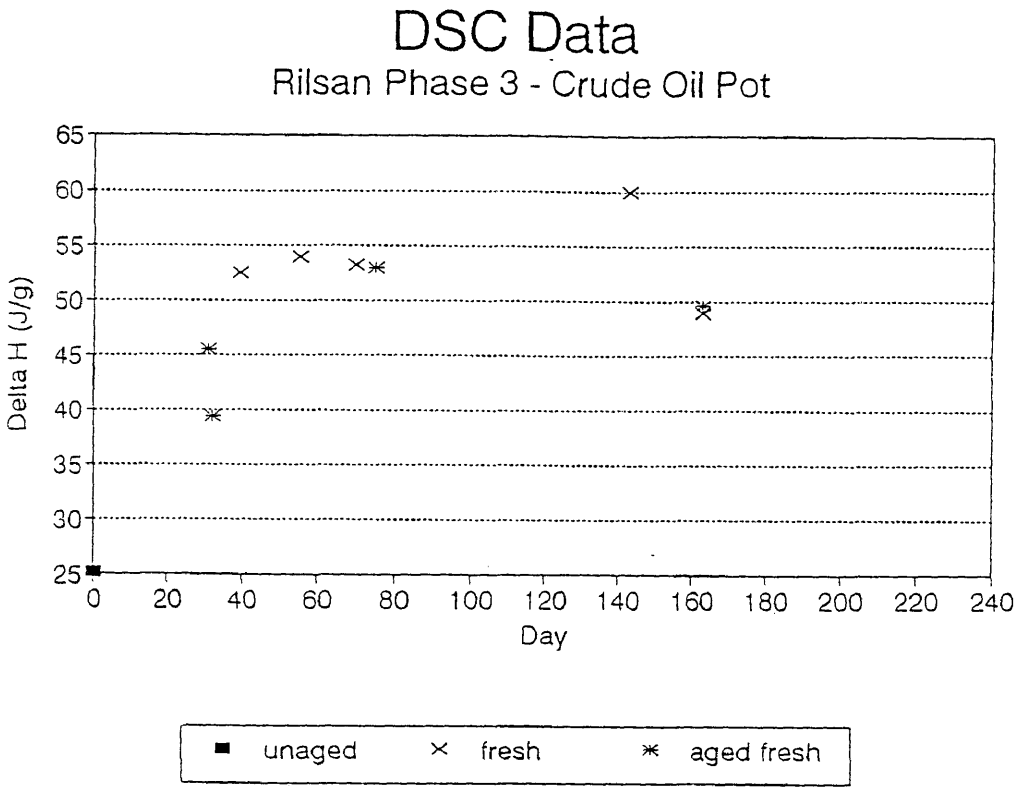

Figure 5-47

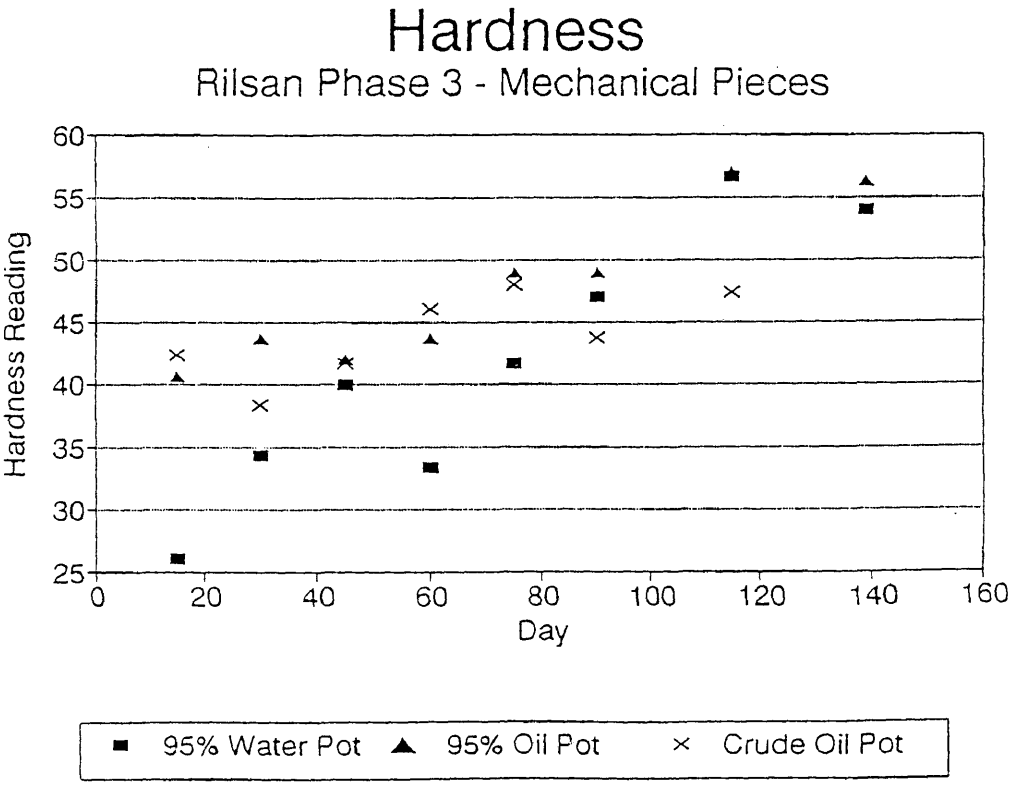

Figure 5-48

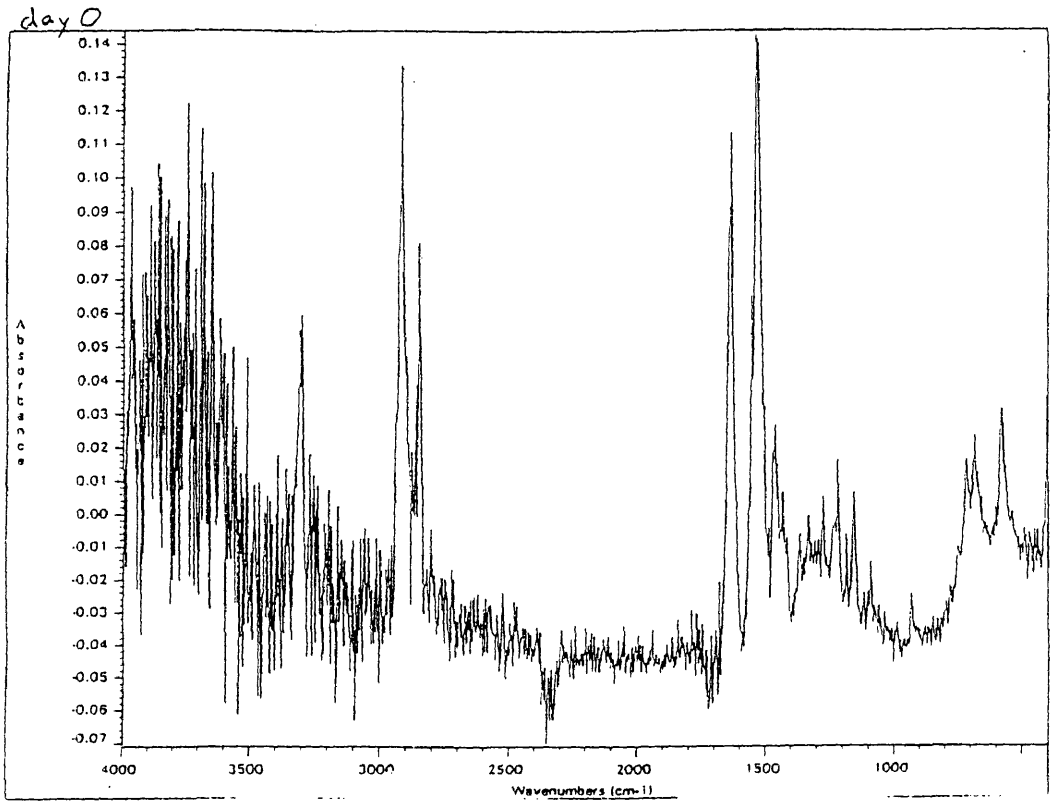

Figure 5-49

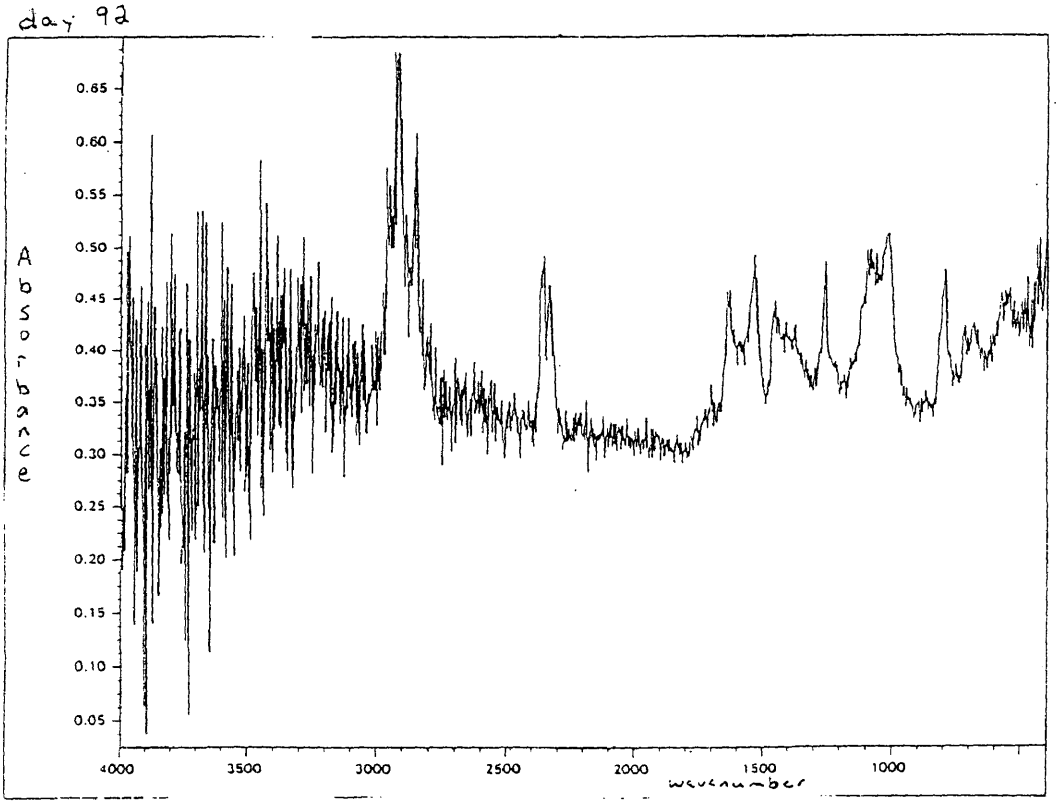

Figure 5-50

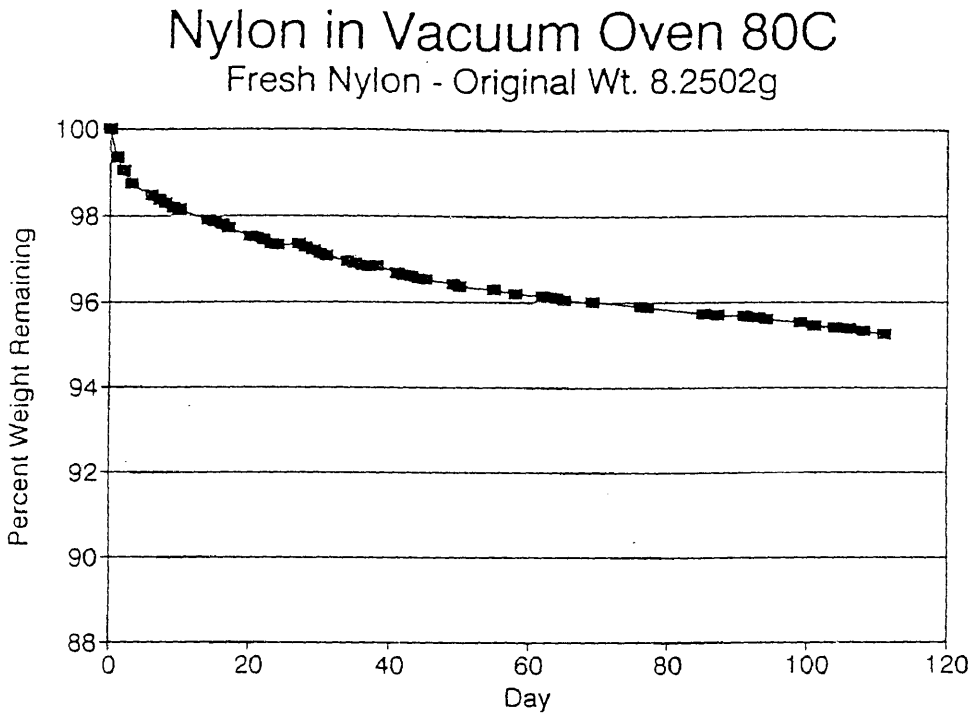

Figure 5-51

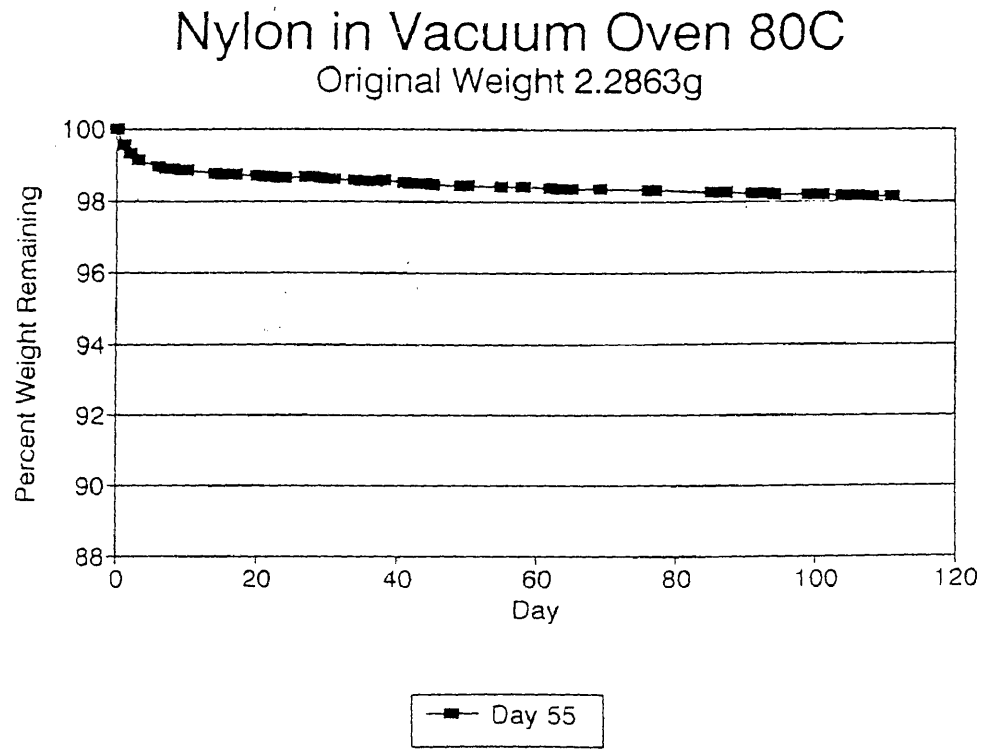

Figure 5-52

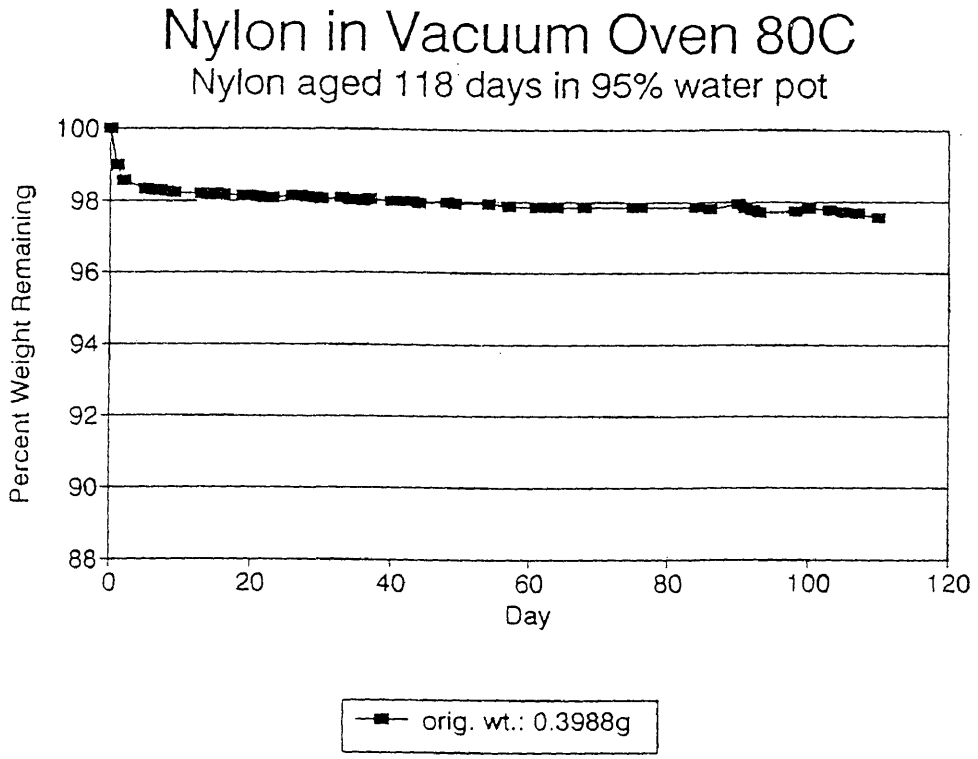

Figure 5-53

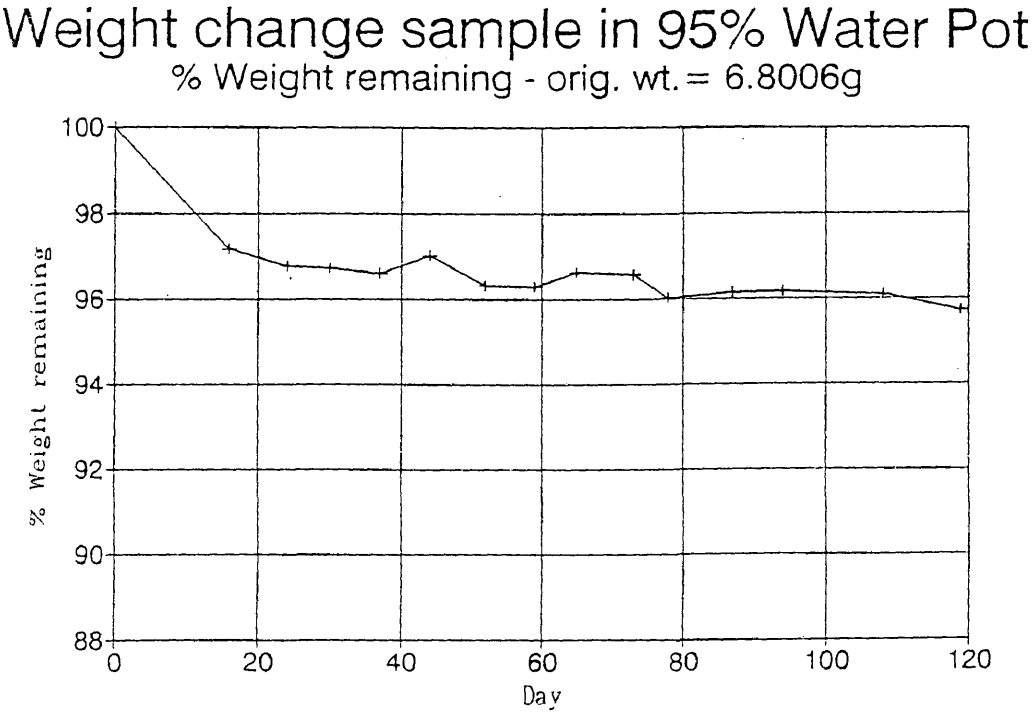

Figure 5-54

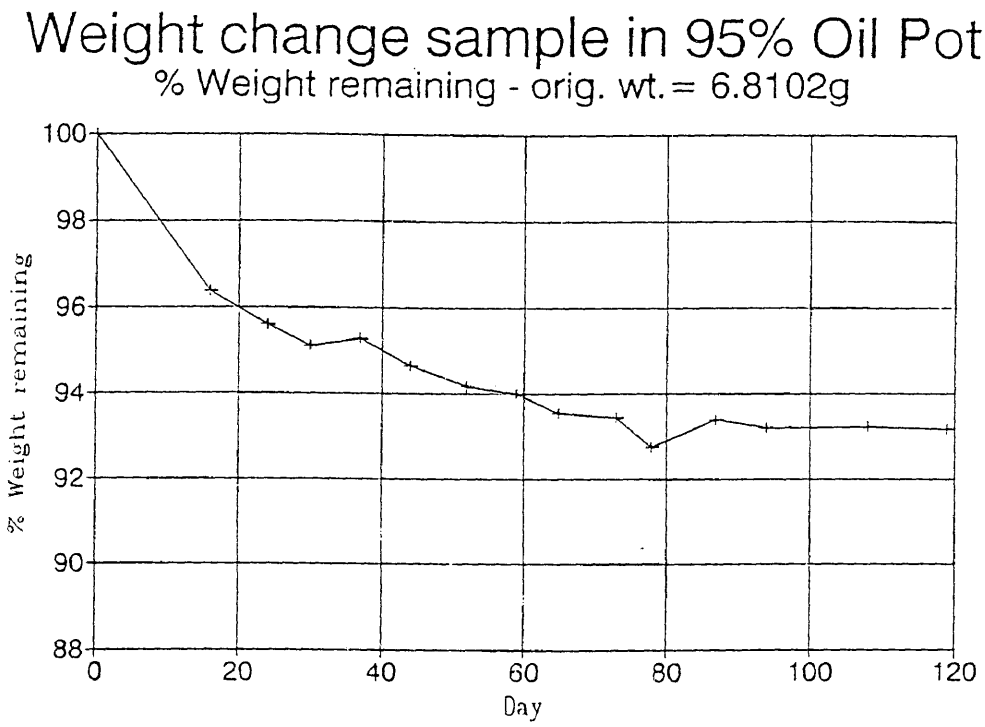

Figure 5-55

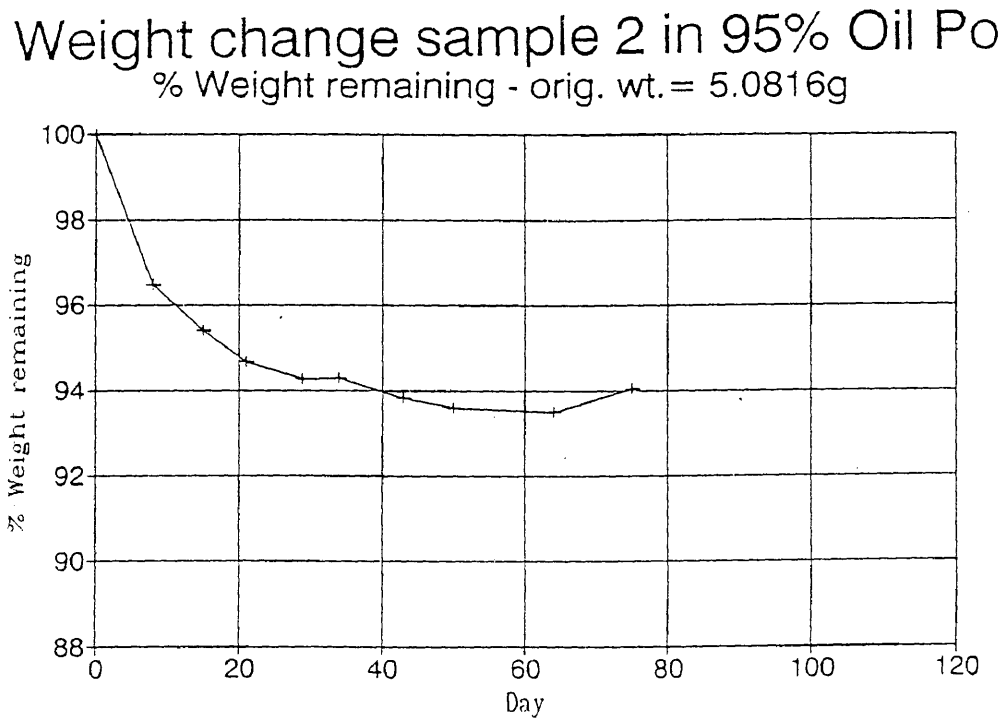

Figure 5-56

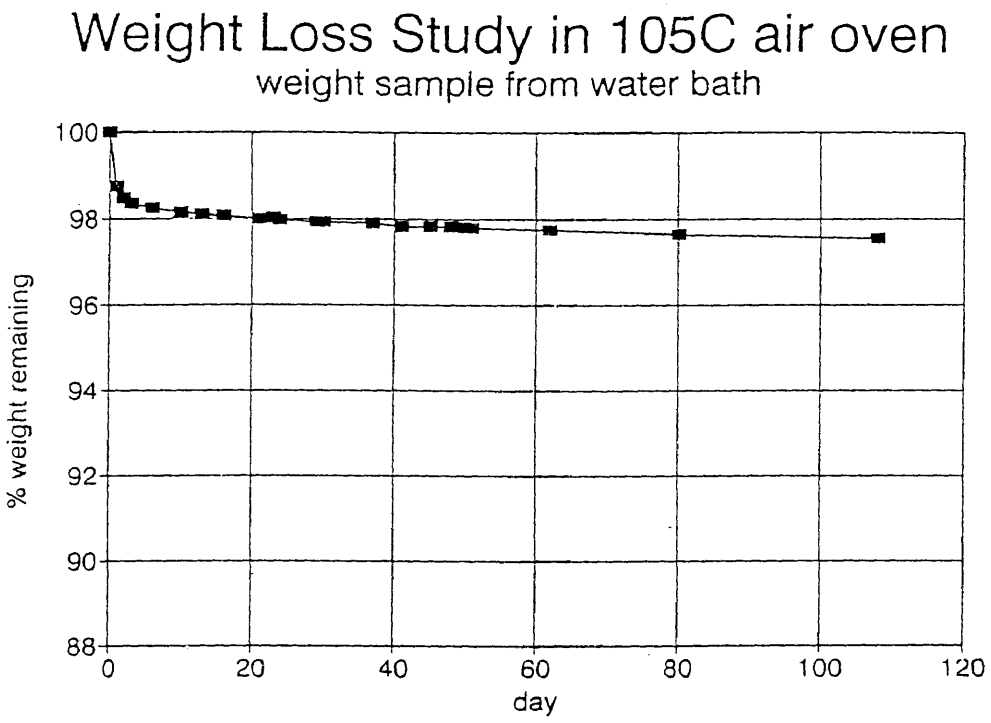

Figure 5-57

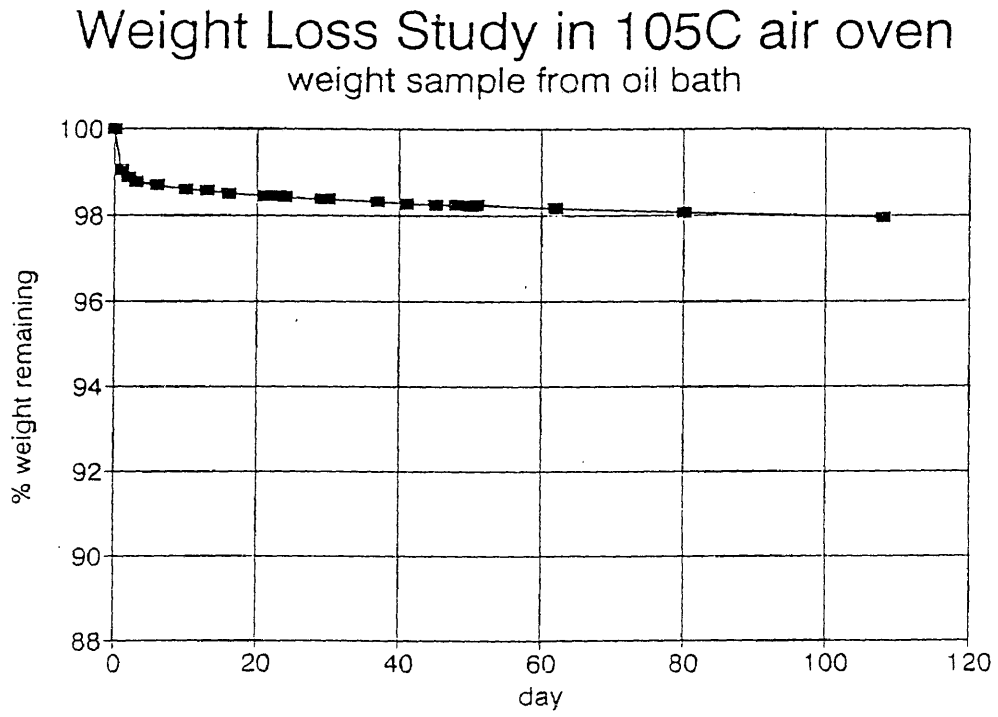

Figure 5-58

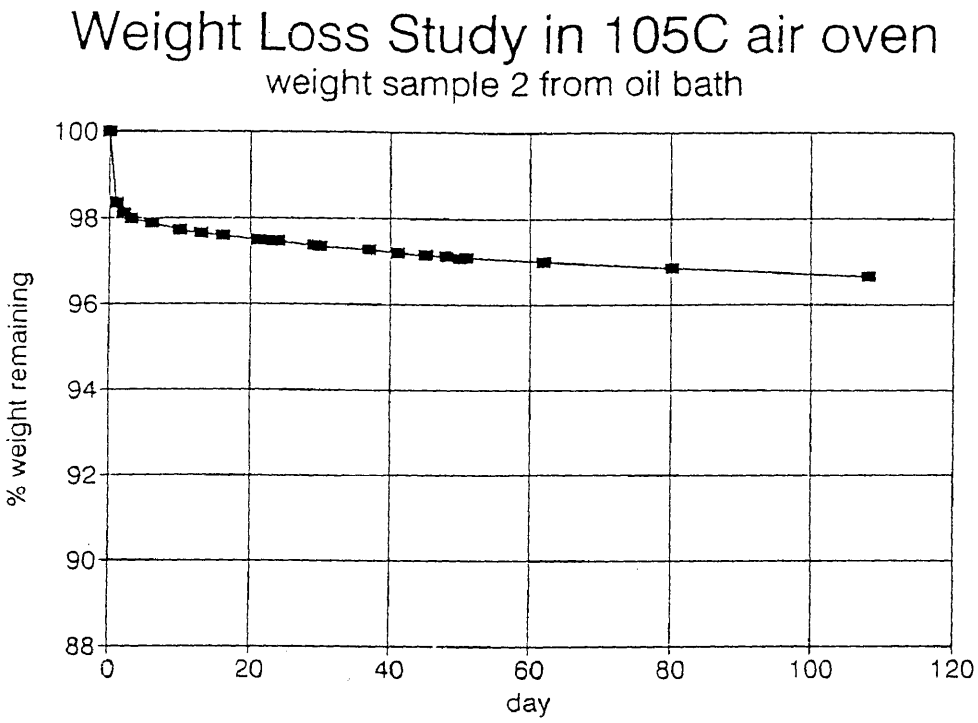

Figure 5-59

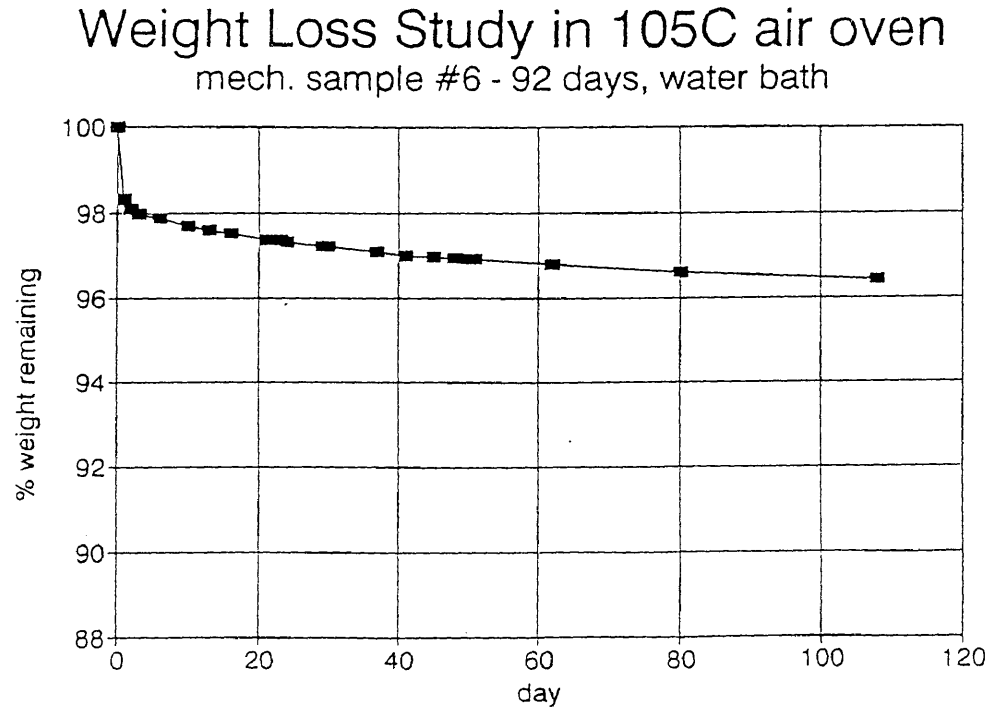

Figure 5-60

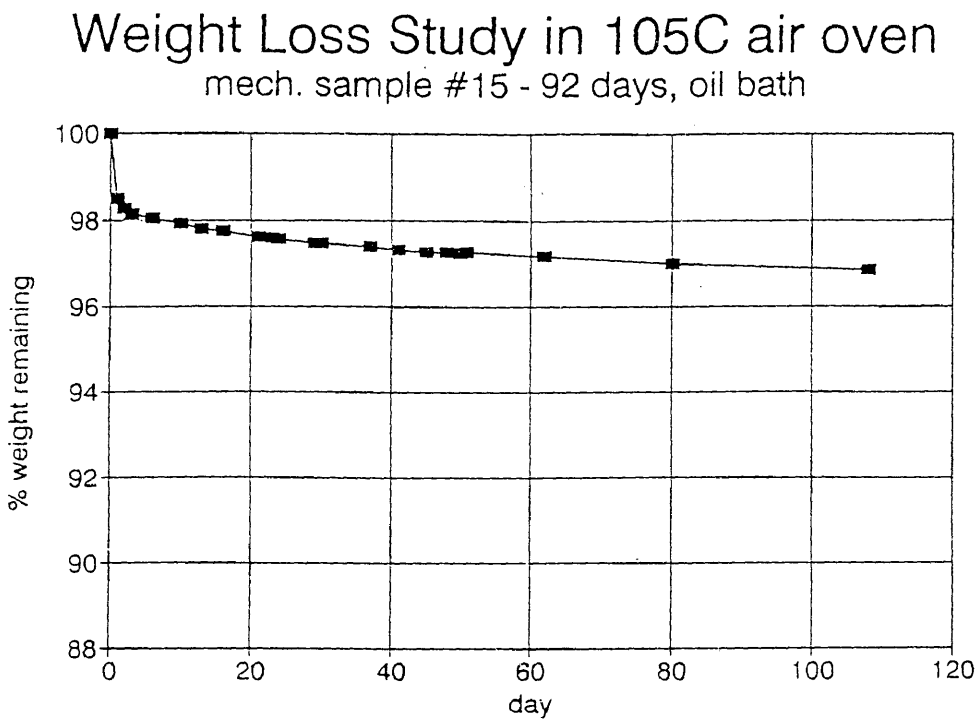

Figure 5-61

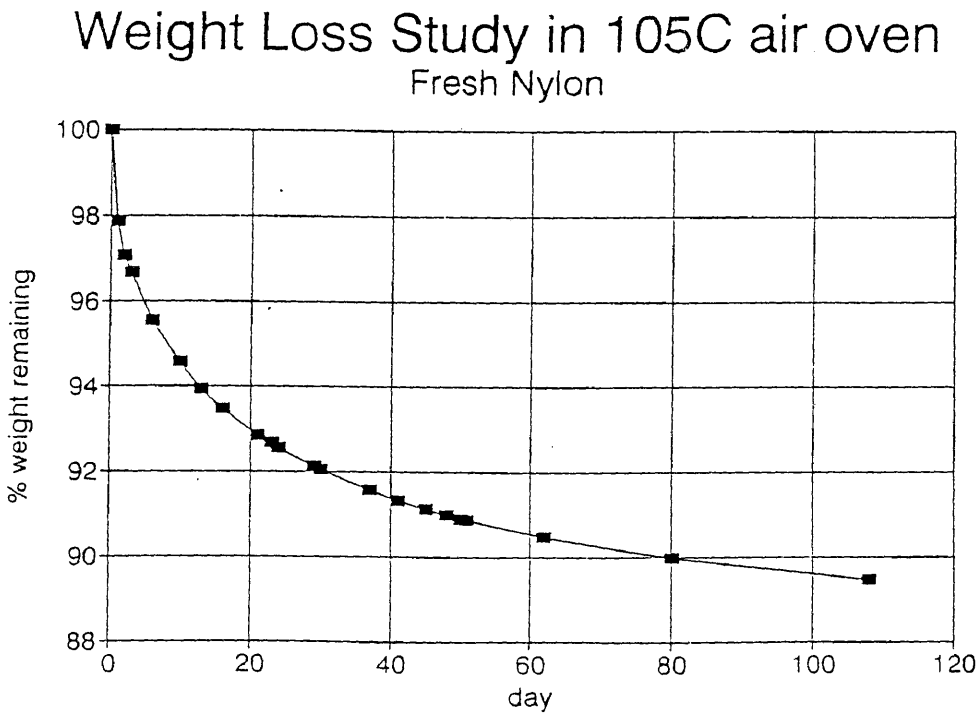

Figure 5-62

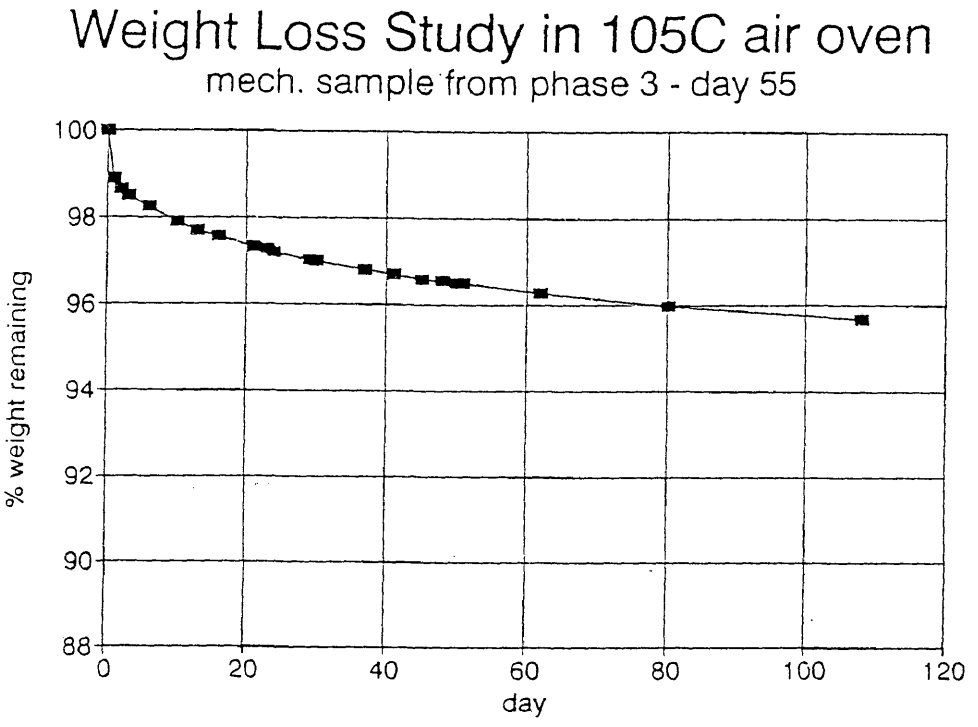

Figure 5-63

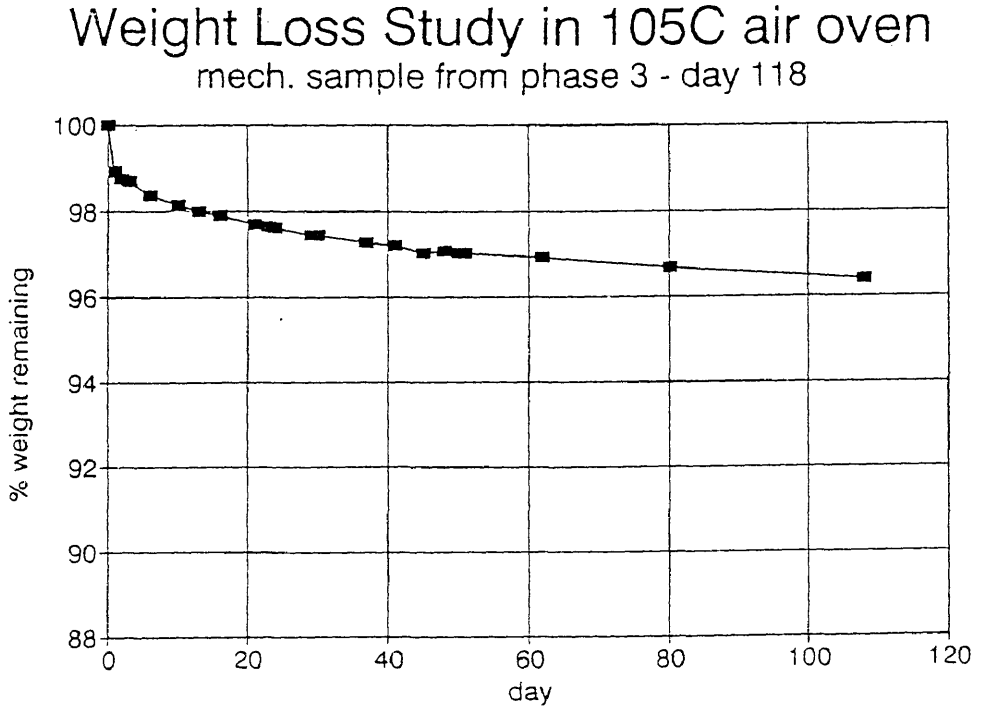

Figure 5-64

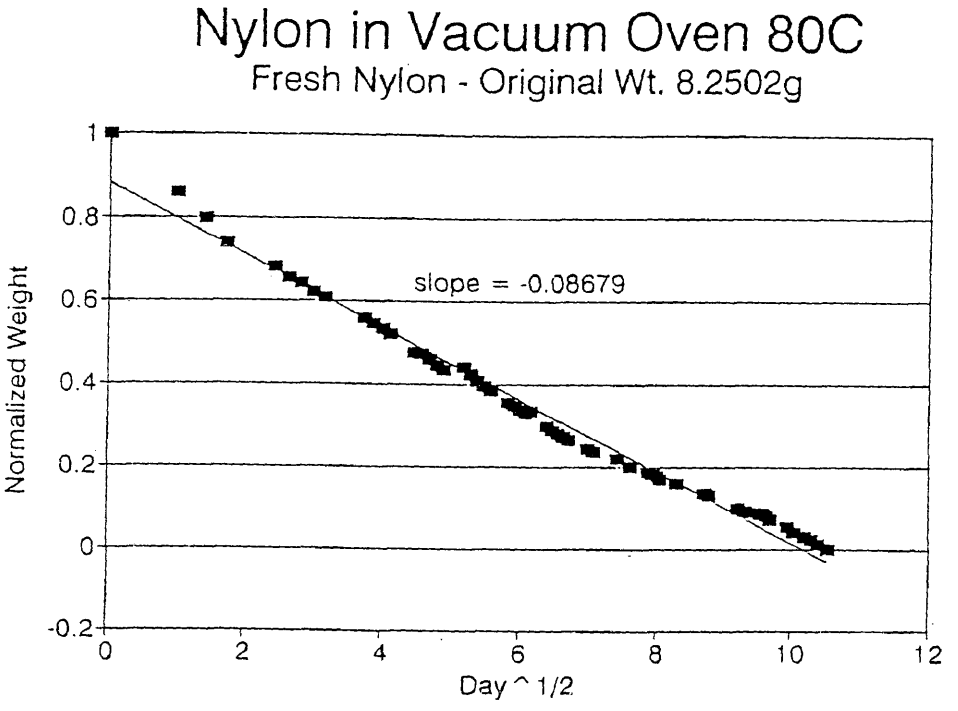

Figure 5-65

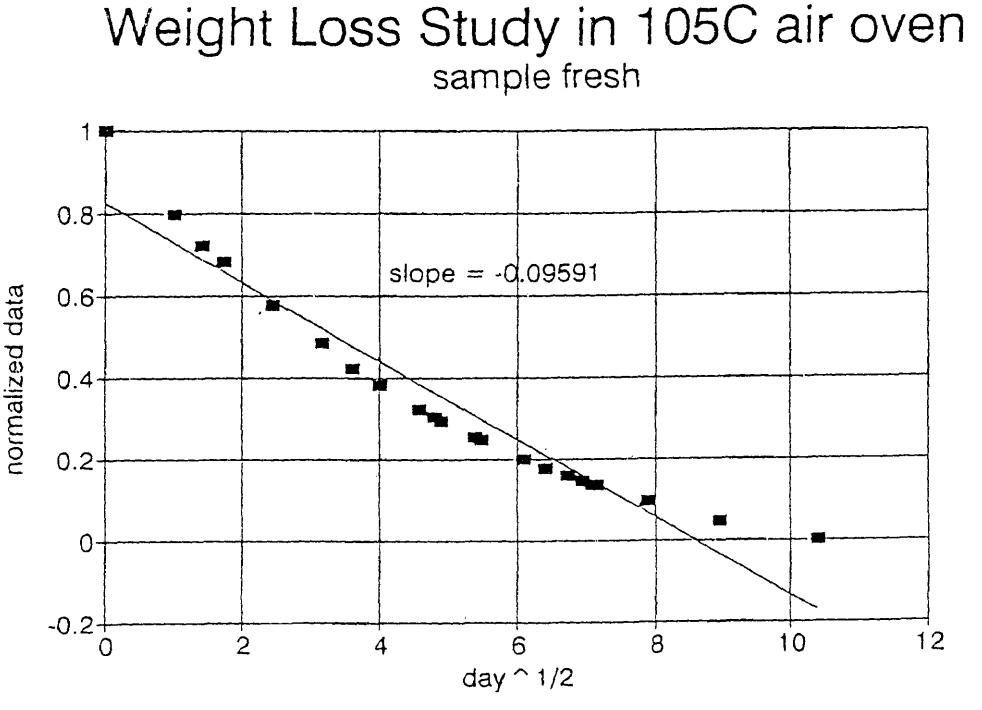

Figure 5-66

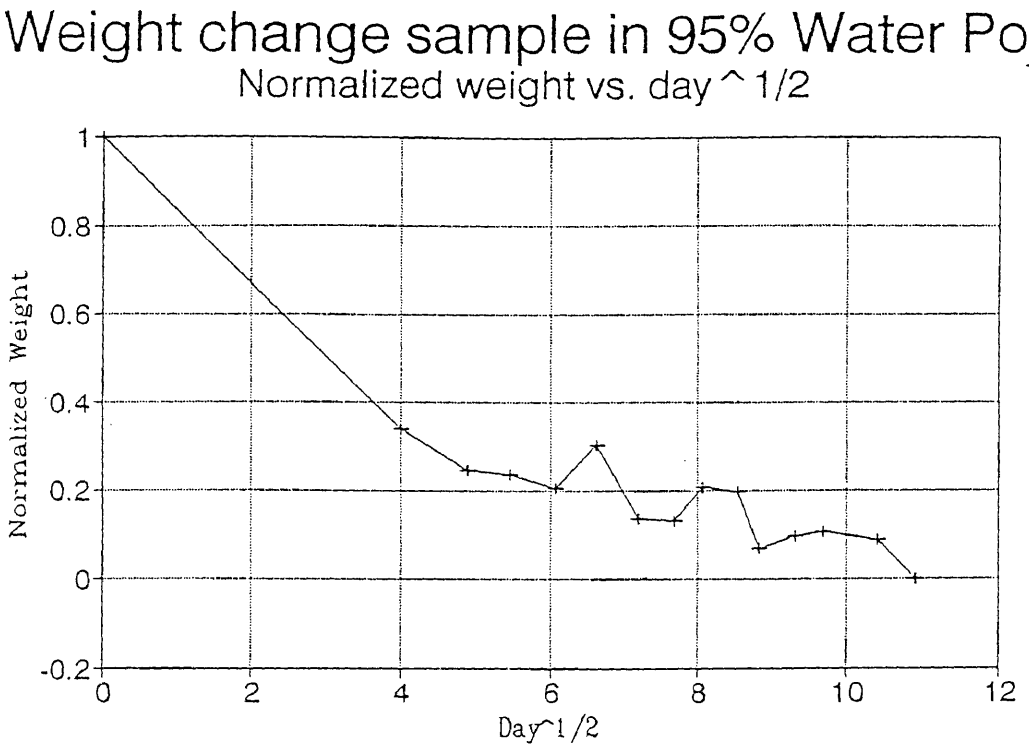

Figure 5-67

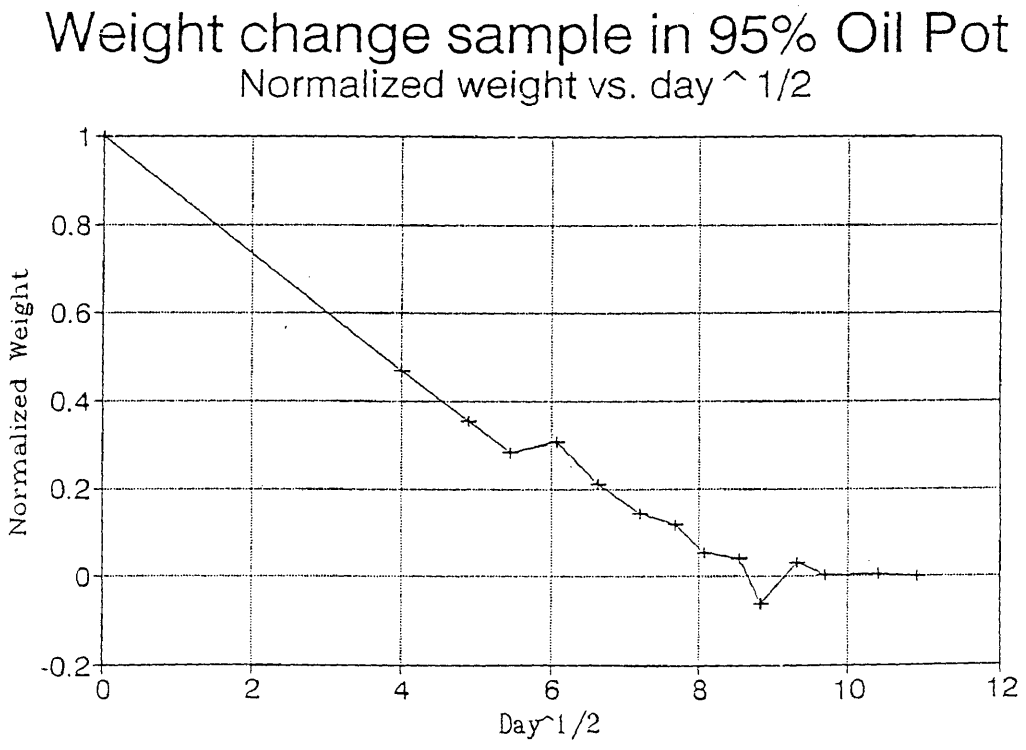

Figure 5-68

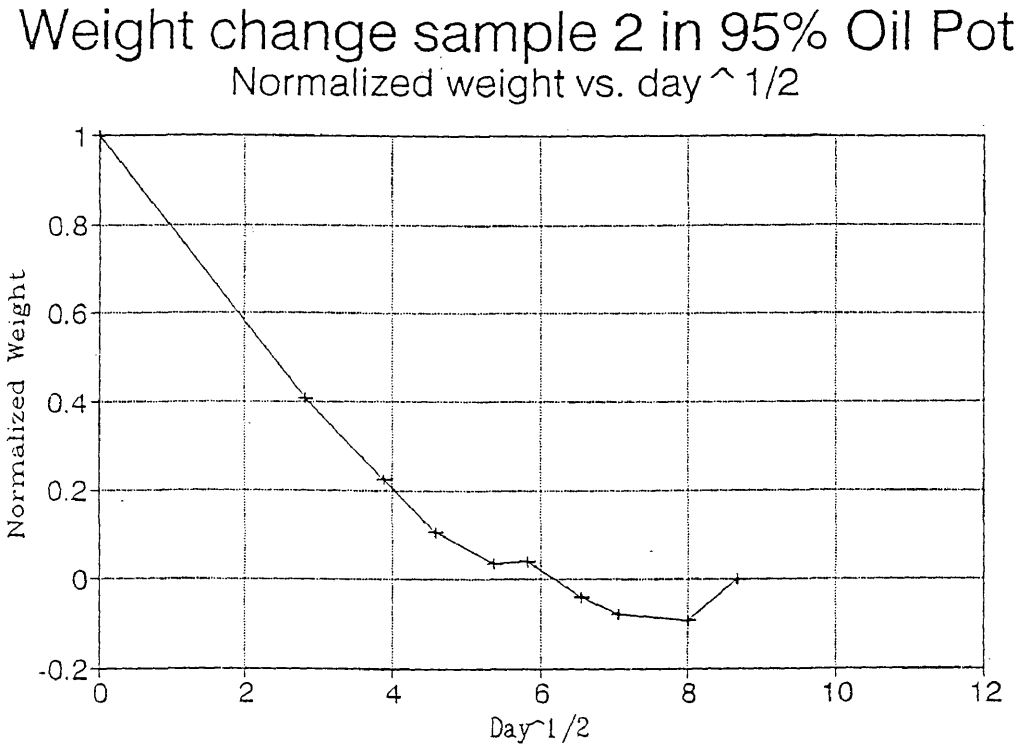
Weight change sample 2 in 95% Oil Pot
Normalized weight vs. day ^ 1/2
Normalized Weight
1
0.8
0.6
0.4
0.2
0
-0.2
0
2
4
6
8
10
12
Day^1/2

Figure 5-69

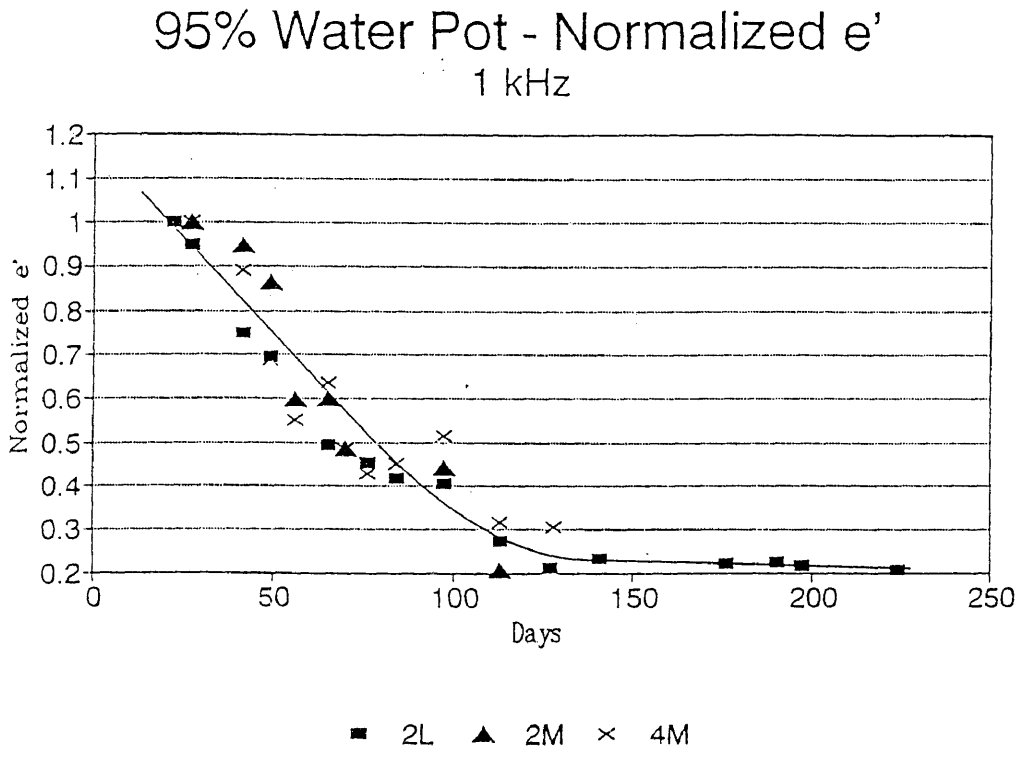

Figure 5-70

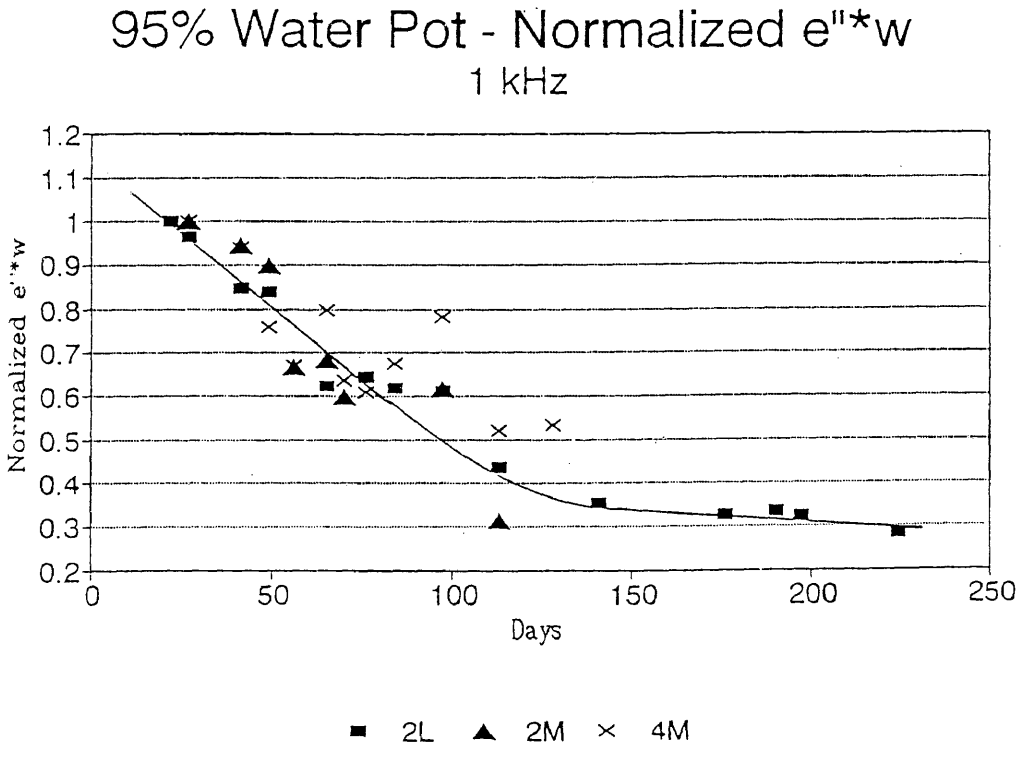

Figure 5-71

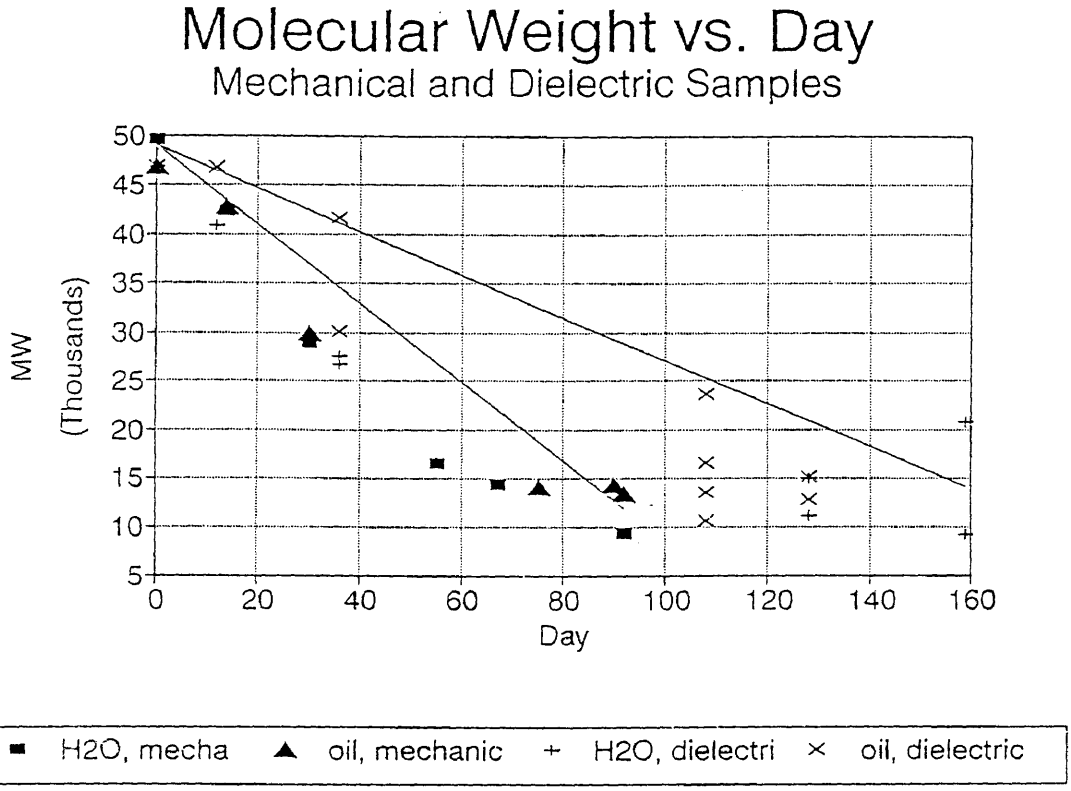
Molecular Weight vs. Day
Mechanical and Dielectric Samples
MW
(Thousands)
50
45
40
35
30
25
20
15
10
5
0
20
40
60
80
100
120
140
160
Day
H2O, mecha
oil, mechanic
H2O, dielectri
oil, dielectric

Figure 5-72

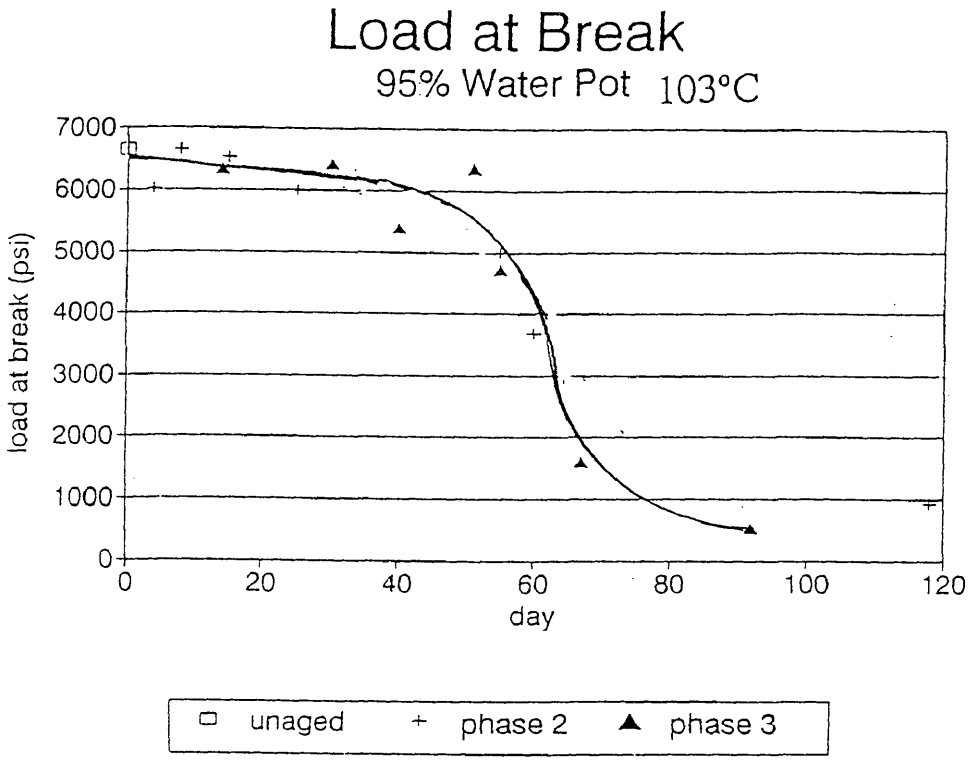

Figure 5-73

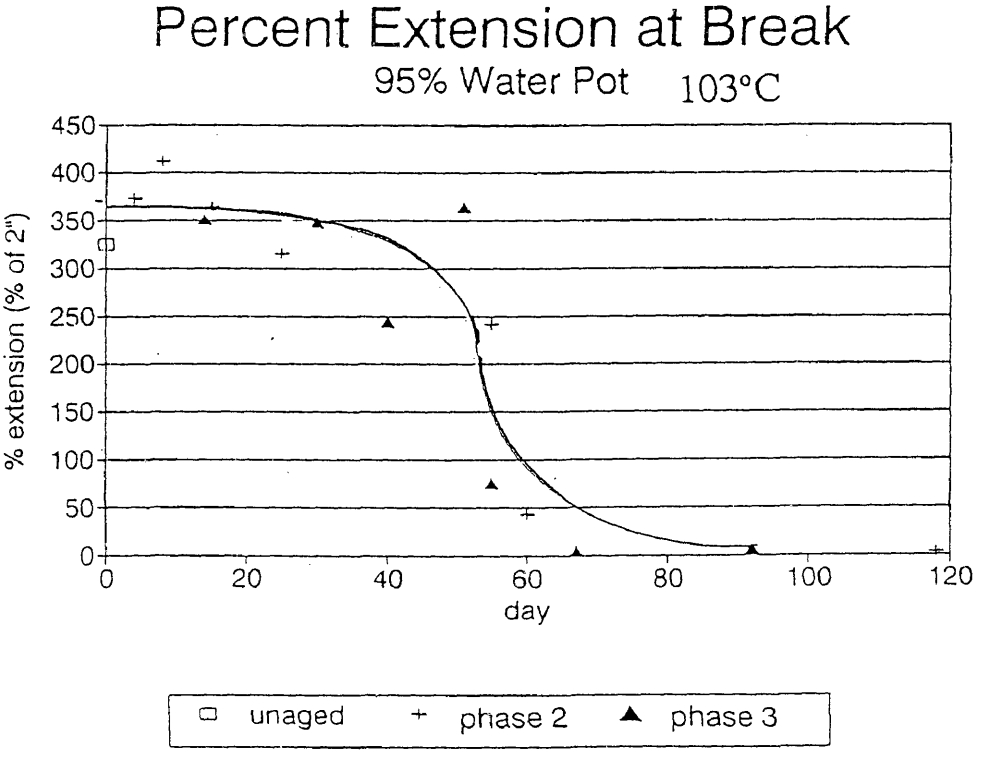

Figure 5-74

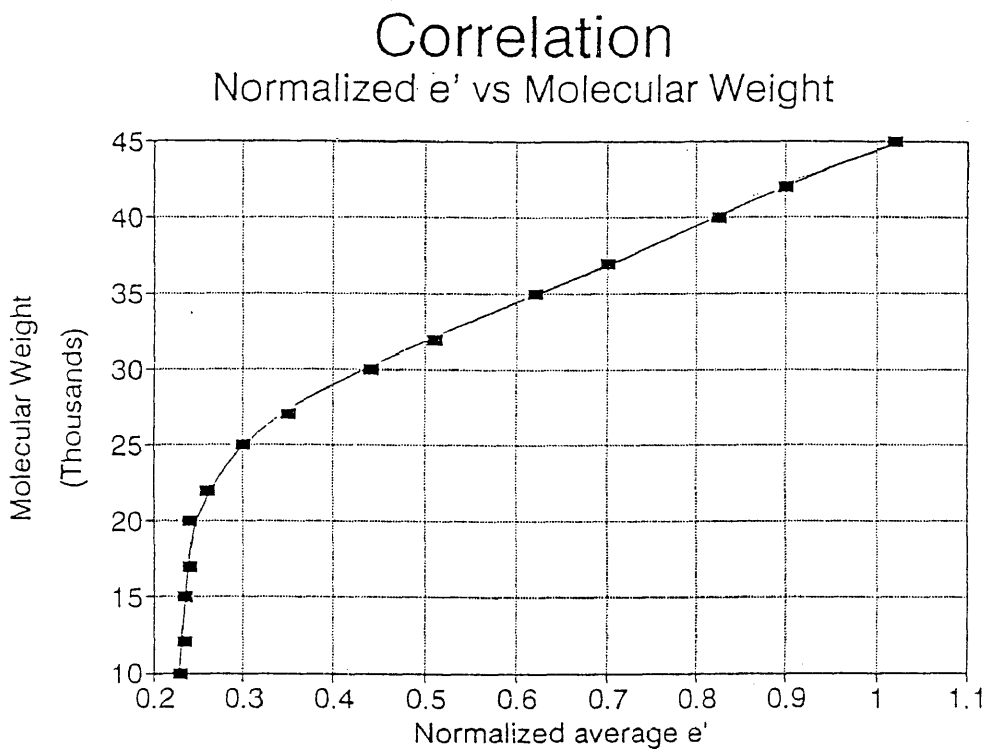

Figure 5-75

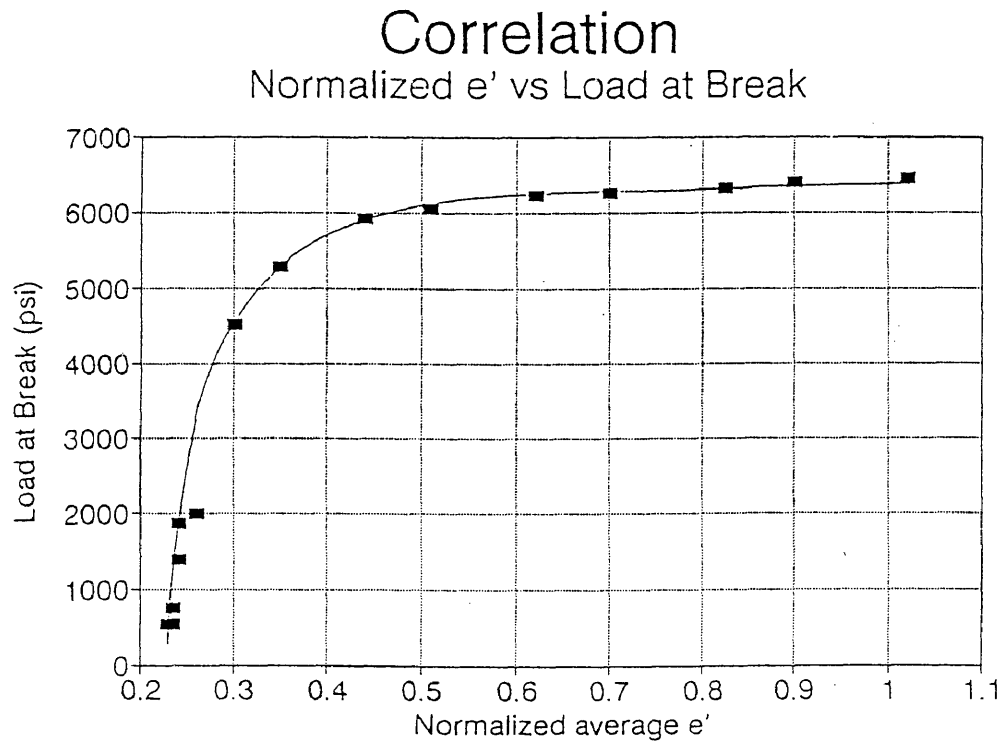

Figure 5-76

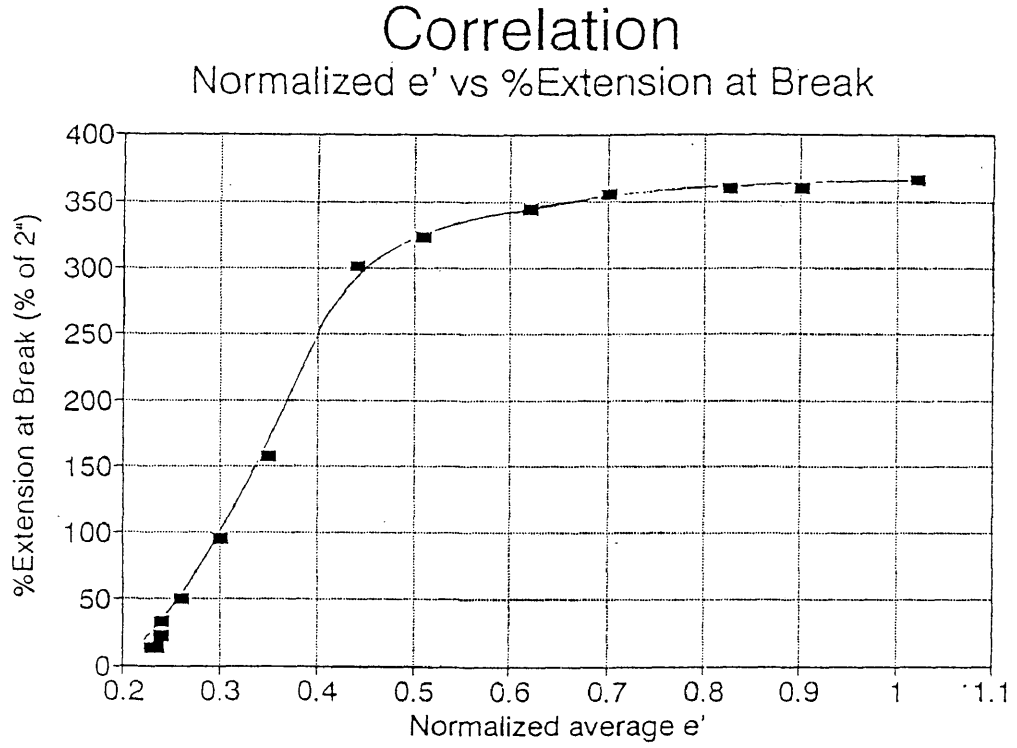

Figure 5-77

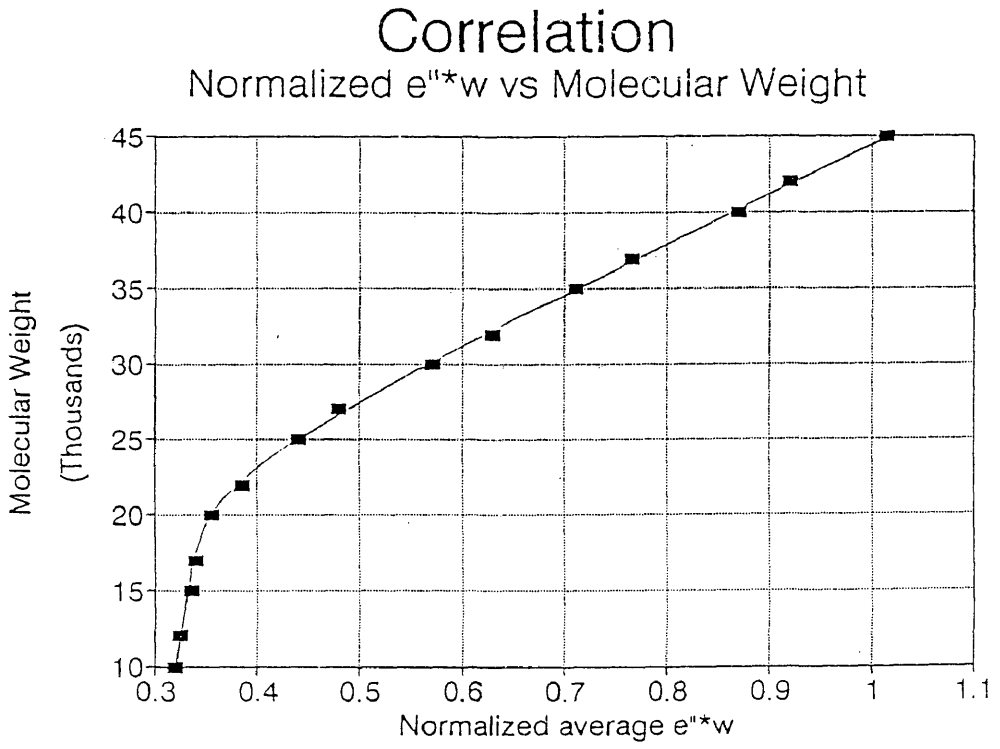

Figure 5-78

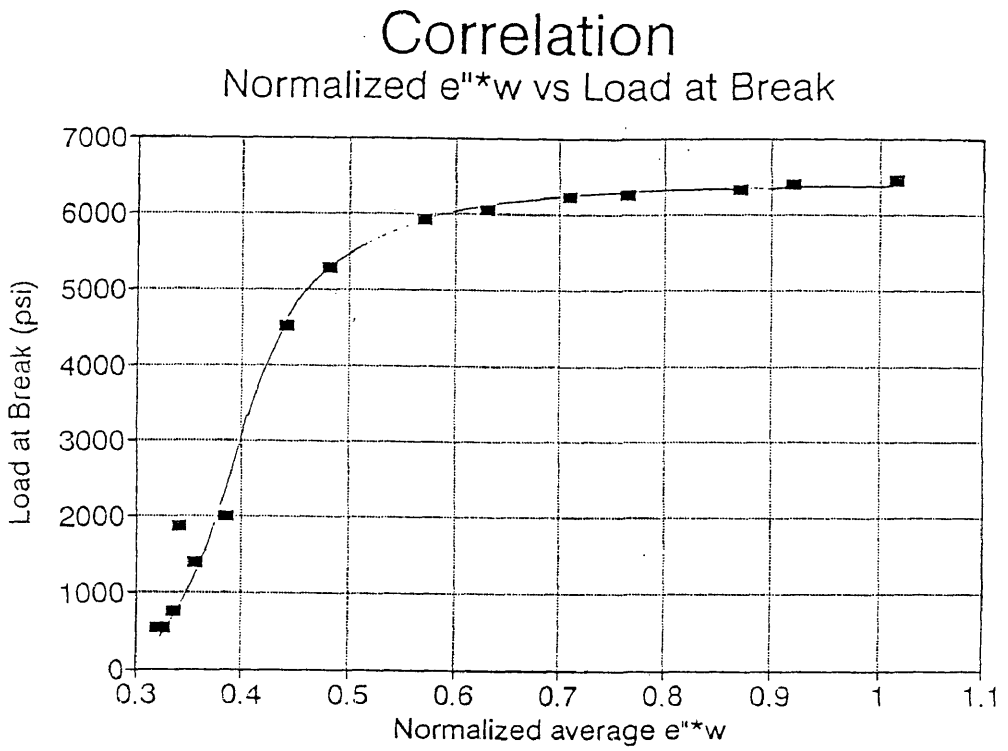

Figure 5-79

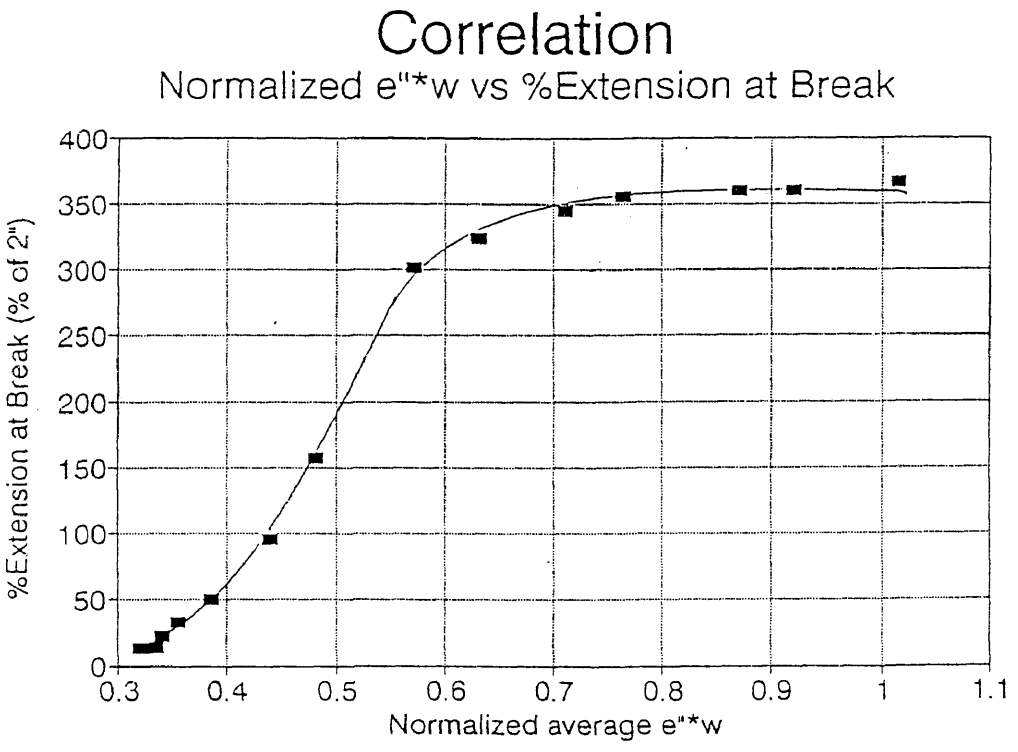

Figure 5-80

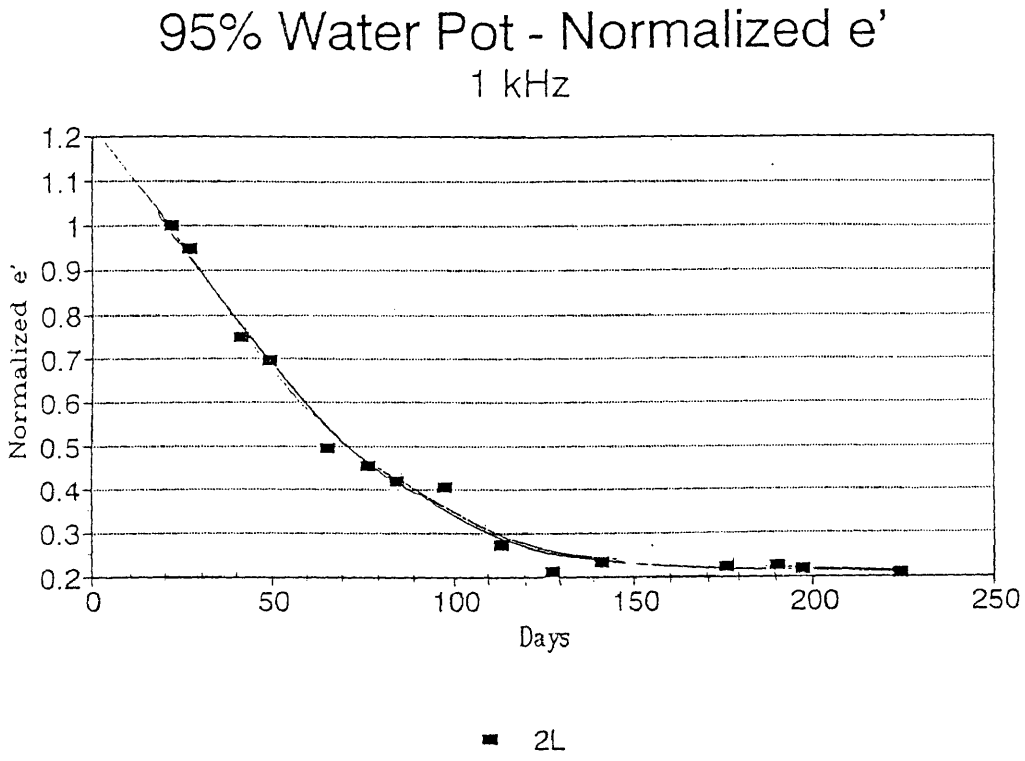

Figure 5-81

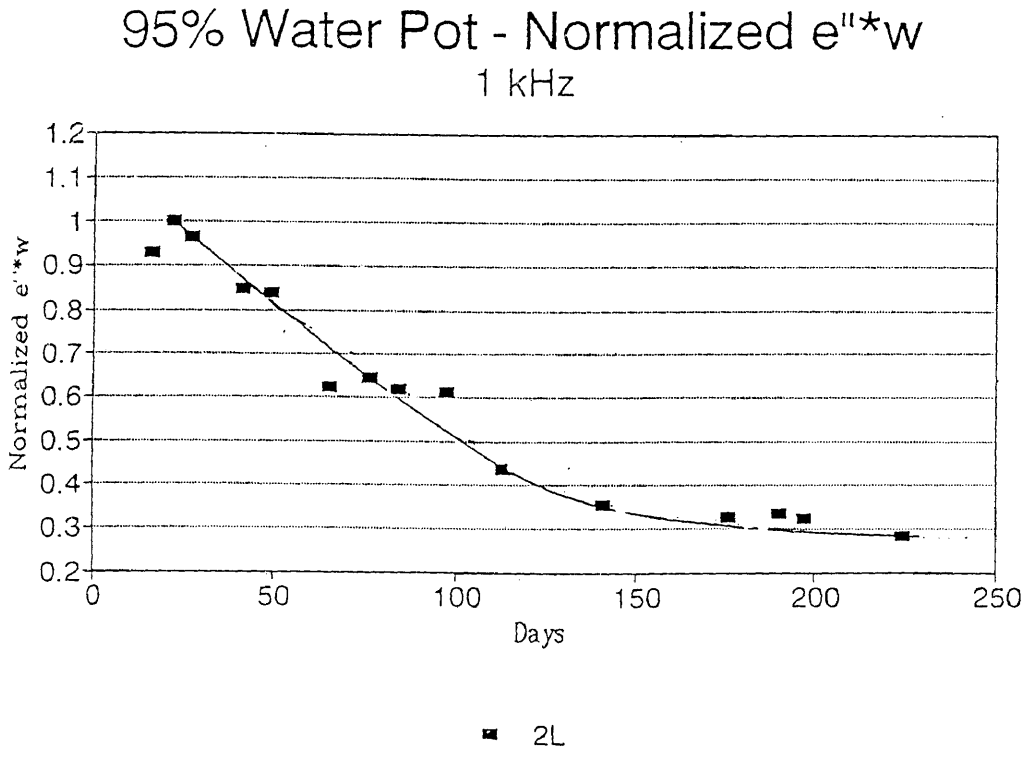

Figure 5-82

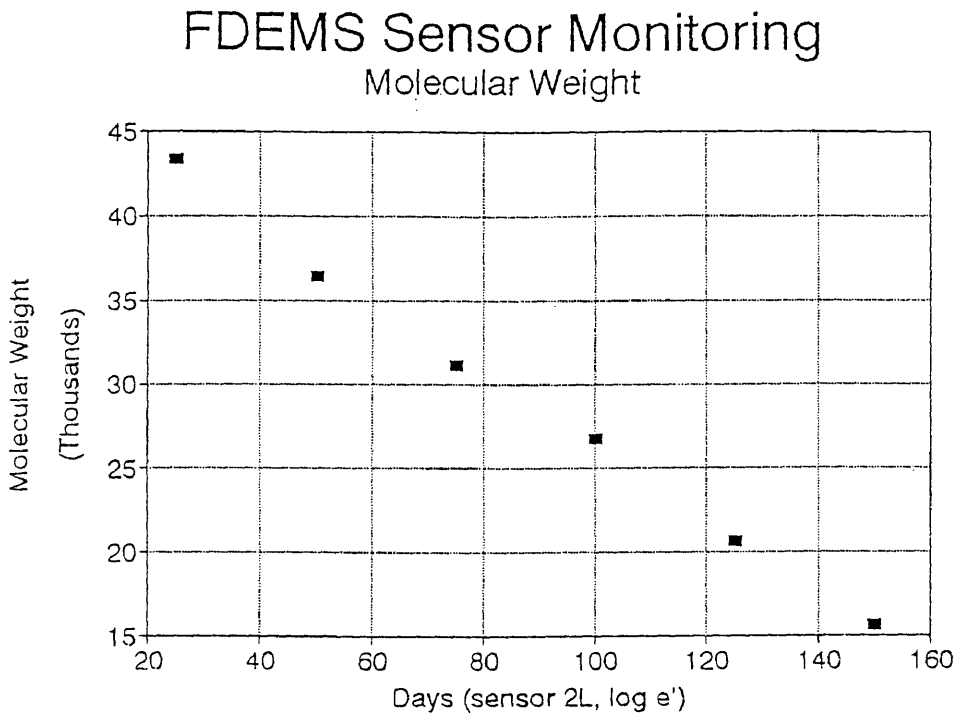

Figure 5-83

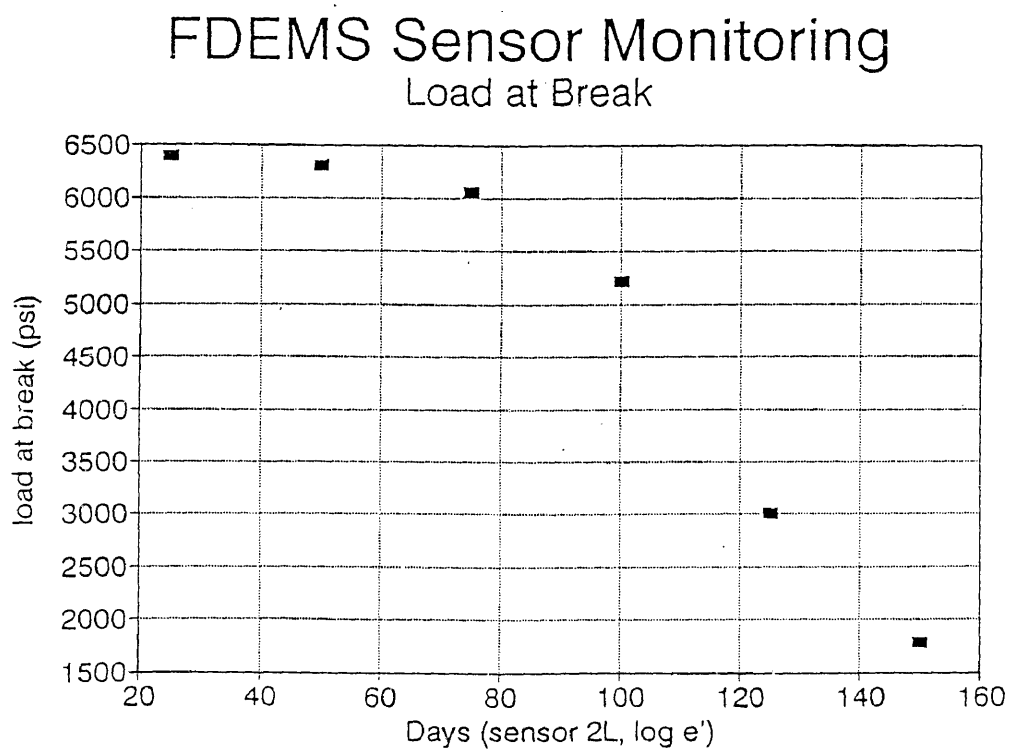

Figure 5-84

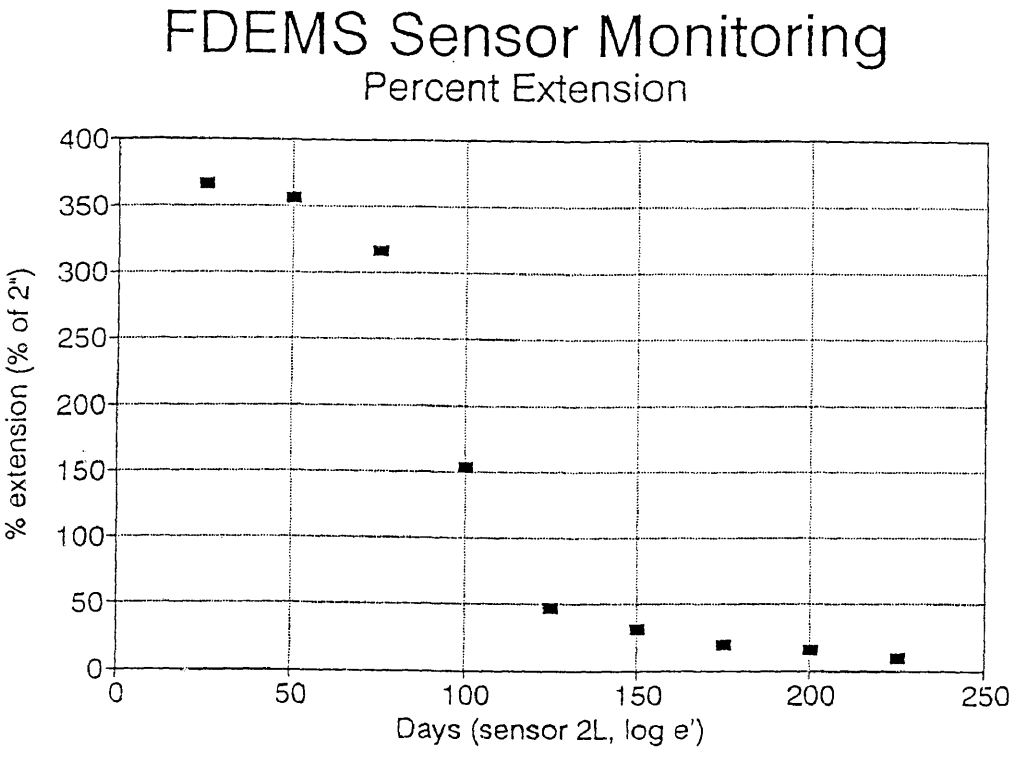

Figure 5-85

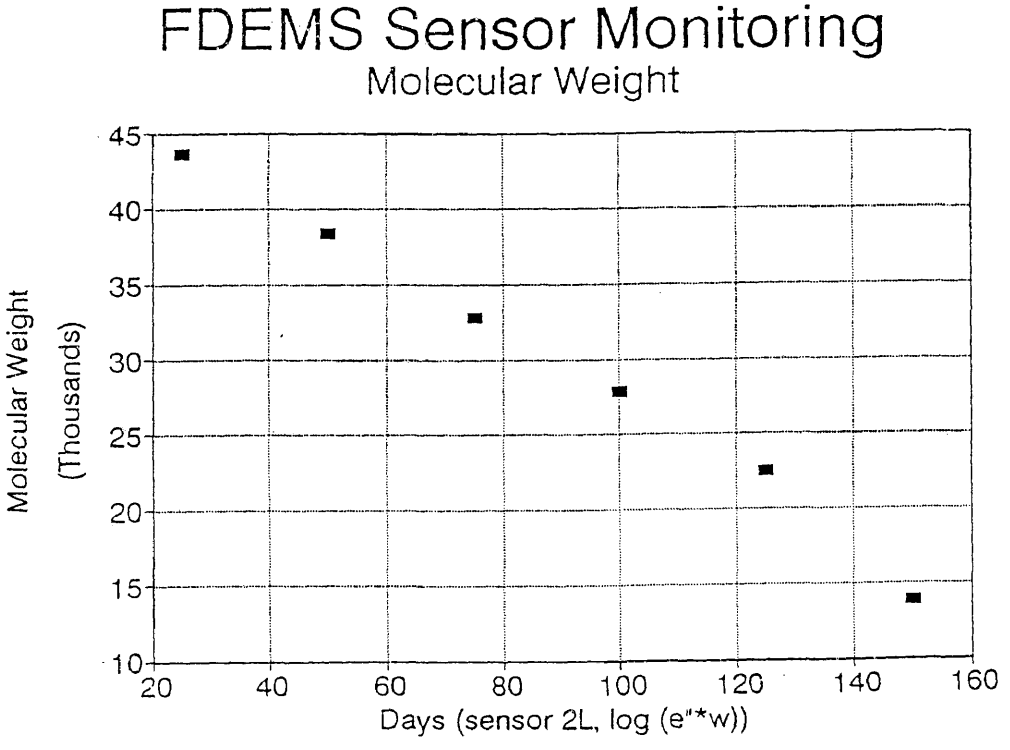

Figure 5-86

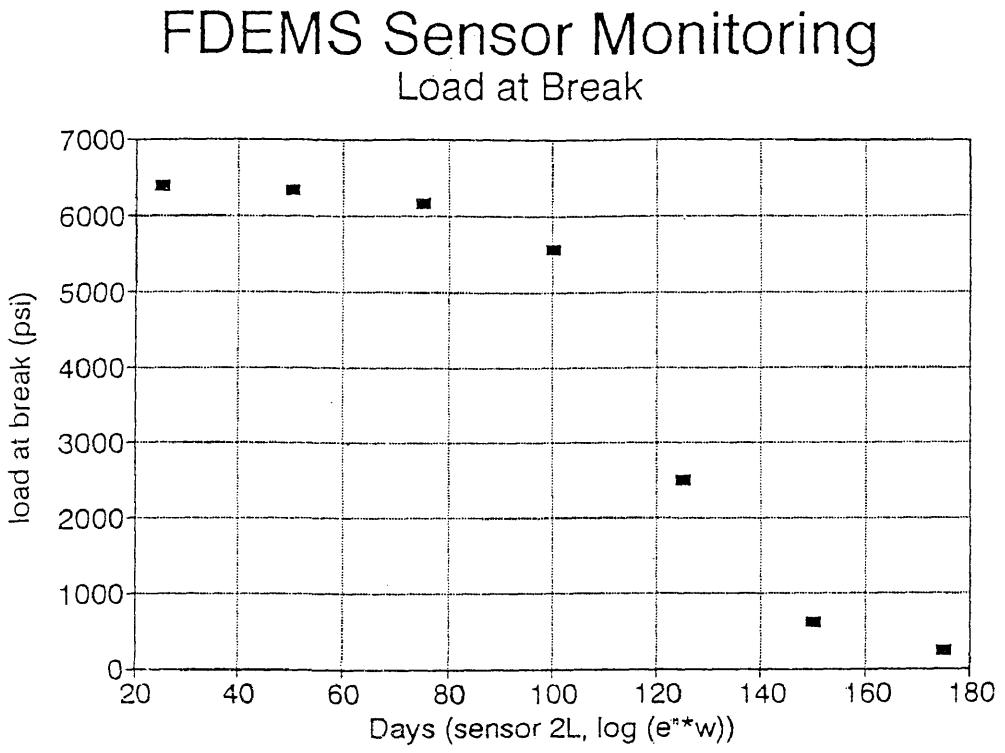

Figure 5-87

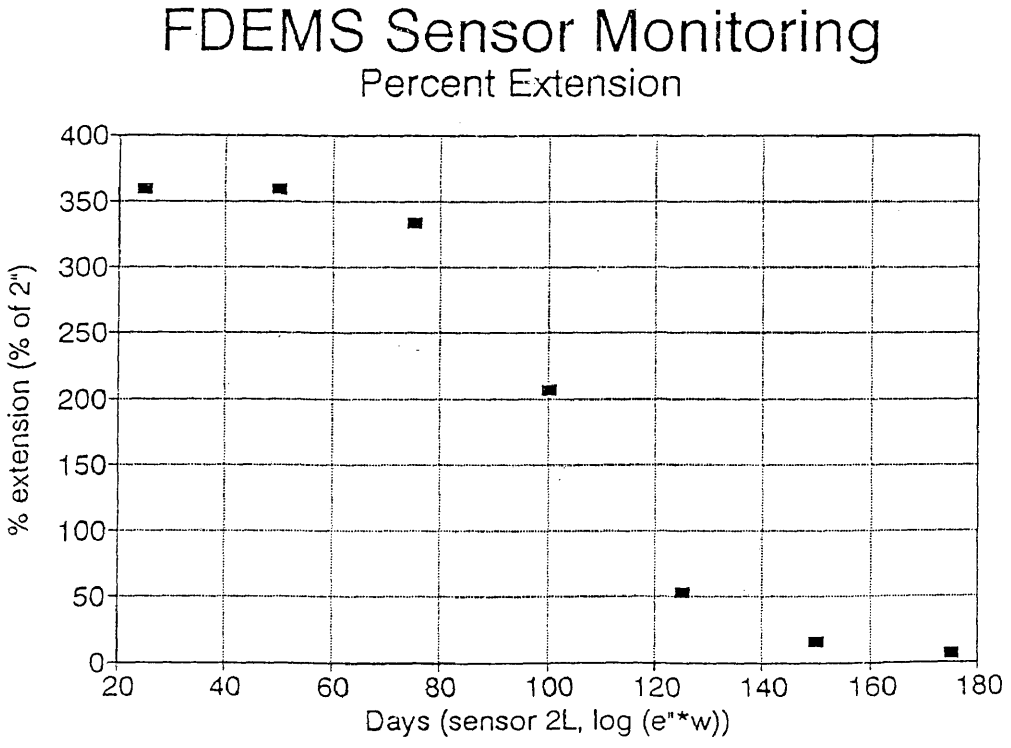

Figure 5-88

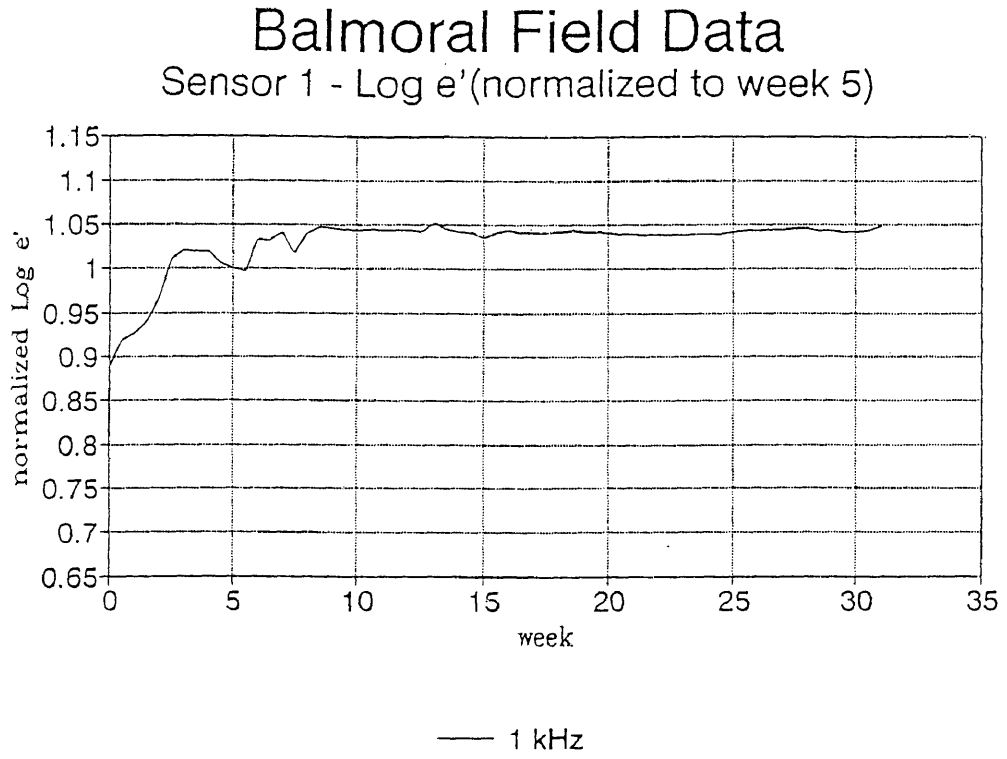

Figure 5-89

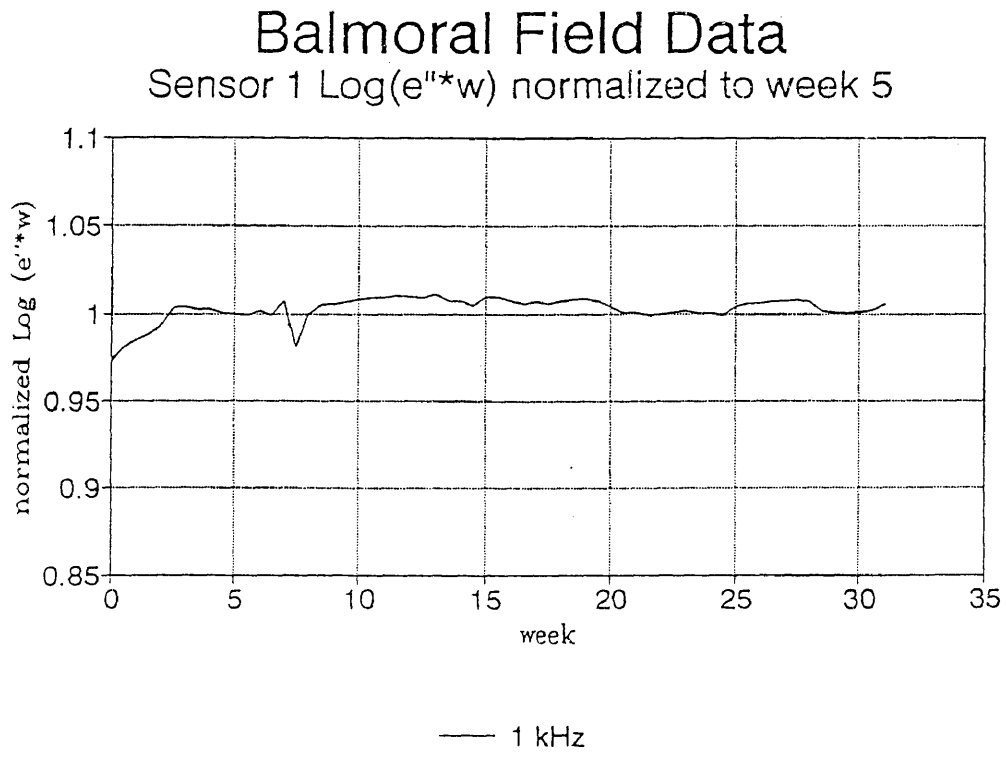

Figure 5-90

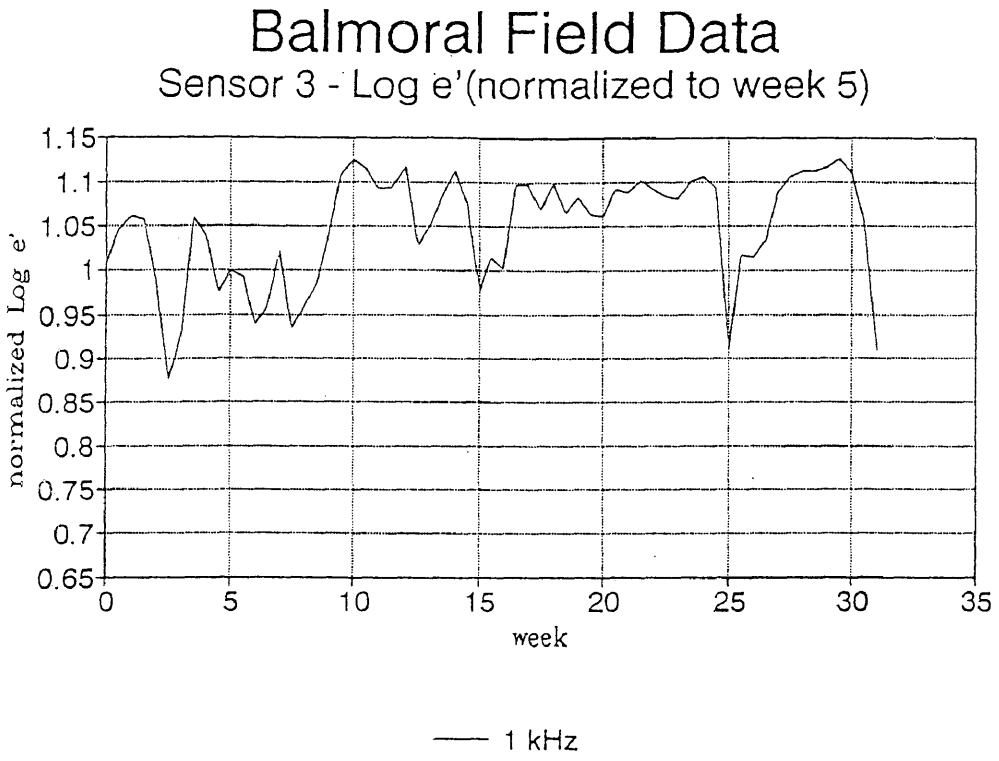

Figure 5-91

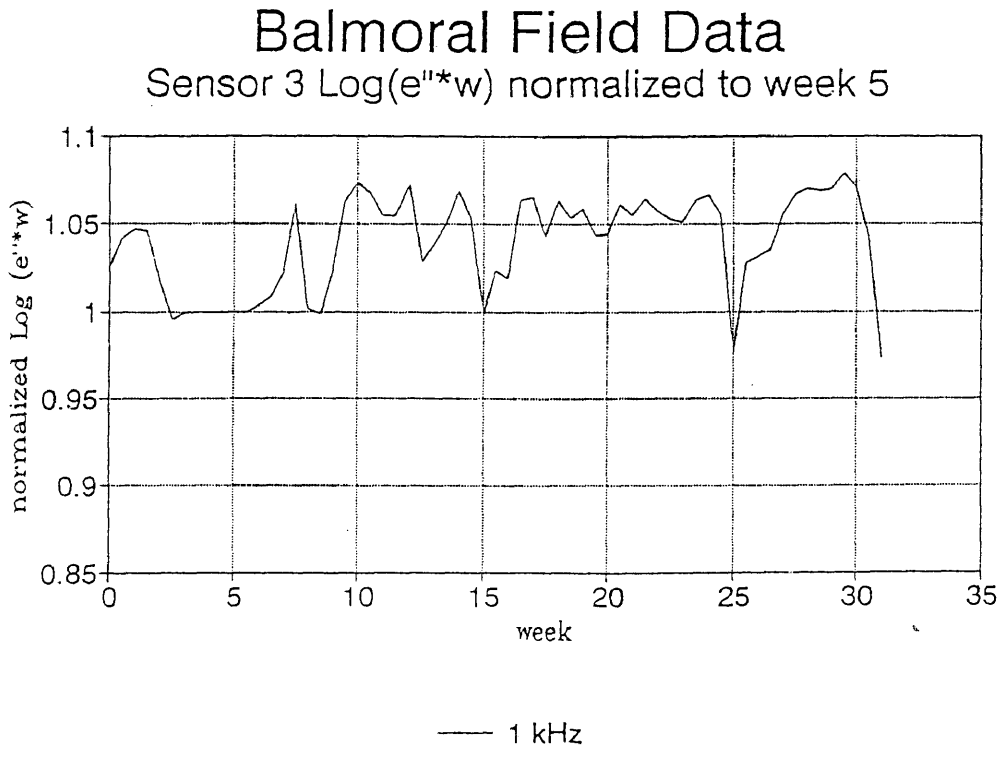

Figure 5-92

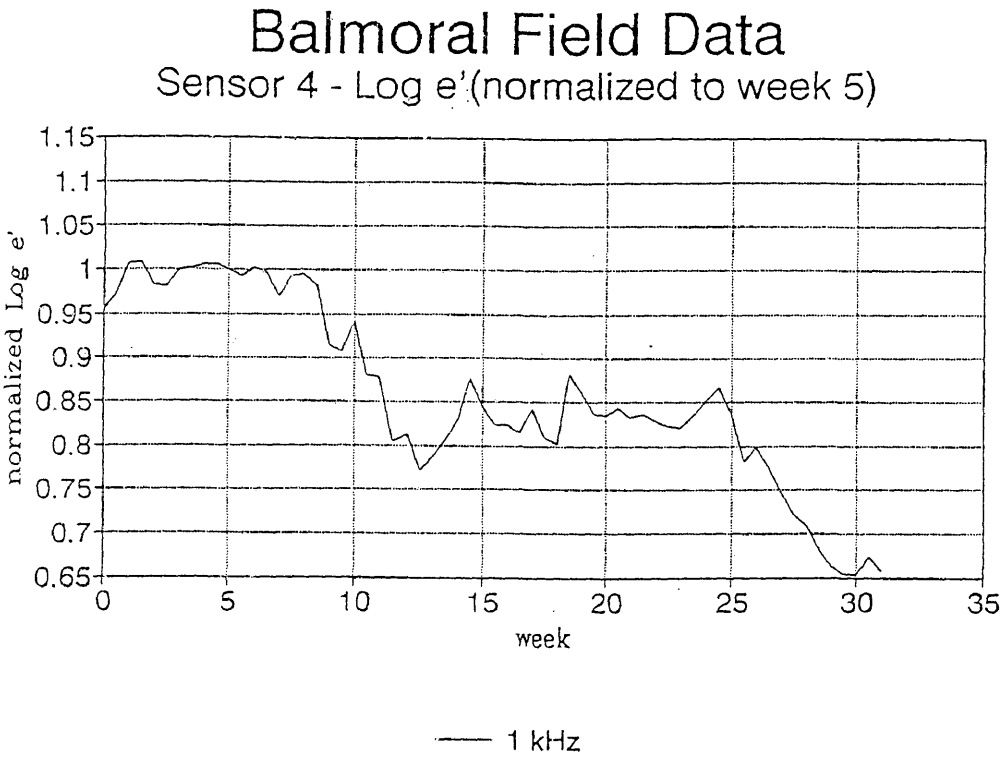

Figure 5-93

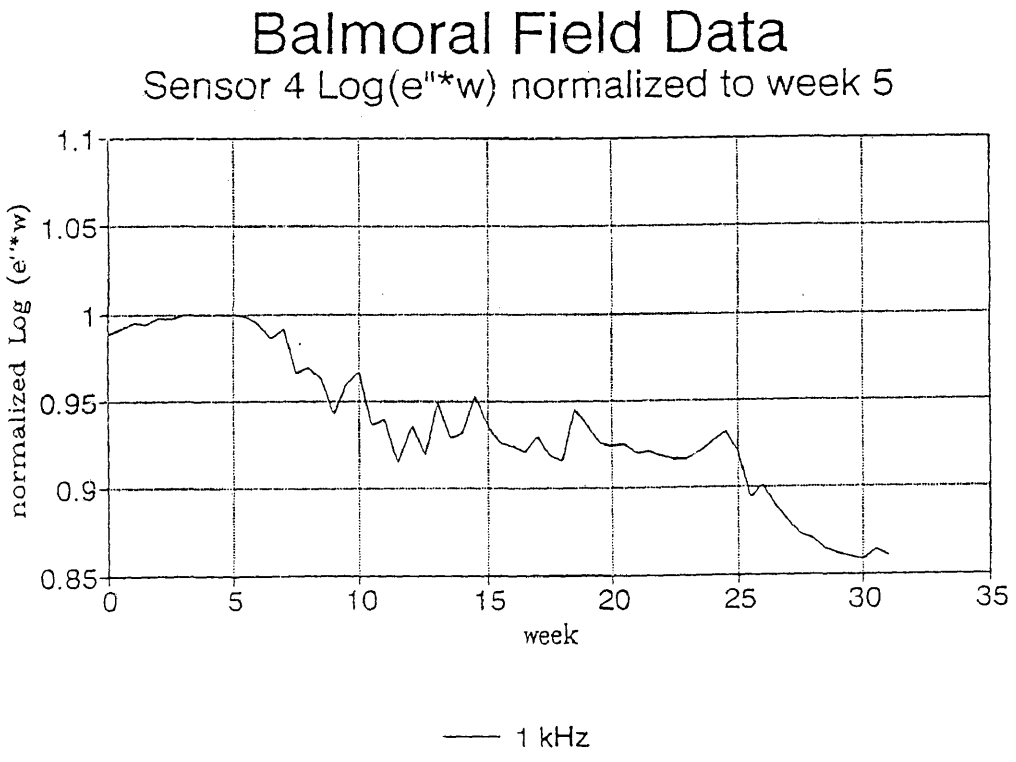

Figure 5-94

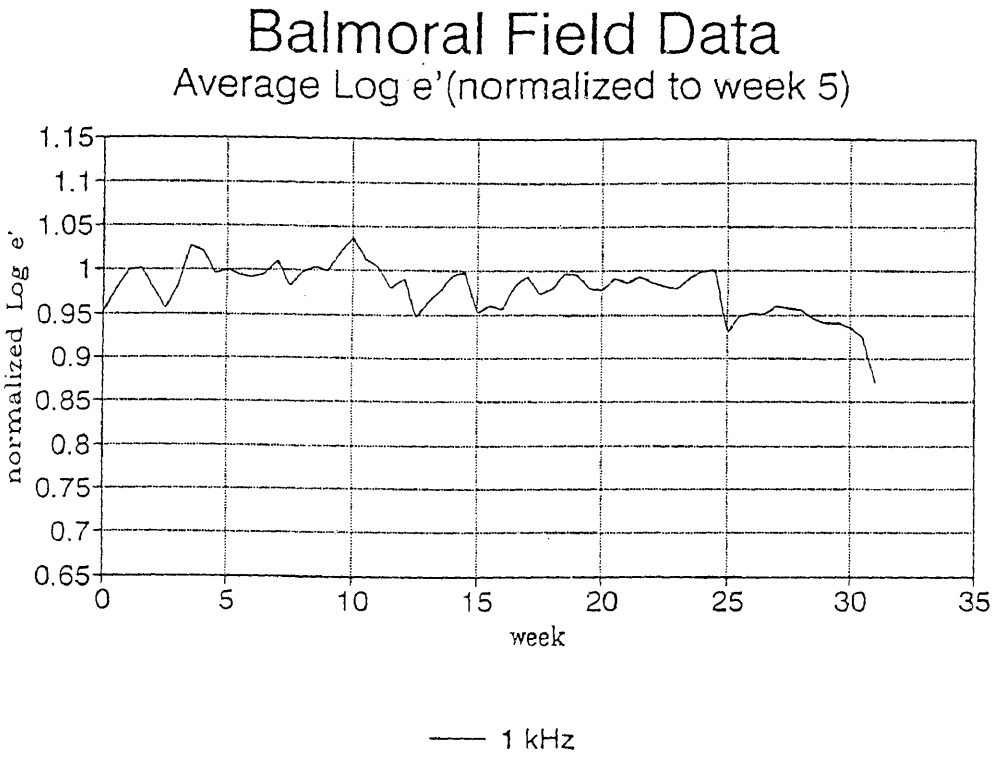

Figure 5-95

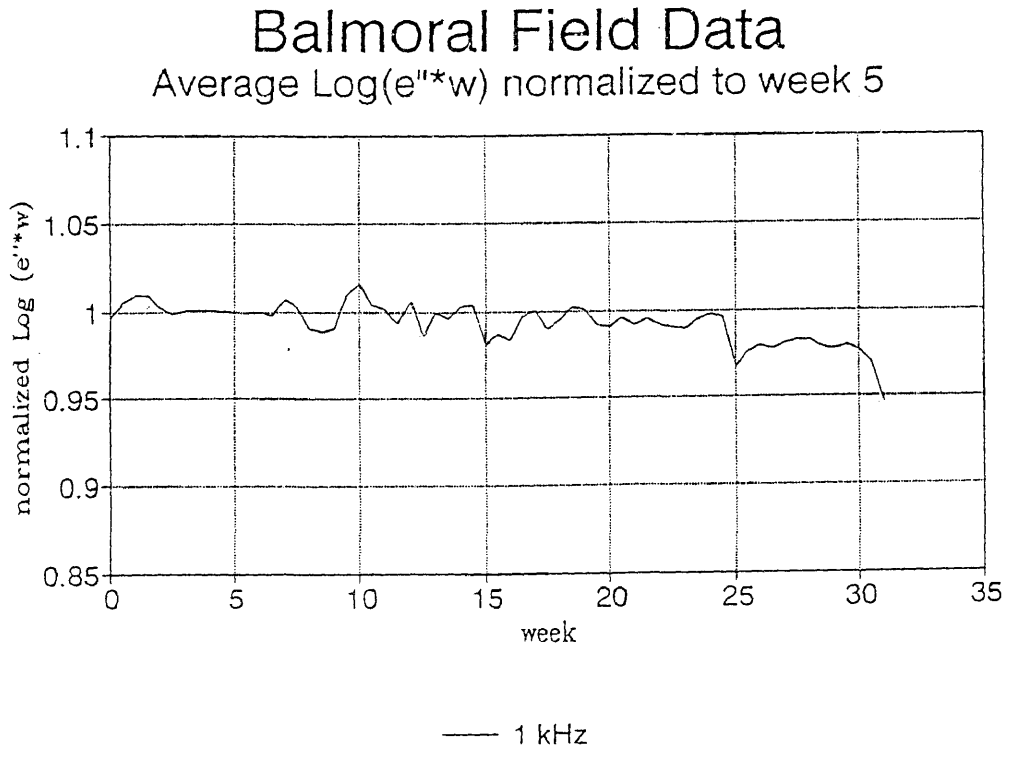

VI. Conclusions

The results from phase 3 (103°C) of the study of Rilsan pipe show that the pipe degrades faster in the CO_2 charged 95% water and 95% oil pots than in the crude oil pot. The dielectric values decrease by one decade for log ϵ' and half a decade for log (ϵ"*ω) for the samples aged in the 95% water and 95% oil pots. The dielectric values of the samples in the crude oil pot decrease at half the rate of the samples in the 95% water and 95% oil pots.

The nylon falls below acceptable mechanical properties after approximately 55 days in both the 95% water and 95% oil pots. Acceptable mechanical properties are defined by Amitec LTD as values above 45% of the original percent extension at break. The mechanical samples in the crude oil pot fall below this value after approximately 120 days. This also shows that samples in the crude oil pot are aging at half the rate of the samples in the 95% water and 95% oil pots. The samples aged in the 130°C 95% water pot of phase 1 fall below acceptable values after 20 days which is about three times as fast as the 103°C 95% water pot.

Molecular weight data shows the same trends as the mechanical data. For a given molecular weight the samples in the crude oil pot take twice as long to reach that point compared to the samples in the 95% water and 95% oil pots. The phase 1 (130°C) samples reach that value about three times as fast. A molecular

weight of 20,000 g/mol corresponds with 45% of the original percent extension at break. The mechanical samples in the 95% water and 95% oil pot fall below this value at about 55 days. The samples in the crude oil pot fall below this value after approximately 120 days. The phase 1 samples (130°C) are below 20,000 g/mol by day 20.

The rate of degradation increases with temperature. The 130°C pot was almost 30° higher and degraded at approximately three times the rate of the 103°C pot. Since the Balmoral field samples are only exposed to temperatures near 70°C, the rate of degradation would be expected to be slower than the 103°C crude oil pot. It can be predicted that this nylon would age at one third the rate of the nylon in the 103°C crude oil pot.

FDEMS measurements, log ϵ' and log(ϵ"*ω), which decrease as degradation proceeds, can be correlated with load at break, percent extension at break and molecular weight. After correlations have been generated, they can be used to predict macroscopic properties from dielectric measurements.

FDEMS in situ monitoring has demonstrated its effectiveness as a non-destructive method of life monitoring. Using FDEMS correlations, mechanical properties can be indirectly monitored. Sections of pipe could be replaced before they fell below the acceptable molecular weight and mechanical property values.

Bibliography

Allcock, H.R. and F.W. Lampe. Contemporary Polymer Chemistry, 2nd edition. Englewood Cliffs, NJ: Prentice Hall, 1990.

Atkins, P.W. Physical Chemistry, 4th edition. New York: W.H. Freeman and Company, 1990.

Bicerano, Jozef. Prediction of Polymer Properties. New York: Marcel Dekker, Inc., 1993.

Birley, A.W., R.J. Heath, and M.J. Scott. Plastics Materials: Properties and Applications, 2nd edition. New York: Chapman and Hall, 1988.

Brandrup, J. and E.H. Immergut, ed. Polymer Handbook, 3rd edition. New York: John Wiley & Sons, 1989.

Chandra, Manas and Salil K. Roy. Plastics Technology Handbook. New York: Marcel Dekker, Inc., 1987.

Chapman, Keith. North Sea Oil and Gas: A Geographical Perspective. North Pomfret, VT: David & Charles, 1976.

Collier's Encyclopedia. 1987.

Crank, J. and G.S. Park, ed. Diffusion in Polymers. New York: Academic Press, 1968.

Cussler, E.L. Diffusion: Mass transfer in fluid systems. New York: Cambridge University Press, 1984.

Deanin, Rudolph D. "Nylon 12." Society of Plastics Engineers Journal. Greenwich, CT: Society of Plastics Engineers, Inc., 1967. vol. 23 no. 9.

Flory, Paul J. Principles of Polymer Chemistry. Ithaca, NY: Cornell University Press, 1953.

Hart, S.M., Masters Thesis, "Intelligent Processing of PMR-15," College of William and Mary, 1992.

Hawkins, W. Lincoln. Polymer Degradation and Stabilization. New York: Springer-Verlag, 1984.

Inoue, M. "Studies on Crystallization of High Polymers by Differential Thermal Analysis." Journal of Polymer Science. Part A. New York: John Wiley & Sons, Inc., 1963.

International Petroleum Encyclopedia. 1983.

Johnson, J.F. and R.H. Cole. Journal of the American Chemical Society. **73** 4536. 1951.

Kranbuehl, David. "Cure Monitoring," Encyclopedia of Composites. New York: VCH Publishers, 1990.

Kranbuehl, D.E., et al. "Dielectric properties of the polymerization of an aromatic polyimide," Polymer. 1986. vol 27.

Kranbuehl, D., D. Hood, L. McCullough, H. Aandahl, N. Haralampus, and W. Newby. "Frequency Dependent Electromagnetic Sensing (FDEMS) For Life Monitoring of Polymers in Structural Composites During Use." 1995.

Kohan, Melvin I., editor. Nylon Plastics. New York: John Wiley & Sons, 1973.

Reich, Leo and Salvatore S. Stivala. Elements of Polymer Degradation. New York: McGraw-Hill Book Company, 1971.

Sears, J. Kern and Joseph R. Darby. The Technology of Plasticizers. New York: John Wiley & Sons, 1982.

Seymour, Ramond B. Plastics vs. Corrosives. New York: John Wiley & Sons, 1982.

Shah, Vishu. Handbook of Plastics Testing Technology. New York: John Wiley & Sons, 1987.

Short, C.K., Masters Thesis, "Characterization of Epoxy Resins For Use in the Resin Transfer Molding Process," College of William and Mary, 1993.

Solomons, T.W. Graham. Organic Chemistry, 4th edition. New York: John Wiley & Sons, 1988.

Sperling, L.H. Introduction to Physical Polymer Science, 2nd edition. New York: John Wiley & Sons, Inc., 1992.

The World Book Encyclopedia. 1993.

VITA

Leslie Christian McCullough

Leslie Christian McCullough was born in Williamsburg, Virginia, April 5, 1972. She graduated from Gaithersburg High School, Gaithersburg, MD in June 1990. She earned a Bachelors of Science degree in Chemistry at the College of William and Mary in Williamsburg, Virginia in May 1994. Afterwards, she enrolled in the Chemistry Graduate Program as a candidate for a Master of Arts at the College of William and Mary and fulfilled requirements in August 1995.